

Covalent and Non-Covalent Donor-Acceptor
Assemblies Based on Porphyrin Building Blocks

A Thesis
Submitted for the Degree of
DOCTOR OF PHILOSOPHY

A. Ashok Kumar



School of Chemistry
University of Hyderabad
Hyderabad - 500 046
India

September 2003

Dedicated to My Parents

Contents

Statement	i
Certificate	ii
Acknowledgements	iii
Synopsis	v
CHAPTER 1: Introduction	1
CHAPTER 2: Materials and Methods	63
CHAPTER 3: A New Nonameric Array Based on Tin(IV) Porphyrin Scaffold	75
CHAPTER 4: A Photochemically-Active Supramolecular Array Assembled <i>via</i> the Complementary Binding Properties of Ruthenium(II) and Tin(IV) Porphyrins	109
CHAPTER 5: A New 'Axial-Bonding' Type Donor-Acceptor System Assembled <i>via</i> Coordination of Zinc(II) Porphyrin with Pyridine-linked Calix[4]diquinone	135
CHAPTER 6: 'Intra-Complex' Electron Transfer in a Series of Quinone-Bound Isomeric Porphyrin-Calix[4]arene Conjugates	167
CHAPTER 7: Conclusions	211
Appendix 1: X-ray Crystallographic Data of [(DTPP)Ru ^{II} (CO)(Py)]	221
Appendix 2: List of Publications	225

Statement

I hereby declare that the matter embodied in this thesis is the result of investigations carried out by me in the School of Chemistry, University of Hyderabad, Hyderabad, India under the supervision of Prof. Bhaskar G. Maiya. In keeping with the general practice of reporting scientific observations, due acknowledgements have been made wherever the work described is based on the findings of other investigators.

A handwritten signature in black ink, appearing to read 'A. Ashok Kumar', written over a horizontal line.

A. Ashok Kumar

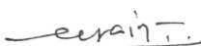
Certificate

Certified that the work contained in this thesis entitled "**Covalent and Non-Covalent Donor-Acceptor Assemblies Based on Porphyrin Building Blocks**" has been carried out by A. Ashok Kumar under my supervision and that the same has not been submitted elsewhere for a degree.


Dean

School of Chemistry

Dean
School of Chemistry
University of Hyderabad
Hyderabad-500 04S. India


Bhaskar G. Maiya

Thesis Supervisor

Acknowledgements

It is with high regards and profound respect I wish to express my deep sense of gratitude to **Prof. Bhaskar** G. Maiya, my supervisor. I owe it to him for introducing me to this field of research and teaching me many principles and techniques. He has always been approachable, helpful and, above all, extremely patient in his guidance throughout my research tenure.

I thank Prof. E. D. **Jemmis**, Dean, School of Chemistry, former Deans and all the faculty members of the school for their help and guidance on various occasions. Special thanks are due to Prof. M. Periasamy.

I also wish to thank Dr. Nick **Bampos**, Dr. Eugene Schultz and Dr. Neil Feeder (University of Cambridge, Cambridge, U. K.) for their help in collecting the NMR, **MALDI-TOF** and X-ray crystallographic data for a few samples.

I am grateful to Prof. N. Periasamy and Dr. Srirama Koti (**TIFR, Mumbai**) and I also thank Dr. P. Ramamurthy, Indira Pyriadharshini and **Karunakaran** (National Centre for Ultrafast processes, Chennai) for their kind help in time-resolved fluorescence studies.

RSIC, Central Drug Research Institute, Lucknow is acknowledged for the FAB mass spectral data.

I thank the authorities of Centre for Modelling, Simulation and Design (CMSD) and also the Universities with Potential for Excellence (UPE) programme of the University of Hyderabad.

I thank my labmates Dr. S. Arounagui, Dr. L. Giribabu, Dr. Easwaramoorthi, Dr. Rajagopal, D. Raghunath Reddy, C. V. Sastri, P. Prashanth Kumar, M. Mariappan, Tamal Ghosh, Premaladha and Narahari for all their help and valuable suggestions.

I would like to thank Mr. Satyanarayana, Mr. Bhaskar Rao, Mrs. Vijayalakshmi and Mr. Venkataramana for their technical assistance. I also thank Mr. Shetty and other non-teaching staff of the school of chemistry for their help.

I thank all my friends and well wishers for making my stay in the campus a memorable one.

Financial assistance from DST and CSIR is gratefully acknowledged.

Lastly, I thank my parents, brother and sister for their love and constant encouragement throughout my career.

Synopsis

This thesis entitled "**Covalent and Non-Covalent Donor-Acceptor Assemblies Based on Porphyrin Building Blocks**" deals with the design, synthesis, spectroscopy and photochemical properties of free-base and **metallo/metalloid** porphyrin based donor-acceptor (D-A) systems in which the D and A subunits are connected to each other by covalent or **non-covalent** interactions. Main observations of the research carried out here include the elucidation of **supramolecular electron/energy** transfer reactions occurring in these D-A systems.

Porphyrins and their metal/metalloid porphyrin derivatives are a versatile class of compounds having applications in various research areas such as **biomimetic** photosynthesis, molecular electronics, molecular catalysis, photodynamic therapy etc. A great variety of D-A type porphyrin systems have been built for use in many of these applications which generally involve photoinduced electron transfer (PET) or electronic energy transfer (EET) as the **key** principles. While majority of the porphyrin-based D-A systems reported so far have been constructed by covalently linking the donor/acceptor subunits at the porphyrin peripheral (i. e. **β -pyrrole and/or meso**) positions, relatively few such systems have been synthesized by utilizing the axial coordinative interactions involving the metal/metalloid center. Three chapters of this thesis discuss the results of investigations on the PET and EET reactions of porphyrin

based, 'axial-bonding' type D-A systems. Similarly, although a great variety of covalently linked porphyrin-quinone systems are reported in the literature," relatively less attention has been paid towards the construction of analogous **non-covalent** D-A systems. One chapter of this thesis deals with the PET reactions occurring between singlet porphyrin and **calixarene-bound** 1, 4-benzoquinone (BQ) in a series of **isomeric** porphyrin-calix[4]arene systems.

Chapter 3 of this thesis reports an 'axial-bonding' type **nonameric** porphyrin array in which a **trimeric** tin(IV) porphyrin is used as the basal scaffolding unit and free-base porphyrins as the axial subunits. The bridge between the axial and peripheral porphyrins is a "C-O-Sn" bond in this array. Detailed studies have been carried out on the chemistry, electrochemistry and photochemistry of the **nonamer**. Next, a different variety of porphyrin **trimer** has been self-assembled by employing the mutually non-interfering coordination properties of the ruthenium(II) and tin(IV) centers to form a 'hetero-metallic' array (Chapter 4). The photo- and electrochemical properties of this array have also been investigated. This axial-bonding theme has been extended to the next chapter, which discusses a D-A system that utilizes the axial bonding ability of a zinc(II) porphyrin to assemble the D and A subunits. A pyridine appended calix[4]diquinone system is shown to axially ligate at the zinc(II) center of **5,10,15,20-tetra(4-methylphenyl)porphyrinato** zinc(II), **[(TTP)Zn^{II}]** (Chapter 5). Systematic investigation on this system reveals a PET between singlet **[(TTP)Zn^{II}]** and the axially bound calix[4]diquinone acceptor.

Finally, covalently linked, **isomeric** free-base and zinc(II) porphyrin-calix[4]arene conjugates have been synthesized in which the calixarene subunit can house a BQ acceptor *via* H-bonding or van der Waals interactions (Chapter 6). Details of PET reactions occurring between the singlet porphyrin and **calixarene-bound** quinone acceptor in these D-A systems have been investigated.

The work embodied in this thesis has been divided into seven Chapters. A brief, **Chapter-wise** account of the results is presented below.

Chapter 1. Introduction

Recent literature on various '**peripherally**'-and 'axially' substituted as well as non-covalently linked porphyrin based D-A systems highlighting their PET and EET reactions have been reviewed in this Chapter.

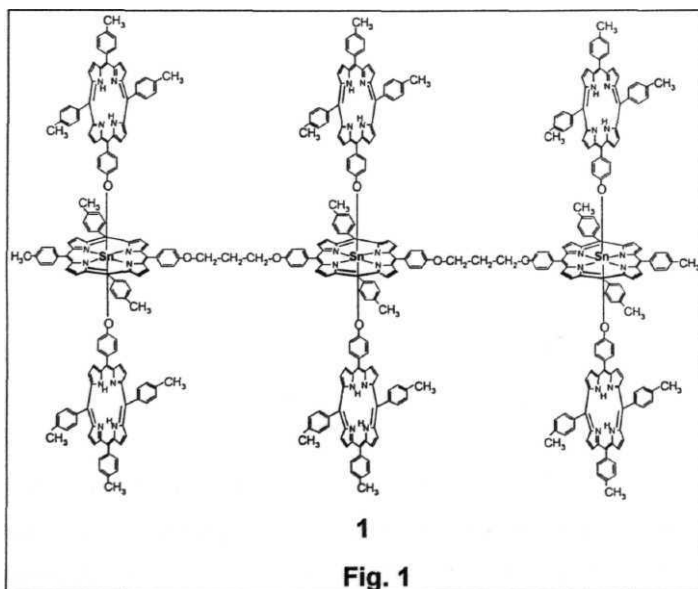
Chapter 2. Material and Methods

This Chapter presents a list of chemicals, a general description of the synthetic procedures and the details of spectroscopic, electrochemical and photophysical techniques employed during the research work.

*Chapter 3. A New **Nonameric** Array Based on **Tin(IV)Porphyrin** Scaffold*

The axial bonding capability of **tin(IV)** porphyrins has been utilized for the design of a hybrid porphyrin nonamer 1, **Fig.1**. The scheme of construction

of this array employs a synthetic protocol involving sequential 'organic' and 'inorganic' reactions conducted respectively, at the peripheral *meso*-phenyl ring and the central tin(IV) ion of the porphyrin scaffold. The architecture of the nonamer is such that it is based on a covalently linked tin(IV) porphyrin trimer, with each of the three tin(IV) centers *trans*-axially ligated to two free-base porphyrins. This extended, "axial-bonding" type architecture of the new array has been investigated by various physical methods that include mass (MALDI-TOF), UV-visible, fluorescence, ^1H NMR (1D and ^1H - ^1H COSY)



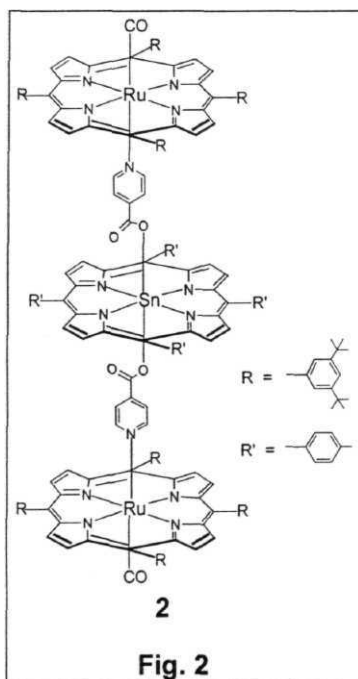
spectroscopies and electrochemical methods. **UV-visible** spectrum of the nonamer is similar to the spectrum of a physical mixture of the corresponding precursor porphyrins in appropriate mole ratio. Cyclic voltammetric data reveal that the oxidation and reduction potentials of the individual porphyrin rings of the nonamer are unaltered in comparison with those of the corresponding porphyrin monomers. Detailed ^1H NMR investigation reveals characteristic ring current induced shifts for the resonances due to protons of the axial free-base porphyrin subunits.

Singlet state activity of **1** has been probed by the steady state fluorescence method with selective excitation into the bands corresponding to the two constituent monomeric species. Analysis of the fluorescence data suggests the occurrence of EET from the basal Sn(IV) porphyrins to the axial free base porphyrins as well as PET from the axial free-bases to the basal metalloid porphyrin.

Chapter 4. A Photochemically Active Supramolecular Array Assembled via the Complementary Binding Properties of Ruthenium(II) and Tin(IV) Porphyrins

A new porphyrin **trimer 2** has been self-assembled by employing the mutually non-interfering coordination properties of ruthenium(II) and tin(IV) centers to form a 'hetero-metallic' array, Fig 2. The precursors employed in **the**

construction of this trimer are penta-coordinated 5,10,15,20-tetra(3,5-di-tert-butylphenyl)porphyrinato ruthenium(II) carbonyl, the hexa-coordinated



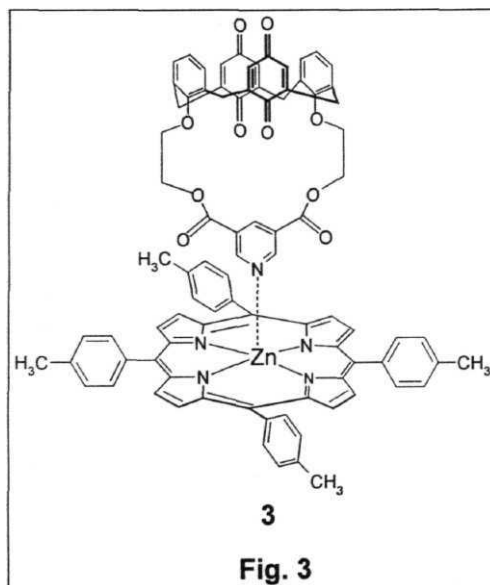
5,10,15,20-tetra(4-methylphenyl) porphyrinato tin(IV) dihydroxide and pyridine-4-carboxylic acid. The trimer has been constructed by both stepwise

and one-pot methods. UV-visible spectrum of **2** is essentially a superposition of the spectra of its constituent monomeric components, and it clearly provides evidence for the absence of any electronic interaction between the porphyrin planes in this array. Structure of the **trimer** is probed by the ^1H -NMR spectroscopic method, monitoring the shielding of protons present on the pyridine linker. Oxidation and reduction potentials of **2**, measured by the differential pulse voltammetric method, are found to be nearly identical to those of the monomers. Results of both steady state and time-resolved fluorescence studies reveal that a PET from the axial ruthenium(II) porphyrin to the singlet excited state of the basal tin(IV) porphyrin is feasible in this trimer.

Chapter 5. A New 'Axial Bonding' Type Donor-Acceptor System Assembled via Coordination of a Zinc(II) Porphyrin with Pyridine-Linked Calix[4]diquinone

This Chapter deals with the synthesis and spectroscopic, redox as well as photochemical behavior of a self-assembled D-A dyad **3** that is formed by the axial coordination of $[(\text{TTP})\text{Zn}^{\text{II}}]$ with a **calix[4]diquinone** bearing a pendant pyridine as the coordinating ligand, Fig. 3. The pyridine ligand **cyclo-25,27-diethoxy 26,28-calix[4]diquinone 3,5- pyridine dicarboxylate (CalixQ-py)** is synthesized in three steps: (i) selective alkylation of tetrahydroxy calix[4]arene with 1,2 **dibromoethane**, (ii) cyclization with cesium salt of 3,5-pyridine dicarboxylic acid and (iii) mild oxidation with aqueous chlorine

dioxide. **CalixQ-py** has been characterized by mass (FAB), UV-visible and ^1H -NMR spectroscopic methods. The well-known ability of zinc(II) porphyrins to form penta-coordinated complexes with coordinating ligands, such as pyridine, has been utilized to construct the novel D-A system **3**.



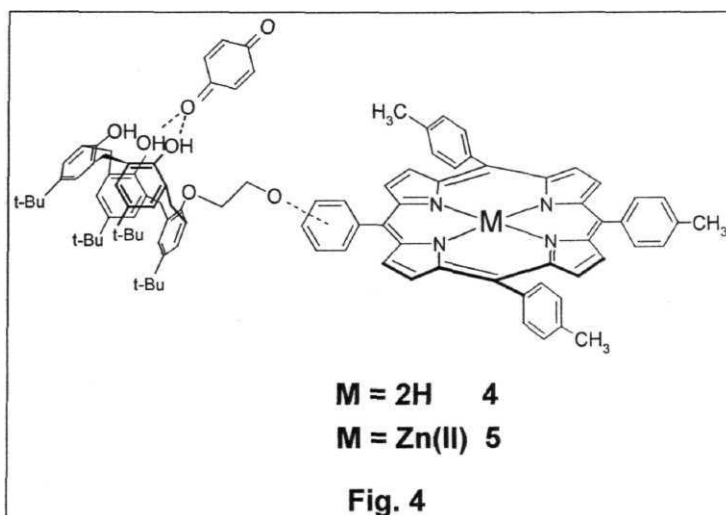
UV-visible titration studies reveal formation of a 1 : 1 complex between $[(\text{TTP})\text{Zn}^{\text{II}}]$ and **CalixQ-py** with a binding constant $K_a = 1685 \text{ M}^{-1}$. ^1H NMR titration studies provide further evidence for this binding. Upfield shifts for a

and β protons of the pyridyl ligand are observed in the presence of $[(TTP)Zn^{II}]$ due to the ring current effect exerted by the porphyrin upon binding. In the steady state and time-resolved fluorescence studies, it is observed that fluorescence quantum yield and lifetime of $[(TTP)Zn^{II}]$ are decreased upon successive addition of **CalixQ-py**. This quenching has been attributed to a PET from the singlet $[(TTP)Zn^{II}]$ to the diquinone acceptor located in the axial direction. Relevant rate constants have been evaluated using both the steady state and the time-resolved emission data.

Chapter 6. 'Intra-Complex Electron Transfer in a Series of Quinone-Bound Isomeric Porphyrin-Calix[4]arene Conjugates

This Chapter deals with the design, synthesis, spectroscopy and singlet state properties of a series of **isomeric porphyrin-calix[4]arene (P-Calix)** conjugates. Free-base derivatives of the isomeric **P-Calix** conjugates (4, see: Fig.4) have been synthesized by reacting 5-(4-hydroxyphenyl)10,15,20-tri(4-methylphenyl) porphyrin, 5-(3-hydroxyphenyl)10,15,20-tri(4-methylphenyl)porphyrin or 5-(2-hydroxyphenyl)10,15,20-tri(4-methylphenyl)porphyrin with 25-(2-bromoethoxy) 26, 27, **28-(trihydroxy)-4-tert-butyl calix[4]arene (Calix-(CH₂)₂Br)** in DMF/K₂CO₃ milieu. The corresponding zinc(II) complexes, 5, are also prepared. All the isomeric **P-Calix** conjugates have been fully characterized for their structural integrity and chemical purity by various physical methods that include mass (MALDI-TOF),

UV-visible, ^1H -NMR and fluorescence spectroscopies and also electrochemical methods.



UV-visible spectral features of the free-base and zinc(II) derivatives of the para and meta isomers and also those of the free-base ortho derivative of these **P-Calix** conjugates are close to the spectral features of their individual constituents. On the other hand, zinc(II) derivative of the ortho **isomer** shows red shifts in the absorbance bands of its calix[4]arene and porphyrin subunits.

Similarly, ^1H NMR data also reveal that resonance positions of the protons on the **calix[4]arene** subunit of this latter derivative are anomalously shielded. These data have been interpreted in terms of a close proximity between the calix[4]arene and porphyrin subunits leading to an intramolecular co-ordination between zinc(II) center of the porphyrin and one of the hydroxyl groups of the calix[4]arene moiety.

The photophysical properties of these isomeric conjugates have been investigated both in the absence and presence of BQ by the steady state and time-resolved fluorescence methods in CH_2Cl_2 and in $\text{THF}/\text{H}_2\text{O}$ (1 : 9, v/v). Binding of BQ by the calix[4]arene host *via* H-bonding interaction in apolar solvents like CH_2Cl_2 and *via* encapsulation in water rich media is well known. This is also expected to be the case with the presently investigated **P-Calix** compounds. Quenching of fluorescence intensity and decrease in singlet state lifetime of the porphyrin fluorophore are observed for each of these complexes upon successive addition of BQ in both CH_2Cl_2 and $\text{THF}/\text{H}_2\text{O}$ media. Rigorous analysis of the data obtained on **P-Calix** conjugates and also on the corresponding reference compounds (i.e. **H2TTP** and **[(TTP)Zn^{II}]**) suggests that the quenching mechanism in these conjugates involves both static and dynamic processes. Thus, the porphyrin fluorescence in these isomeric **P-Calix** conjugates is quenched, in part, by an intra-complex electron transfer from the singlet porphyrin to the 'complexed' quinone. The observation that the intra-

complex electron transfer rate varies in the order: ortho > meta > **para**, has been interpreted in terms of distance and orientation dependence of the PET.

Chapter 7. Conclusions

This Chapter presents general conclusions based on the investigations carried out in this work.

CHAPTER 1

Introduction

Porphyrin chemistry has undergone a resurgence over the past few years due to its potential applications in research areas such as biomimetic photosynthesis, molecular electronics, supramolecular catalysis, organic synthesis, magnetic resonance imaging (MRI), photodynamic therapy (PDT) etc. Photochemically active donor-acceptor (D-A) systems based on variously substituted **monomeric** and oligomeric porphyrin species are of immense utility in many of these applications, with the key photochemical reactions associated being (i) photoinduced electron transfer (PET) and (ii) excitation energy transfer (EET). This thesis deals with the design, synthesis and photochemical properties of D-A systems derived from 'axial' and/or 'peripheral' substitution of free-base and metalloporphyrins.

1. 1 Basic theory of PET and EET reactions

Molecules, upon photoexcitation become powerful donors or acceptors and hence, can be involved in electron and/or energy transfer reactions. Photoinduced electron transfer reaction has attracted the interest of chemists in many respects that include synthesis of organic molecules, development of solar energy storage/conversion systems and understanding of **natural/artificial**

photosynthetic **systems**.¹⁻⁴ Similarly, excitation energy transfer reactions are also important from the point of view of photosynthetic antenna function,⁵ polymer photophysics,⁶ molecular electronic devices **etc.**^{7,8} Equally significant is the theoretical understanding of the electron and energy transfer reactions and, this has added further impetus to the study of these important **processes**.⁹⁻¹⁴ Fig. 1. 1 depicts pathways through which electron and energy transfer processes can occur. In electron transfer, the excited state (*) can act either as a donor (D) or as an acceptor (A) whereas in energy transfer, the excited state will always be a donor.

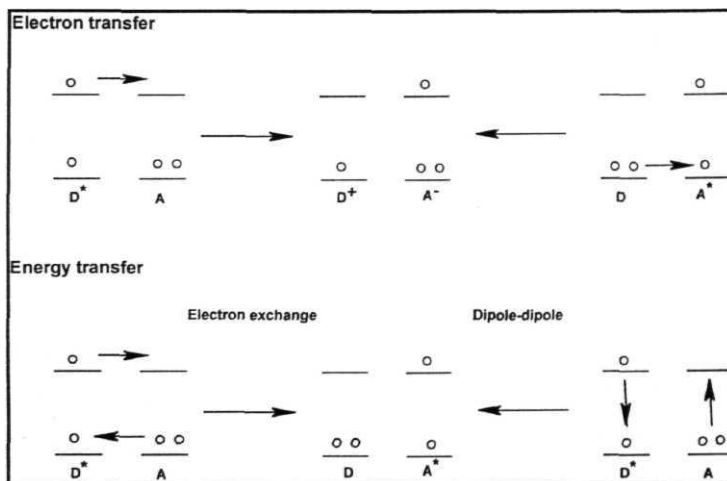


Fig. 1. 1

Marcus theory of electron transfer process provides a convenient way of discussing certain key aspects involved in the PET reactions.⁹⁻¹² According to this theory, rate constant for the electron transfer (k_{ET}) is given by the expression

$$k_{ET} = k_{el} \nu_n \exp(-\Delta G^\circ + \lambda) / 4k_B T \quad (1.1)$$

Here, k_{el} is the electronic transmission coefficient, ν_n is the frequency of nuclear motion through the transition state, ΔG° is the standard Gibbs free energy change for the overall ET reaction, λ is the reorganization energy needed to orient the initial complex to have a suitable configuration for electron transfer, k_B is the Boltzmann's constant, and T , the absolute temperature. ΔG^\ddagger is the free energy of activation, and it is related to ΔG° and λ , the reorganization energy, by the expression

$$\Delta G^\ddagger = (\lambda + \Delta G^\circ)^2 / 4\lambda \quad (1.2)$$

For exoergic reactions, when $-\Delta G^\circ < 0$, k_{ET} increases with increasing exoergicity. It reaches a maximum at $-\Delta G^\circ = \lambda$ and decreases again when $-\Delta G^\circ > \lambda$. This region of decrease of k_{ET} with respect to increasing exoergicity is termed as the "Marcus inverted region".

Electronic energy transfer reactions can, in principle, operate by two mechanisms:

- (i) Dipole-dipole mechanism which involves mutual Coulombic interaction of electrons (based on **Forster's theory**)¹
- (ii) Exchange mechanism which involves mutual exchange of electrons (based on **Dexter's theory**)¹⁴

Forster has developed an expression for the rate of electronic energy transfer due to dipole-dipole interaction in terms of the experimentally obtainable parameters. According to this theory, the rate constant for energy transfer, k_{EnT} , is given by equn. 1.3

$$k_{EnT} = \frac{8.8 \times 10^{-25} \kappa^2 \phi_D}{n^4 \tau_D R^6} \int F_D(\bar{\nu}) \epsilon_A(\bar{\nu}) \bar{\nu}^{-4} d\bar{\nu} \quad (1.3)$$

In the above equation, $\bar{\nu}$ is the wave number, $F_D(\bar{\nu})$ is the spectral distribution of the donor emission in quanta normalized to unity, $\epsilon_A(\bar{\nu})$ is the molar extinction coefficient for the acceptor absorption and n is the refractive index of the **solvent**. κ^2 is a function of relative orientation of transition dipole moments of the donor and the acceptor. ϕ_D is the quantum yield of donor emission, τ_D is the donor emission lifetime (in seconds) and R is the distance between the donor and acceptor molecules (in centimeters).

From the photophysical point of view, the fundamental processes that take place from the singlet state are depicted in Fig. 1.2.

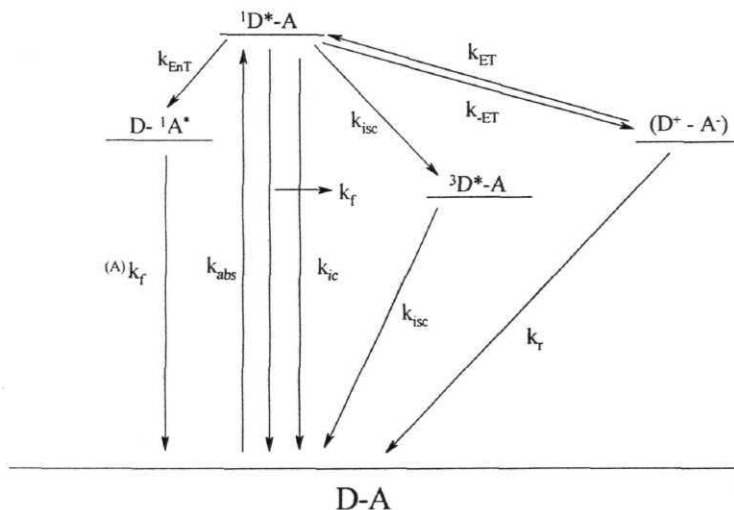


Fig. I. 2

Here, superscripts 1 and 3 refer to the singlet and the triplet states, respectively. k_f ($^{(A)}k_f$), k_{ic} , k_{isc} , k_{ET} , k_{-ET} , k_r and k_{EnT} are the rate constants for fluorescence, internal conversion, **intersystem** crossing, forward electron transfer, reverse electron transfer, charge recombination and energy transfer reactions, respectively. For an efficient **electron/energy** transfer to occur, k_{ET} and k_{EnT}

have to compete with other processes *viz.* fluorescence, internal conversion, intersystem crossing etc.

Table 1. 1 summarizes determinants of EET and PET reactions derived from the theories of electron and energy transfer reactions as well as the processes competing with these reactions discussed above.

Table 1. 1

Determinants of electron and energy transfer

Electron transfer	Distance and orientation (electronic coupling, orbital overlap); Free energy change (driving force); Reorganization in D and A; Orientation polarization of medium
Excitation energy transfer	Distance and orientation (coupling of excited states); Spectral overlap of emission and absorption of D and A; refractive index of the medium.

Processes competing with electron and energy transfer

Electron transfer	(i) Nonradiative relaxation of D* by photoisomerization and other conformational changes; Excited state proton transfer; Intersystem crossing; Chemical reactions;
	(ii) Back reaction to the ground state D-A
<u>Excitation energy transfer</u>	<u>Same as (i)</u>

1. 2 PET and EET in biological and a biological systems

As mentioned in the previous section, many applications of porphyrins rely on the photochemical characteristics of these **macrocyclic** compounds. In recent years, considerable development that has taken place in areas such as biomimetic photosynthesis, photodynamic therapy and molecule based optoelectronics seems to have provided greater impetus to research related to photochemistry of porphyrins. A brief introduction to these biological and abiological issues, as applied to the theme of the present thesis is presented below.

Photosynthesis is responsible for our oxygenic atmosphere. Both PET and EET are important and prevalent phenomena in natural photosynthesis. For example, antenna function of the photosynthetic systems involves singlet-singlet (s-s) energy transfer between two chlorophyll (**Chl**) molecules and also that between carotenoids (*Car*) and **Chl**. In addition, carotenoids provide photoprotection by rapidly quenching the triplet states of **Chl** by triplet-triplet (t-t) energy transfer thus preventing **Chl** sensitized production of singlet oxygen.

The electron transfer events of photosynthesis take place within a highly specialized reaction center (RC) complex. Detailed structural information for several bacterial reaction centers are now available from x-ray crystallographic investigations.^{15 - 24} The RC of *Rhodobacter spheroides* (RhS) comprises of four bacteriochlorophylls (**BChl**) including those of the so-called 'special pair', two bacteriopheophytins (*BPhe*), two quinones (Q) and a carotenoid polyene. In

addition, this RC has two branches - L and M. The photosynthetic process begins within the reaction center by excitation of the "special pair" *BChl*. This excitation usually occurs through s-s energy transfer from antenna molecules. Within 2 - 4 ps of excitation, singlet state of the special pair donates an electron to one of the *BPhe* molecules with a quantum yield of essentially unity. The *BPhe* radical anion transfers an electron to the neighbouring *Q*, again with a quantum yield of ~ 1 . The net result of this multistep electron transfer sequence is the generation of a spatially separated, charge transfer state comprising the oxidized 'special pair' and the reduced quinone.

A detailed understanding of these natural reactions has been greatly aided by studies of electron and energy transfer in synthetic model systems. A great number of substituted porphyrins and metallo/metalloid porphyrins have been synthesized as photosynthetic model systems; a number of reviews/monographs on this topic are now **available**.^{1,5,25-39}

Currently, design of molecule based optical devices is receiving world-wide attention. Molecular rectifiers, transistors, wires, photodiodes etc. are being designed by utilizing the chemistry of excited- and charge transfer states of both inorganic and organic **molecules**.^{7, 8,39} The design of a 'molecular wire' is one among the many important aspects of research in this subject. Many 'molecular wires' based on porphyrin arrays are being **devised**.⁴⁰⁻⁴⁵

The following sections deal with a survey of recent literature on porphyrin-based oligomeric- and D-A systems as relevant to the present study.

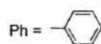
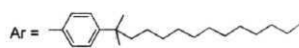
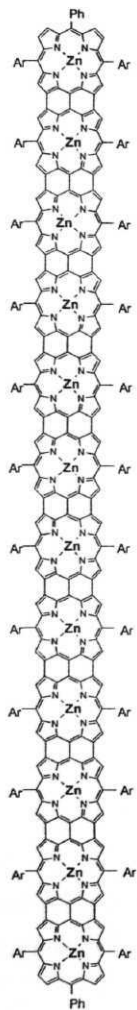
1. 3 Porphyrin oligomers

A great variety of **covalently/non-covalently** linked porphyrin dimers and higher oligomers have been reported in the literature and multistep energy- and electron transfer reactions have been elucidated in some of these systems. In the following discussion, recent studies on the oligomeric porphyrins are highlighted.

1. 3. 1 Covalently linked linear oligomers

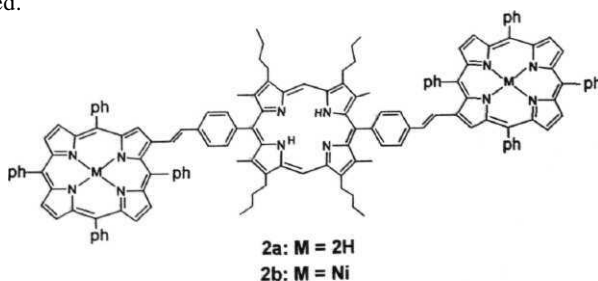
Among the first examples of linear dimers are those which have been developed by Kong and Loach and also by Boxer and **Bucks**⁴⁶⁻⁴⁸

Linear porphyrin oligomers formed by conjugated bridging of porphyrin subunits have been the focus of current interest because of their potential application in non-linear optics, organic semiconductors and light harvesting antenna systems. Osuka and co-workers have been synthesized **meso-meso/ β - β** linked, linear **dimeric**, trimeric, **tetrameric**, pentameric, hexameric, nonameric and **12-meric** porphyrin **arrays**.⁴⁹⁻⁶⁶ Mutual electronic and excitonic interactions between the individual porphyrin units has been demonstrated in these arrays. The Soret bands of the arrays have observed to be split depending upon the number of porphyrins in a given array and this has been explained in terms of the exciton coupling theory. In addition, absorption bands become increasingly red-shifted and intensified upon increasing the number of porphyrins, reaching to the infrared frequency range. The completely fused **12-meric** array 1 has

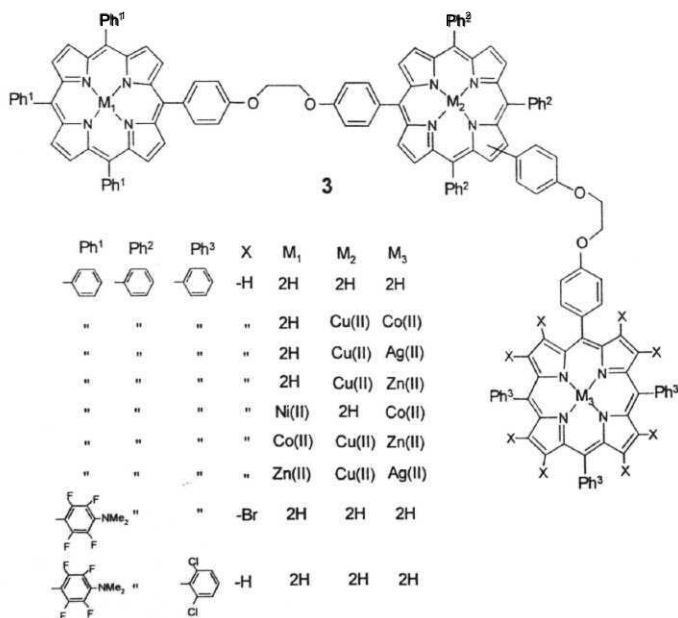


planar, tape-shaped structure and it displays extremely red-shifted absorption bands, reflecting the extensively conjugated electronic system. With an increase in the number of porphyrins in this series of arrays, the fluorescence spectra also become broader and red-shifted without significant decrease in the fluorescence quantum yield, reflecting their stretched conformations that do not allow the formation of a singlet-excitation-energy trapping site. The same group has also reported 1,4-phenylene-linked zinc(II) porphyrin oligomers and demonstrated excitonic interactions between the porphyrin units.^{67,68} While similar **meso-meso** linked porphyrin trimers have been reported by Segawa and co-workers,⁶⁹ acetylenyl bridged porphyrin arrays have been reported by Therien and co-workers.⁷⁰⁻⁷⁶ In the latter arrays, efficient electronic interactions between the porphyrinic subunits has been demonstrated by the application of fluorescence and absorption spectroscopies and also by electrochemistry.

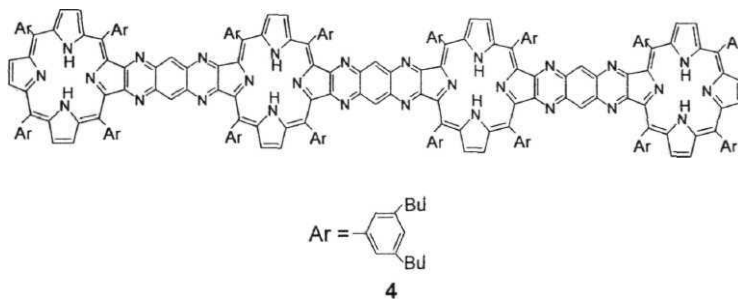
Burrell *et al.* have synthesized linear trimers **2** *via* aldehyde appended porphyrin subunits.⁷⁷ The utility of aldehyde appended porphyrin unit as a building block for construction of larger linear arrays has also been demonstrated.⁷⁸



Krishnan and Sen have reported novel hybrid porphyrin trimers **3** in which the monomers bear different metal centers **and/or** different peripheral substituents.⁷⁹ The Q and B bands in the UV-visible spectra of these trimers are red-shifted and broadened in comparison with those of the corresponding monomers. It has been reported that fluorescence of the distal free-base porphyrin is quenched by the non-fluorescent octabromoporphyrin due to spin-orbit coupling or other non-radiative deactivation mechanisms.



Crossley and co-workers⁴¹⁻⁴⁵ have synthesized linear and bent porphyrin arrays by fusing individual porphyrin units through rigid aromatic units. Compound 4 is an illustrative example. Crossley and co-workers have also discussed relationship between the inter-ring coupling responsible for electron or hole conduction and oligomer size in this class of arrays. The advantage of this system is that it is completely rigid, spans large distances and possesses a sizable, switchable electronic coupling between its ends.



The first quinone substituted **trimer** was synthesized by Sessler and co-workers.^{80,81} Porphyrin \rightarrow quinone electron transfer in this system is over a distance comparable to that found in the natural photosynthetic reaction centers and has been shown to be efficient enough to use this system as a model for studying long range electron transfer mechanisms. In an analogous study, Osuka

et al. have reported tetrads consisting of 1,2-phenylene-bridged zinc(II) diporphyrin, zinc(II) porphyrin, pyromellitimide and quinone subunits.⁸²

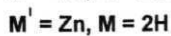
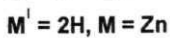
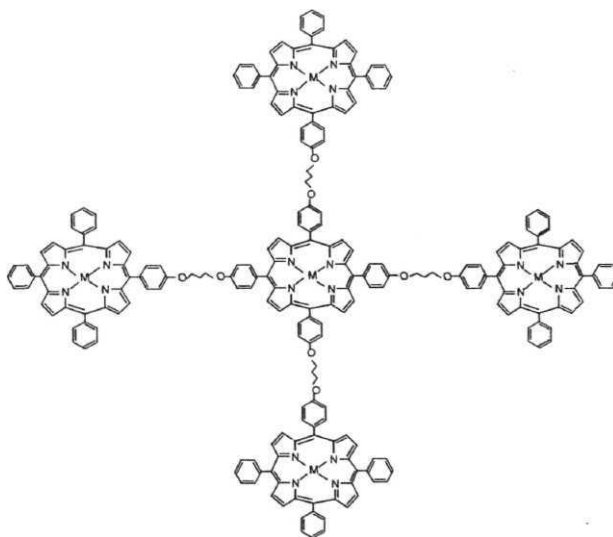
1. 3. 2 Covalently linked branched chain oligomeric porphyrin arrays

Based on the architecture of antenna chlorophyll systems, porphyrin oligomers have been fashioned to generate the so-called "light-harvesting arrays". A number of conformationally restricted porphyrins such as face-to-face porphyrins, stacked porphyrins and other rigidly linked systems have been studied.^{83,92} These are mostly **dimeric** systems and will not be discussed here.

Yeow *et al.* have reported a series of first, third and fifth generation dendrimers consisting of 4, 16 and 64 porphyrin **chromophores**, respectively. In these dendrimers, they have observed depolarization of the fluorescence as compared to the monoporphyrin model compound, indicating that electronic energy transfer takes place between the chromophores within the dendrimers. Aida and co-workers have reported a series of first, second and third generation zinc(II) porphyrin dendrimers having a free-base porphyrin core.^{94,95} By the application of pico- and **femto**- second time-resolved fluorescence spectroscopic techniques, they have demonstrated that the quenching of zinc(II) porphyrin fluorescence increases as the **dendrimer** generation increases.

Pentameric porphyrins comprising a central porphyrin that is covalently linked to four others are among the interesting examples of the branched chain oligomeric arrays. These species were designed to serve as light harvesting

models and for use in potential photovoltaic cells. The ether-bridged pentameric arrays **5** were first reported by **Milgrom**.⁹⁶ Harriman and co-workers have demonstrated an efficient Forster-type EET from the antenna zinc(II) porphyrins to the central free-base porphyrin in these systems.⁹⁷

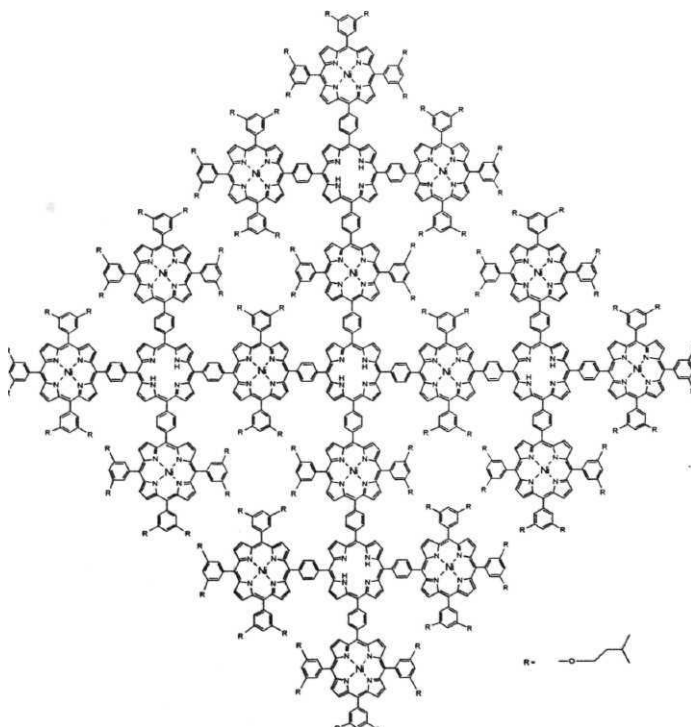


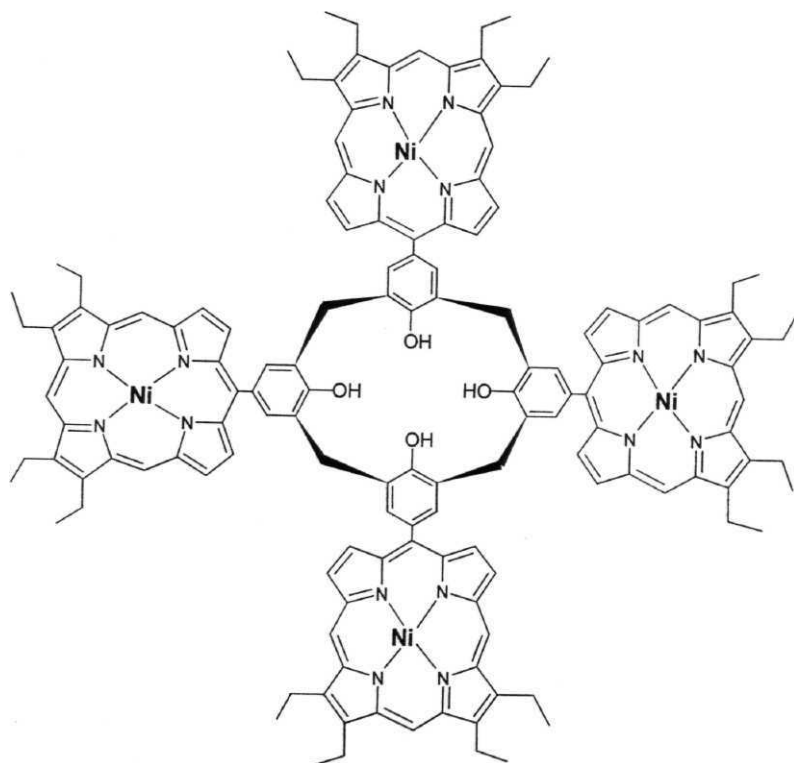
Wennerstrom *et al.* have further modified the architecture of 5 and designed a rigid **pentamer** incorporating the phenyl bridges.⁹⁸ Similarly, with a view to increase the conjugation between the **porphyrin** subunits, a diarylethyne bridged **pentameric** array was synthesized." This array has been tailored in such a way that the centre-to-centre inter-porphyrin distances are $\sim 20 \text{ \AA}$, making the porphyrin units close enough for rapid energy transfer but far enough to preclude any competing electron transfer quenching reactions. Detailed spectral and electrochemical studies have been carried out on the zinc(II) and free-base derivatives of this system.¹⁰⁰

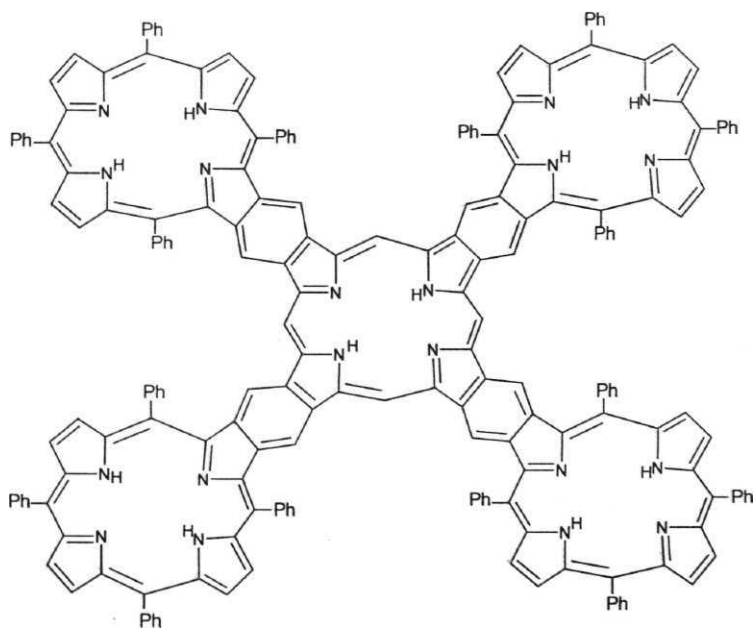
Sakata and co-workers have reported an **aryl** linked henicosamer porphyrin array 6 which they termed as a "*mandala-patterened bandanna*" porphyrin.¹⁰¹ The compound has been characterized by MALDI-TOF and scanning and tunneling microscopic techniques. Smith and co-workers have reported the porphyrin array 7 consisting of four porphyrins that are fused at the lower rim of the calix[4]arene unit.¹⁰² This array possesses strong ion binding properties, potentially leading to a class of new molecular receptors for the development of efficient sensors. The same group has further reported a P-pyrrole linked cruciform pentamer 8.¹⁰³

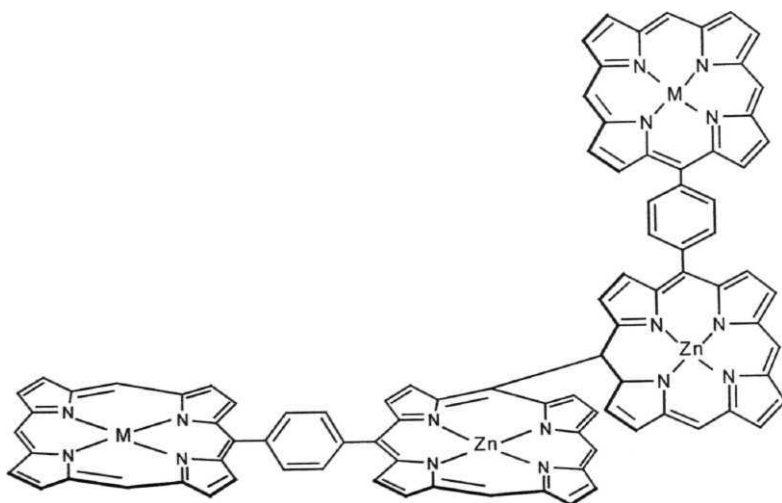
Osuka and co-workers have reported several meso-meso linked 'windmill and grid like' porphyrin arrays having potential application as light harvesting antenna complexes.¹⁰⁴ Array 9 is an illustrative example. In the UV-visible spectra of these arrays, the Soret band gets split due to exciton

interaction between the individual porphyrin units. Steady state fluorescence spectra of these arrays show dual emission emanating from the peripheral porphyrin rings and the diporphyrin core. The reduced fluorescence intensity of peripheral porphyrin rings suggested a s-s energy transfer to diporphyrin core.







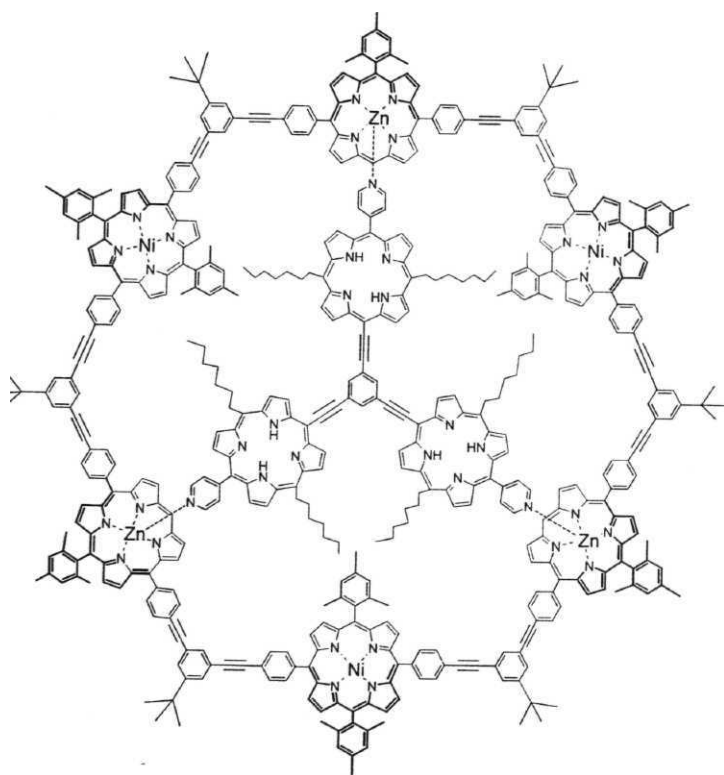


9a: M = Zn

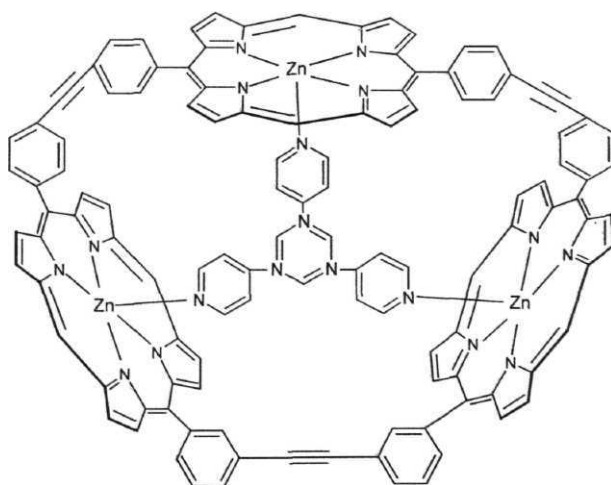
9b: M = Ni

The same group has recently reported 126-mer, 512-mer, 768-mer and 1024-mer porphyrin arrays *via* Ag^I-promoted oxidative coupling reaction.¹⁰⁵ A cyclic hexamer 10 consisting of three zinc(II) porphyrins which can accommodate a star shaped guest (a trimeric free-base porphyrin) inside its cavity has been reported by Gossuer and co-workers¹⁰⁶⁻¹⁰⁸ Singlet excited state energy transfer from the zinc(II) chelates to free-base porphyrins has been observed in these arrays and an overall intramolecular energy transfer efficiency was estimated to be 98%. Ambroise *et al.* have reported a light harvesting array of seven porphyrins in a 'wheel and spoke' architecture.¹⁰⁹ Here, a shape-persistent cyclic array of six zinc(II) porphyrins provides an effective host for a dipyridyl-substituted free-base porphyrin, yielding a self-assembled structure. Energy transfer occurs quantitatively from the uncoordinated to the pyridyl-coordinated zinc(II) porphyrins in this cyclic array. On the other hand, EET from the coordinated zinc(II) porphyrin to the guest free-base porphyrin is less efficient and is attributed to a Forster process.

Cyclic porphyrin oligomers have been synthesized in efforts to mimic gross structure of the photosynthetic reaction center and enzymatic catalysis.¹¹⁰⁻¹²² In their efforts to mimic bacterial photosynthetic reaction center, Dubowchik and Hamilton have reported cyclic tetrameric and hexameric entities.¹¹⁰⁻¹¹² During their studies on supramolecular catalysis using macrocyclic systems, Sanders and co-workers have developed an 'extended conjugation' approach



to synthesize various **oligomeric porphyrins**.¹¹⁰⁻¹²² Specifically, in an effort to create a system in which convergent binding sites are positioned in such a way that substrate molecules can be held in close proximity, they have synthesized a cyclic porphyrin system 11. More recently, they have also reported porphyrin dendrimers using a similar synthetic strategy.¹²²



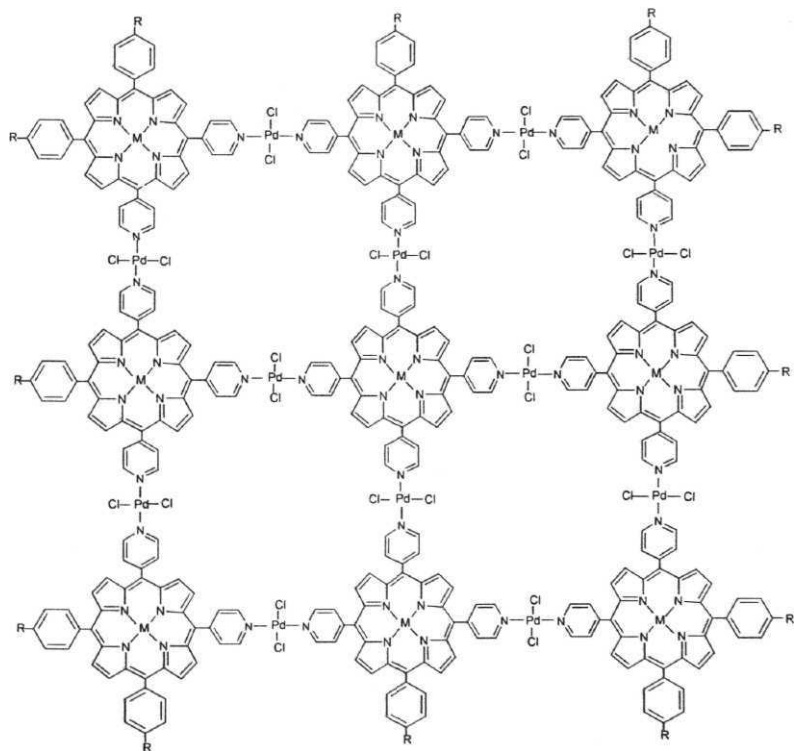
11

1. 3. 3 Porphyrin oligomers linked by metal coordination

In recent years, ordered **supramolecular** arrays formed by self-assembly of porphyrin units *via* metal (metalloid) ion coordination are being investigated with views to design molecular optical/electronic devices and model biological energy or charge transfer **reactions**.^{123, 124}

For example, a diethynyl-linked zinc(II) porphyrin **dimer** which forms a self-assembled "ladder" by coordinate-covalent linkage between 1,4-diazabicyclo [2.2.2] octane (DABCO) and the central zinc(II) ions has been reported.⁴⁰ The ladder formation has been established by NMR and UV-visible methods. It has been suggested that similar polymeric ladders would be good candidates as a low-band-gap materials. Drain and Lehn have utilized the pyridine nitrogen coordination of cis- and trans- substituted **meso-dipyridyl** porphyrins with cis or trans- substituted palladium(II) or platinum(II) ions to construct arrays which are characterized by the 'square' architecture.¹²⁵ Drain *et al.* have further reported **nonamer** 12 that is constructed by the coordination of porphyrin exocyclic pyridyl groups to palladium(II) dichloride **units**.¹²⁶ Recently, Slone and Hupp have constructed a cyclic porphyrin tetramer with the help of coordination at the rhenium(I) **site**.¹²⁷

Ordered supramolecular arrays have also been synthesized by connecting metalloporphyrins to other porphyrin subunits *via* pyridine bridges, further illustrating the utility of coordinate-covalent bond formation reaction in



M = 2H or Zn

12a: R = methyl

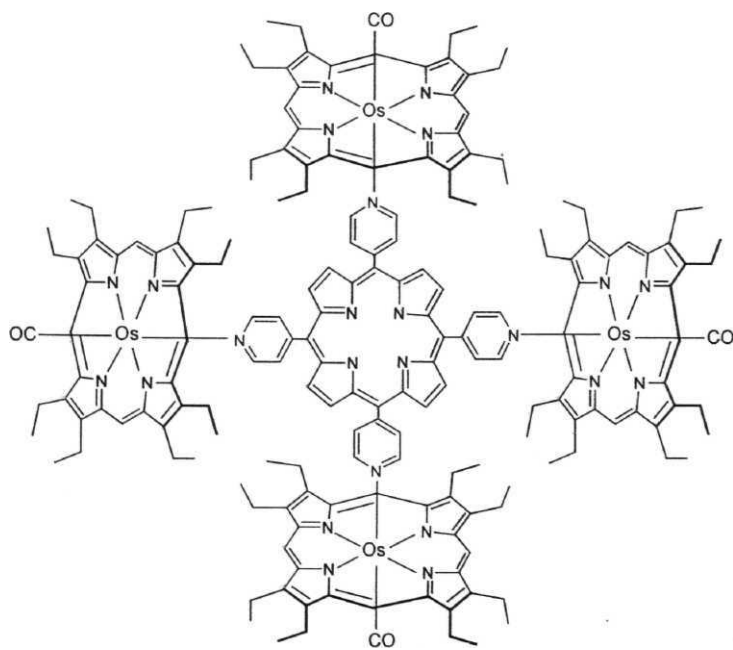
12b: R = *tert*-butyl

porphyrin array building **process**.¹²⁸⁻¹³⁵ Imamura and co-workers have synthesized pentamer 13 consisting of four osmium(II) porphyrins linked non-covalently to a central **tetrapyrrolyl** porphyrin.¹³¹ They have also reported ruthenium(II) porphyrin-based **dimeric**, **trimeric** and **tetrameric** arrays.^{133,134}

Solid-state multichromophoric assemblies have an advantage over solution species because, with a suitable design strategy, one could interlink an unlimited number of metallo- and metal-free porphyrins, either through hydrogen bonding or coordination bonds, into rigid and highly organized **supramolecular arrays**.¹³⁶⁻¹³⁹ By utilizing the exterior **functionality** of **metallated** tetraaryl porphyrins, Robson and co-workers have synthesized, novel 3D and large open channel **networks**.¹³⁷⁻¹³⁸ Sharma *et al.* have also reported similar multichromophoric supramolecular **arrays**.¹³⁹

Wojaczynski and Latoz-Grazynski have reported novel porphyrin **trimers** formed by a "head-to-tail" arrangement of the monomeric **subunits**.¹⁴⁰⁻¹⁴² For example, **oligomerization** of an iron(III) porphyrin, by axial linkage of the central iron atom of one porphyrin to the p-position of another, yielded a "cyclic" **trimer**.¹⁴⁰ Similar structures have been architected using gallium(III) and manganese(III) as the metal **centers**.^{141, 142}

Self-assembly of oligomers in solution has been reported by Hunter and co-workers wherein coordination of zinc(II) or cobalt(II) porphyrins by pyridine ligands is used to construct oligomeric assemblies. • In an analogous



approach, Sanders and McCallien have utilized **5,15-dioxoporphyrins** as supramolecular building blocks to synthesize a **pentameric** assembly. Here, four zinc (II) dioxoporphyrin molecules are linked to a central tetrapyridyl porphyrin by **zinc-pyridyl** bonding.

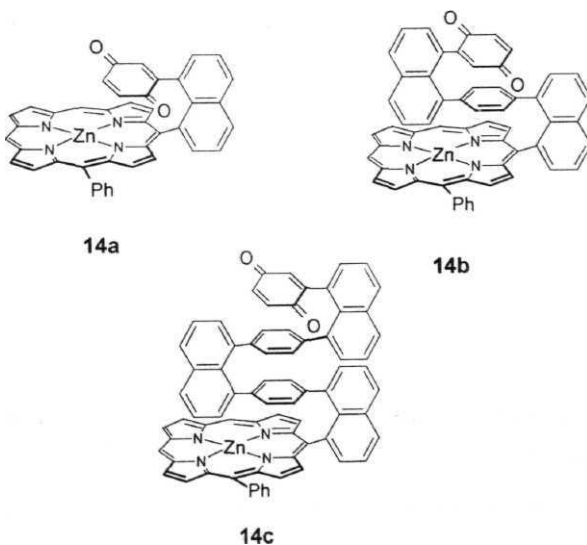
1. 4 Porphyrin-based **covalent and non-covalent D-A** systems

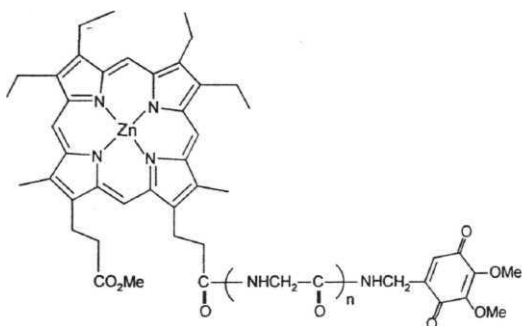
Porphyrins having peripheral (i.e., β -pyrrole or *meso*-positions) and/or axial substituents have been extensively investigated over the last few decades. Porphyrins substituted with donor or acceptor groups at these sites are of interest to the present study.

1. 4. 1 D-A systems involving covalent linkage at the porphyrin peripheral position/s

Earlier reports on EET and PET reactions of porphyrin-based D-A systems are abound with studies on covalently linked complexes and these have been reviewed in many recent **accounts**.^{1,2,5,24-38} Kong and Loach have synthesized the ester-linked porphyrin-quinone (P-Q) dyad in 1978 and the corresponding amide linked dyad was reported in 1979 by Tabushi and co-workers.¹⁴⁹ These latter systems were subsequently investigated for their photophysical properties by Ho *et al.*¹⁵⁰ Since then, a number of porphyrin-based D-A systems have been synthesized and their photophysical properties studied in detail. Discussion on a few recent examples follow.

Therein and co-workers have reported distance dependence of electron transfer in a rigid, cofacially compressed, π -stacked porphyrin-bridge-quinone systems **14**.¹⁵¹ Photoinduced charge separation and thermal charge recombination reactions of **14** were investigated by pump-probe transient absorption spectroscopy. Hayashi *et al.* have reported the D-A system **15** in which a quinone is connected through peptide bonds to the one of the propionate side chain of the porphyrin.¹⁵² Both steady state fluorescence and transient spectroscopic measurements have suggested that an intramolecular





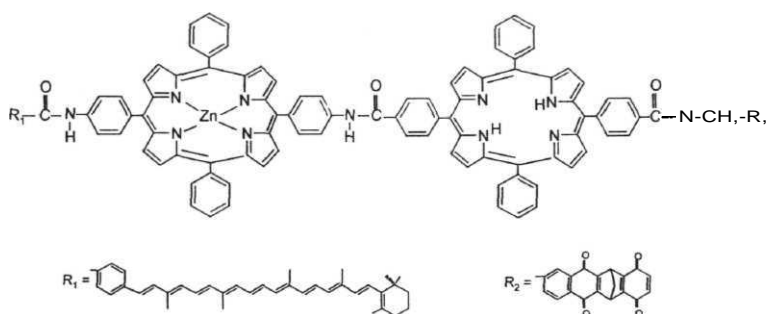
15a: n = 0

15b: n = 1

15c: n = 2

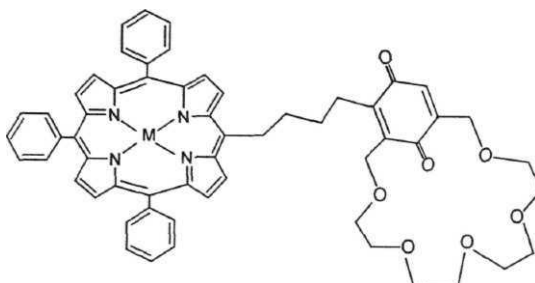
electron transfer from photoexcited zinc(II) porphyrin to the covalently linked quinone takes place in the system. Gust, Moore and their co-workers have reported triads, tetrads and pentads based on carotene, porphyrin and quinone **subunits**.^{153,154} One example is the pentad system 16, which consists of two covalently linked porphyrin moieties: one containing a zinc(II) ion (**P_{Zn}**) and other present as the free-base (**P**). The **metallated** porphyrin bears a carotenoid (**C**) polyene and other a diquinone species (**Q_A-Q_B**).¹⁵³ The carotenoid absorbs light in spectral regions where the porphyrin does not absorb strongly and transfers singlet excitation energy to the porphyrin. Excitation of the free-base porphyrin of the pentad yields an initial charge separated state, **C-P_{Zn}-P⁺-Q_A-**

QB, and subsequent electron transfer steps lead to a final charge separated state $C-P_{Zn}-P^+-Q_A-Q_B$ with an overall quantum yield of 0.83.



16

Porphyrins substituted with multiple crown ether voids have been investigated in great detail.¹⁵⁴⁻¹⁶⁰ A recent study has investigated a porphyrin substituted with a redox active crown ether (17) as a biomimetic model.¹⁶⁰ Folding of the **crown-ether-quinone** moiety towards the porphyrin and 'intramolecular' PET has been demonstrated in this system at the room temperature. At low temperatures, however, PET has been shown to be absent.



17a: M = 2H

17b: M = Zn

In an attempt to mimic photosynthetic energy transfer reactions and to develop molecular devices, porphyrin systems, as energy acceptors, have been covalently linked to carotenoid, cyanine dye and anthracene donor subunits to generate molecular dyads.^{5, 161} Lindsey *et al.* have synthesized a series of porphyrin-cyanine dye dyads to mimic the phycobilisome action of photosynthesis.¹⁶¹

1. 4. 2 D-A systems involving non-covalent interactions at the porphyrin peripheral position/s

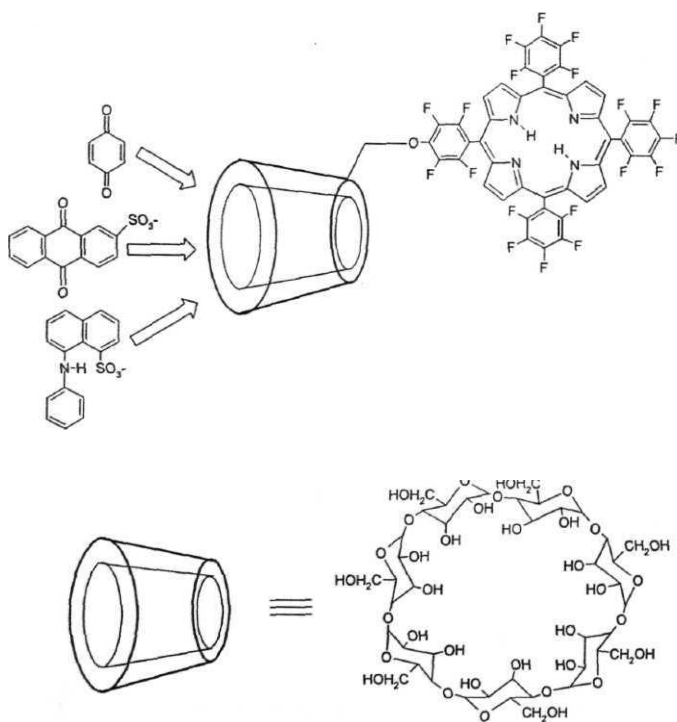
D-A systems bound by non-covalent interactions can be expected to provide a better understanding of the biological energy/electron transfer processes as, in

natural systems these processes proceed through complex non-covalently bound protein pathways. This consideration has led to the construction of porphyrin-based D-A systems that are characterized by either coordinative, H-bonding or nucleic acid base-pairing interaction between the donor and the **acceptor**.^{37, 38, 162-179}

D'Souza *et al.* reported that free-base and zinc(II) porphyrins bearing either one, two or four hydroquinone entities at the **meso** positions can bind quinones in solutions *via* a quinhydrone pairing **mechanism**.¹⁸⁰⁻¹⁸² Electrochemical and ¹H NMR studies carried out on these systems have revealed that the quinhydrone complexes are stabilized by H-bonding in addition to the charge transfer interactions. Singlet emission studies have shown that fluorescence quenching of the porphyrin increases with an increase in the number of receptors. This indicates that the H-bonding plays an important role in the quinhydrone formation. Recently, Branda and co-workers have reported a photocontrolled PET process between an urea porphyrin and the cis and trans isomers of a carboxylate substituted phenoxynaphthacequinone that is bound to the urea porphyrin *via* hydrogen **bonding**.¹⁸³ Cyclic voltammetric and steady state fluorescence emission studies have revealed that PET is more favored in the cis **isomer** rather than the trans **isomer**.

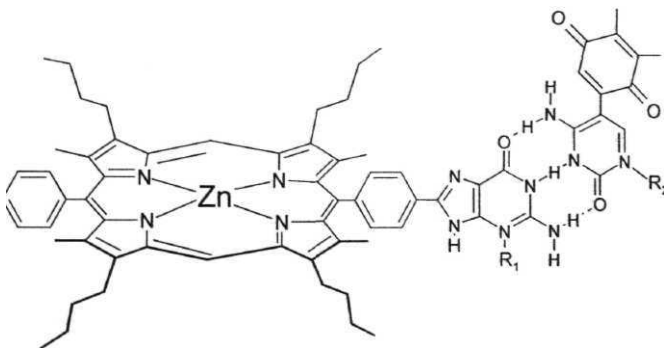
Lang *et al.* have reported a new porphyrin-cyclodextrin conjugate **18**.¹⁸⁴ This conjugate shows a marked tendency to form chiral assemblies in aqueous

solutions. The key role of cyclodextrin in the formation of a porphyrin-based supramolecular complex is confirmed by steady state and time-resolved fluorescence spectroscopies. Fluorescence intensity of the conjugate is



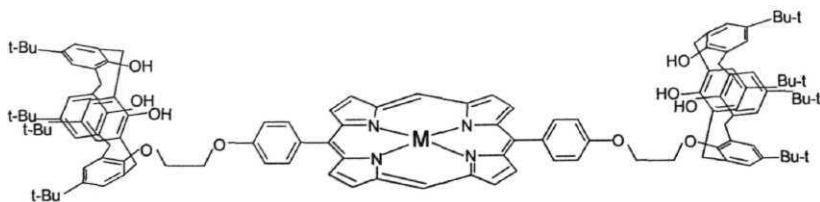
quenched by the addition of 1,4-benzoquinone, anthraquinone-2-sulfonate or 8-anilino-1-naphthalene sulfonic acid guests. All these quenchers form inclusion complexes within the porphyrin-bound cyclodextrin in aqueous media. The quenching of fluorescence has been interpreted in terms of a PET between the singlet porphyrin and the quinone guests within the conjugate (monomer or aggregate).

Sessler and co-workers have presented another approach to design non-covalently linked porphyrin-quinone systems typified by structure 19. As seen, the porphyrin and quinone subunits bear guanosine and cytidine substituents respectively, as the recognition sites to form Watson - Crick hydrogen-bonded pair.¹⁷⁹ Upon addition of increasing concentration of quinone to zinc(II)



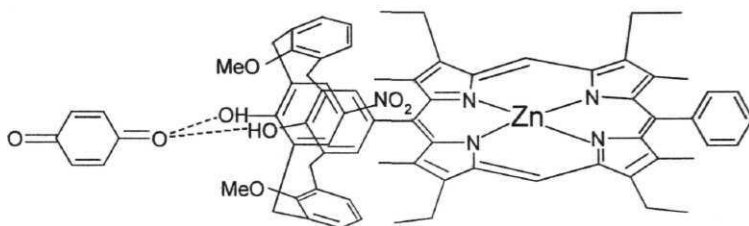
porphyrin, quenching of fluorescence due to the zinc(II) porphyrin was observed in the steady state and time-resolved fluorescence experiments. These results indicate a PET between the singlet porphyrin to the quinone.

In a seminal work, Weiss and co-workers have reported a porphyrin-calix[4]arene conjugate, 20, in which a porphyrin is covalently linked to two calixarene[4]arene units which serve as the binding sites for the quinone *via n-n* stacking inside their **cavities**.¹⁸⁵ Upon increasing addition of quinone to the conjugate, quenching of fluorescence was observed due to an 'intra-complex' PET from singlet state of the porphyrin to the encapsulated quinone. Sessler, Arimura and their co-workers have reported calixarene- porphyrin systems 21 and 22, in which a quinone acceptor can bind to the calixarene *via* supramolecular contacts. Fluorescence studies reveal the occurrence of an 'intra-complex' PET from singlet porphyrin to the **calixarene-bound** quinone.^{186, 187}

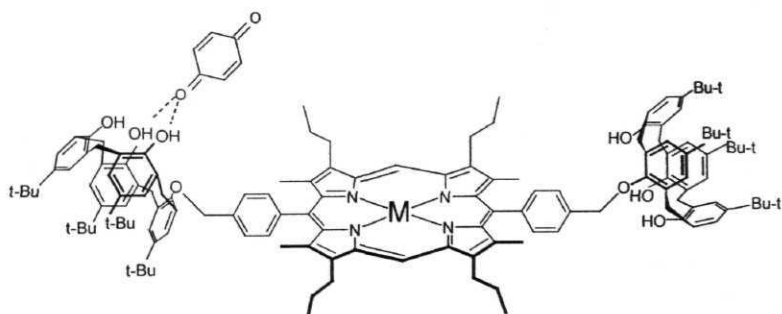


M = 2H, Zn

20



21



M = 2H, Zn

22

1. 4. 2 D-A systems assembled *via* axial coordination of metallo/metalloid porphyrins

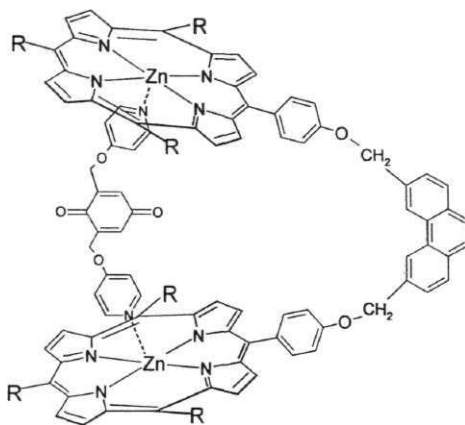
Although synthesis and spectral studies of porphyrins containing almost every element of the periodic table are now well known, reports dealing with investigations on PET and EET reactions between metallo/metalloid porphyrin excited states and the axially ligated electron donors or acceptors are scarce. This contrasts the innumerable studies carried out on the PET and EET reactions of metallo/metalloid porphyrins linked, at their peripheral positions, with donor/acceptor subunits. A few important examples among the recently reported D-A systems involving axial substitution of porphyrins are discussed below.

Hoshino *et al.* have studied ligand assisted PET from metalloporphyrins to 'methyl(mono) viologen'.¹⁸⁸ Detailed electrochemical and photochemical investigations have been carried on σ -bonded indium(III), gallium(III) and tin(IV) porphyrins by Kadish and co-workers.¹⁸⁹ Generation of 'zwitterionic' species has been noticed upon laser flash excitation of these systems. While Segawa *et al.* have reported axially substituted dialkoxo phosphorus(V) porphyrin derivatives,¹⁹⁰ Rao and Maiya have reported aryloxo derivatives of phosphorus(V) porphyrin based trimers and D-A systems.^{191,192} Steady state fluorescence data of the latter systems has been interpreted in terms of a PET reaction from the axial aryloxo 'donor' ligands to the singlet phosphorus(V) porphyrin.

Recently Reddy and Maiya have reported a series of ‘axial-bonding’ type phosphorus(V)porphyrin-azoarene **conjugates**.^{193,194} Here, they have demonstrated that the cis-trans isomerization of the axial azoarene subunits leads to fluorescence 'on-off' switches of the basal phosphorus(V) porphyrin *via* a PET mechanism. Shimidzu and co-workers have reported a series of "wheel and axle" type phosphorus (V) porphyrin arrays in which porphyrin units are linked to each other *via* the central phosphorus **atoms**.¹⁹⁵⁻¹⁹⁹ The excited state properties of a few compounds in this series of oligomers have been investigated. **Electrochemically** synthesized D-A polymers, which contain axial oligothiophene and basal phosphorus (V) porphyrin subunits have also been reported.¹⁹⁹

Hunter and Shannon have reported an intramolecular PET in a **supramolecular** D-A complex **23**.²⁰⁰ Here, the quencher quinone is held within the macrocyclic receptor by a combination of hydrogen bonding to the amide protons and *n* - *n* stacking with the phenyl rings in the cyclic frame work. The whole quencher-receptor assembly was then attached to the axial position of a zinc(II) porphyrin **chromophore** *via* coordination of the peripheral pyridyl group of the macrocyclic receptor. In an elegant study, Sakata *et al.* have investigated a dipyrityl-quinone bound zinc(II) porphyrin dimer **24**.^{201,202} UV-visible studies revealed formation of a 1:1 complex between the host (diporphyrin) and the guest (quinone) molecules. Intramolecular PET from singlet state of the

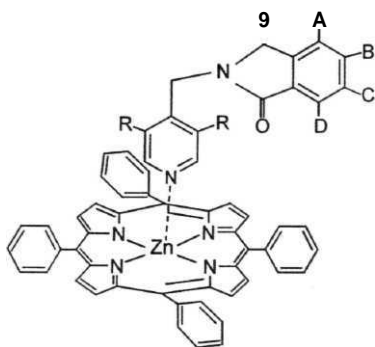
Otsuki *et al.* have reported the energy gap dependence of the rate of electron transfer in supramolecular D-A assemblies of the type 25.²⁰³ Complexation of pyridine nitrogen with the zinc (II) center was confirmed by



24

UV-visible and NMR spectroscopic methods. Fluorescence from singlet state of zinc(II)porphyrin is quenched in the complex due to electron transfer to the **imide** acceptor. The extent of fluorescence quenching of the zinc(II) porphyrin depends on the reduction potential of the acceptor molecule.

Recently **Flamigni *et al.*** have reported the self assembly of a bis-zinc(II) porphyrin host and a bis(pyridyl)naphthalenediimide / bis(pyridyl)phenyldiimide guest.^{204,205} **Complexation** between the guest and the host was investigated by UV-visible and ¹H NMR spectroscopic methods. Steady state and time-

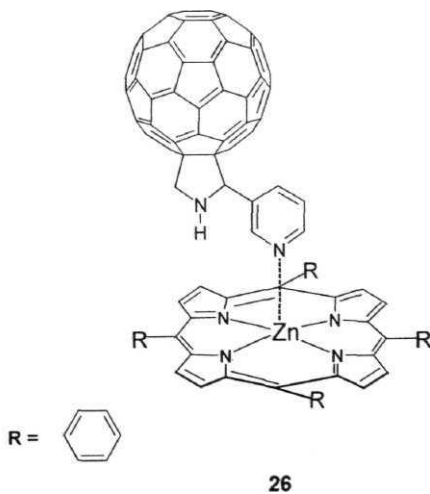


25

	R	A	B	C	D
25a	H	H	(CO) ₂ N	C ₆ H ₁₃	H
25b	OEt	H	H	H	H
25c	OEt	F	H	F	H
25d	OEt	F	F	F	F
25e	OEt	NO ₂	H	H	H
25f	OEt	H	NO ₂	H	H
25g	OEt	H	(CO) ₂ N	C ₆ H ₁₃	H

resolved emission and also transient absorption spectroscopic studies revealed that quenching of porphyrin fluorescence is due to a PET from singlet porphyrin host to **diimide** guest.

D'Souza's group and also a few others have reported porphyrin-fullerene D-A systems.²⁰⁶⁻²¹⁸ Dyad 26, in which a pyridine appended fullerene is axially ligated to the zinc(II) porphyrin through coordinative interaction, is an



illustrative example. **UV-visible** and ^1H NMR spectral studies have revealed a 1:1 complex formation between the pyridine-fullerene and zinc(II) porphyrin.

Singlet emission studies have showed efficient fluorescence quenching due to the occurrence of a PET from the excited zinc(II) porphyrin to the axially positioned fullerene.

1. 5 Summary

The basic principles involved in electron- and energy transfer reactions occurring in porphyrin-based arrays and D-A systems, as applicable to the subject matter of the present thesis, are presented in this chapter.

This thesis has been divided into seven chapters.

Chapter 1 gives a general introduction to the basic principles involved in electron- and energy transfer reactions. It also includes a survey of the recent literature on oligomeric porphyrins and various peripherally- and axially substituted, porphyrin-based D-A systems highlighting their PET and EET reactions.

Chapter 2 presents a list of chemicals, a general description of the synthetic procedures and details of the spectroscopic, electrochemical and magnetic resonance techniques employed during the research work.

Chapter 3 presents the results of spectroscopic, electrochemical and photochemical studies carried out with a new, monomeric tin (IV) porphyrin based array.

Chapter 4 is concerned with the design, synthesis, characterization and photochemistry of a self-assembled trimeric array consisting of a central tin(IV) porphyrin and two axial ruthenium(II) porphyrins.

Chapter 5 discusses the design, synthesis and spectroscopy as well as PET reactions of a self-assembled D-A dyad consisting of a zinc(II) porphyrin donor and a pyridine appended calix[4]diquinone acceptor.

Chapter 6 deals with PET reactions occurring in a series of isomeric porphyrin-calix[4]arene conjugates that are bound to quinone acceptors.

Chapter 7 presents general conclusions based on the results obtained during this research work.

References

1. *Photoinduced Electron Transfer*, Parts A-D; For, M. A.; Chanon, M.; Eds.; Elsevier: Amsterdam, 1988.

2. *Photoinduced Electron Transfer* A series in *Topics in Current Chemistry* Mattay, J.; Ed.; **Springer-verlag**: New York, 1991.
3. Marcus, R. A.; Sutin, N. *Biochim. Biophys. Acta* **1985**, *811*, 262.
4. *Photosynthesis*; **Amesz, J.**; Ed.; Elsevier: Amsterdam, 1987.
5. Gust, D.; Moore, T. A.; Moore, A. L. *Acc. Chem. Res.* **1993**, *26*, **198**.
6. Guillet, J. E. in *Polymer Photophysics and Photochemistry*; Cambridge University Press: Cambridge, 1985.
7. Bloor, D. *Physica Scripta.* **1991**, *39*, 380.
8. Pope, M. *Mol. Cryst. Liq. Cryst.* **1993**, *228*, 1.
9. Marcus, R. A. *J. Chem. Phys.* **1956**, *24*, **966**.
10. Marcus, R. A. *J. Chem. Phys.* **1965**, *43*, 679.
11. Marcus, R. A. in *Light Induced Charge Separation in Biology and Chemistry*; Gerischer, H.; Katz, J. J., Eds.; Verlag **Chemie**: Berlin, 1979, p 15.
12. Marcus, R. A. *Angew. Chem. Int. Ed. Engl.* **1993**, *32*, 1111 (and references therein).
13. Forster, Th. *Discuss. Faraday Soc.* **1959**, *27*, 7.
14. Dexter, D. L. *J. Chem. Phys.* **1953**, *21*, 836.
15. Deisenhofer, J.; Epp, O.; Mikki, K.; Huber, R.; Michel, H. *J. Mol. Biol.* **1984**, *180*, 385.
16. Deisenhofer, J.; Epp, O.; Mikki, K.; Huber, R.; Michel, H. *Nature*, **1985**, *318*, 618.

17. Chang, C. H.; Tiede, D.; Tang, J.; Smith, U.; **Norris, J.; Schiffer, M.** *FEBS Lett.* **1986**, 205, 82.
18. **Allen, J. P.**; Feher, G.; Yeates, T. O.; **Rees, D. C.**; Deisenhofer, J.; Michel, H.; Huber, R. *Proc. Natl. Acad. Sci. USA* **1986**, 83, 8589.
19. **Allen, J. P.**; Feher, G.; Yeates, T. O.; **Komiy, H.**; **Rees, D. C.**; *Proc. Natl. Acad. Sci. USA* 1987, 84, 5730.
20. Yeates, T. O.; **Komiy, H.**; Chirino, A.; **Rees, D. C.**; **Allen, J. P.**; Feher, G. *Proc. Natl. Acad. Sci. USA* **1988**, 85, 7993.
21. El-Kabbani, O.; Chang, C. H.; Tiede, D. M.; **Norris, J.**; **Schiffer, M.** *Biochemistry* **1991**, 30, 5361.
22. **Ermler, U.**; Fritzsche, G.; Buschanan, S. K.; Michel, H. *Structure* **1994**, 2, 925.
23. Deisenhofer, J.; Epp, O.; Sinning, I.; Michel, H. *J. Mol. Biol.* **1995**, 246, 429.
24. Connolly, J. S. In *Photochemical Conversion and Storage of Solar Energy*; Rabani, J., Ed.; The **Weizman** Science Press : Jerusalem, 1982, Part A, p. 175.
25. *Photochemistry of Polypyridine and Porphyrin Complexes*; Kalyanasundaram, K.; Academic Press : London, **1992**.
26. Harriman, A. in *Supramolecular Photochemistry*; Balzani, V.; Reidel, D.; Boston, 1987, p.207.

27. Wasielewski, M. R. In *Photoinduced Electron Transfer*, Part D, Fox, M. A.; Channon, M.; Eds.; Elsevier : Amsterdam, 1988, Chapter 1.4.
28. Gust, D.; Moore, T. A. *Science* **1989**, 244, 35.
29. *The Porphyrins*, Dolphin, D.; Ed.; Academic Press: New York, 1979, Vols. 1-7
30. Gust, D.; Moore, T. A. *Top. Curr. Chem.* **1991**, 159, 103.
31. Wasielewski, M. R. *Chem. Rev.* **1992**, 92, 435.
32. Fox, M. A. *Photochem. Photobiol.* **1990**, 52, 617.
33. Kurreck, H.; Huber, M. *Angew. Chem. Int. Ed. Engl.* 1995, 34, 849.
34. Morgan, B.; Dolphin, D. *Structure and Bonding* **1987**, 64, 115.
35. Baldwin, J. E.; Perlmutter, P. *Top. Curr. Chem.* **1984**, 121, 181.
36. Pullerits, T.; Sundstrom, V. *Acc. Chem. Res.* **1996**, 29, 381.
37. Hayashi, TV, Ogoshi, H. *Chem. Soc. Rev.* **1997**, 26, 355.
38. Ward, M. D. *Chem. Soc. Rev.* **1997**, 26, 365.
39. Yamamoto, M.; Ito, S.; Ohmori, S. In *Photochemical Processes in Organized Molecular Systems*; Honda, K.; Ed: Amsterdam, 1991; p 329
40. Anderson, H. L. *Inorg. Chem.* **1994**, 33, 972.
41. Crossley, M. J.; Burn, P. L. *Chem. Commun.* **1987**, 39.
42. Crossley, M. J.; Burn, P. L. *Chem. Commun.* **1991**, 1569.
43. Crossley, M. J.; Govenlock, L. J.; Prashar, J. *Chem. Commun.* **1995**, 2379.
44. Crossley, M. J.; Burn, P. L.; Langford, S. J.; Prashar, J. K. *Chem. Commun.* 1995, 1921.

45. Reimers, J. R.; Lu, T. X.; Crossley, M. J.; Hush, N. S. *Chem. Phys. Lett.* **1996**, 256, 353.
46. Kong, J.; Loach, P. A. In *Frontiers of Biological Energetics: From Electrons to Tissues* Dutton, P. L.; Scarpa, S. Eds.; Academic : New York, 1987; Vol.1, p.73.
47. Anton, J. A.; Kong, J. A.; Loach, P. A. *J. Heterocycl. Chem.* **1976**, 13, 717.
48. Boxer, S. G.; Bucks, R. R. *J. Am. Chem. Soc.* **1979**, 101, 1883.
49. Aratani, N.; Cho, H.Y.; Ahn, T. K.; Cho, S.; Kim, D.; Sumi, H.; Osuka, A. *J. Am. Chem. Soc.* **2003**, 125, 9668.
50. Tsuda, A.; Nakano, A.; Osuka, A. *Chem. Commun.* **2003**, 1096.
51. Aratani, N.; Osuka, A.; Cho, H.Y.; Kim, D. *J. Photochem. Photobiol., C: Photochem Rev.*, **2002**, 21, 1.
52. Cho, H.Y.; Jeong, D.H.; Cho, H.S.; Kim, D. Matsuzaki, Y.; Tanaka, K.; Tsuda, A.; Osuka, A. *J. Am. Chem. Soc.* **2002**, 124, 14642.
53. Jeong, D. H.; Yoon, M. -C; Jang, S. M.; Kim, D.; Cho, D. W.; Yoshida, N.; Aratani, N.; Osuka, A. *J. Phys. Chem. A* **2002**, 106, 2359.
54. Song, N. W.; Cho, H. S.; Yoon, M.-C; Aratani, N.; Osuka, A.; Kim, D. *Bull. Korean Chem. Soc.* **2002**, 23, 271.
55. Kim, Y. H.; Cho, H. S.; Kim, D.; Kim, S. K.; Yoshida, N.; Osuka, A. *Synth. Metal.* **2001**, 117, 183.
56. Aratani, N.; Osuka, A. *Org. Lett.*, **2001**, 3, 4213.
57. Tsuda, A.; Osuka, A. *Science*, **2001**, 293, 79.

- 58. Tsuda, A.;** Furuta, H.; Osuka, A. *J. Am. Chem. Soc.* **2001**, *123*, 10304.
59. Piet, J. J.; Taylor, P. N.; Wagewijs, B.R.; Anderson, H.L.; Osuka, A.;
Warman, J.M. *J. Phys. Chem. B* **2001**, *105*, 97.
60. Tsuda, A.; Furuta, H.; Osuka, A. *J. Am. Chem. Soc.* **2001**, *123*, 10 304.
61. Tsuda, A.; Nakano, A.; Furuta, H.; Yamochi,; Osuka, A. *Angew. Chem. Int. Ed.* **2000**, *39*, 558.
62. Tsuda, A.; Nakano, A.; Furuta, H.; Yamochi,; Osuka, A. *Angew. Chem. Int. Ed.* **2000**, *39*, 558.
63. Aratani, N.; Osuka, A.; Kim, D.; Kim, Y. H.; Jeong, D. H. *Angew. Chem.* **2000**, *39*, 1458.
64. Nakano, A.; Osuka, A.; Yamazaki, I.; Yamazaki, T.; Nishimura, Y. *Angew. Chem. Int. Ed. Engl.* **1998**, *37*, 3023.
65. Ogawa, T.; Nishimoto, Y.; Yoshida, N.; Ono, N.; Osuka, A. *Chem. Commun.* **1998**, 337.
66. Osuka, A.; Shimidzu, H. *Angew. Chem. Int. Ed. Engl.* **1997**, *36*, 135.
67. Osuka, A.; Maruyama, K. *Chem. Letts.* **1993**, 949.
68. Osuka, A.; Tanabe, N.; Nakajima, S.; Maruyama, K. *J. Chem. Soc, Perkin Trans. 2* **1996**, 199.
69. Susumu, K.; Shimidzu, T.; Tanaka, K.; Segawa, H. *Tetrahedron Lett.* **1996**, 8399.
- 70. Susumu, K.;** Therien, M. *J. Am. Chem. Soc.* **2002**, *124*, 8550.
71. Fletcher, J.; Therien, M. *Inorg. Chem.* **2002**, *41*, 331.

72. Fletcher, J. T.; Therien, M. J. *J. Am. Chem. Soc.* **2000**, *122*, 12393.
73. Shediach, R.; Gray, M. H. B.; Uyeda, H. T.; Johnson, R. C.; Hupp, J. T.; Angiolillo, P. J.; Therien, M. J. *J. Am. Chem. Soc.* **2000**, *122*, 7017.
74. Kumble, R.; Palese, S.; Lin, V. S.-Y.; Therien, M. J.; Hochstrasser, R. M. *J. Am. Chem. Soc.* **1998**, *120*, 11489.
75. Lin, V. S.-Y.; Therien, M. J. *Chem. Eur. J.* **1995**, *1*, 645-651.
76. Lin, V. S.-Y.; DiMagno, S. G.; Therien, M. J. *Science* **1994**, *264*, 1105.
77. Burrell, A. K.; Officer, D. L.; Reid, D. C. W. *Angew. Chem. Int. Ed Engl.* **1995**, *34*, 900.
78. Higuchi, H.; Shimizu, K.; Ojima, J.; sugiura, K.-i.; Sakata, Y. *Tetrahedron Lett.* **1995**, *36*, 5359.
79. Sen, A.; Krishnan, V. *Tetrahedron Lett.* **1998**, *39*, 6539.
80. Sessler, J. L.; Capuano, V. L. *Angew. Chem. Int. Ed. Engl.* **1990**, *29*, 1134.
81. Sessler, J. L.; Capuano, V. L.; Harriman, A. *J. Am. Chem. Soc.* **1993**, *115*, 4618.
82. Osuka, A.; Yamada, H.; Maruyama, K.; Ohno, T.; Nozaki, K.; Okada, T.; Tanaka, Y.; Mataga. *Chem. Lett.* **1995**, 591.
83. Tran-Thi, T. H.; Lipskier, J. R.; Maillard, P.; Momenteau, M.; Lopez-castillo, J. -M.; Jay-gerrin, J. -P. *J. Phys. Chem.* **1992**, *96*, 1073.
84. Wasielewski, M. R.; Niemezyk, M. P.; Svec, W. A. *Tetrahedron Lett.* **1982**, *23*, 3215.
85. Nagata, T.; Osuka, A.; Maruyama, K. *J. Am. Chem. Soc.* **1990**, *112*, 3054.

86. Abdalmuhdi, I.; Chang, C. K. *J. Org. Chem.* **1985**, *50*, 411.
87. Osuka, A.; Ida, K.; Maruyama, K. *Chem. Lett.* **1989**, **741**.
88. Osuka, A.; Nagata, T.; Maruyama, K. *Chem. Lett.* **1991**, 481.
89. Osuka, A.; Nakajima, S.; Maruyama, K.; Mataga, N.; Asahi, T.; Yamazaki, I.; Nishimura, Y.; Ohino, T.; Nozaki, K. *J. Am. Chem. Soc.* **1993**, *115*, 5477.
90. Osuka, A.; Yamada, H.; Maruyama, K.; Ohno, T.; Nozaki, K.; Okada, T.; Tanaka, Y.; Mataga, N. *Chem. Lett.* **1995**, 591.
91. Osuka, T.; Taniguchi, S.; Nozaki, K.; Ohno, T.; Mataga, N. *Tetrahedron Lett.* **1995**, *36*, 5781.
92. Osuka, A.; Lin, B. -I.; Maruyama, K. *Chem. Lett.* **1993**, 949.
93. Yeow, E. K. L.; Ghiggino, K. P.; Reek, J. N. H.; Crossley, M. J.; Bowman, A.W.; Schenning, A.P.H.J.; Meijer, E.W. *J. Phys. Chem. B* **2000**, *104*, 2596.
94. Choi, M. S.; Aida, T.; Yamazaki, T.; Yamazaki, I. *Chem. Eur. J.* **2002**, *6*, 2667.
95. Choi, M. S.; Aida, T.; Yamazaki, T.; Yamazaki, I. *Angew. Chem. Int. Ed. Engl.* **2001**, *40*, 3803.
96. Milgrom, L. R. *J. Chem. Soc. Perkin Trans.2* **1983**, 2535.
97. Davila, J.; Harriman, A.; Milgrom, L. R. *Chem. Phys. Lett.* **1987**, *136*, 427.
98. Wennerstrom, O.; Ericsson, H.; Raston, I.; Svensson, S.; Pimlott, W. *Tetrahedron Lett.* **1989**, *30*, 1129.
99. Prathapan, S.; Johnson, T. E.; Lindsey, J. S. *J. Am. Chem. Soc.* **1993**, *115*, 7519.

100. Seth, J.; Palaniappan, V.; Johnson, T. E.; Prathapan, S.; Lindsey, J. S. *J. Am. Chem. Soc.* **1995**, *117*, 5231.
101. Sugiura, K.; Tanaka, H.; Matsumoto, T.; Kawai, T.; Sakata, Y. *Chem. Lett.* **1999**, 1193.
102. Khoury, R.G.; Jaquinod, L.; Aoyagi, K.; Olmstead, M.M.; Fisher, A.J.; Smith, K.M. *Angew. Chem. Int. Ed.* **1997**, *36*, 2497.
103. Vincente, M. G. H.; Cancilla, M. T.; Lebrilla, C. B.; Smith, K. M. *Chem. Commun.* **1998**, 2355.
104. Nakano, A.; Osuka, A.; Yamazaki, I.; Yamazaki, T.; Nishimura, Y. Itaya, A.; Murakami, M.; Miyasaka, M. *Chem. Eur. J.* **2001**, *7*, 3134.
105. Nakano, A.; Osuka, A.; Yamazaki, I.; Yamazaki, T.; Nishimura, Y. *Angew. Chem. Int. Ed. Engl.* **1998**, *37*, 3023.
106. Rucareanu, S.; Mongin, O.; Schuwey, A.; Hoyler, N.; Gossauer, A. *J. Org. Chem.* **2001**, *66*, 4973.
107. Mongin, O.; Hoyler, N.; Gossauer, A. *Eur. J. Org. Chem.* **2000**, 1193.
108. Mongin, O.; Schuwey, A.; Vallot, M. A.; Gossauer, A. *Tetrahedron Lett.* **1999**, *40*, 8347.
109. Ambroise, A.; Li, J.; Yu, L.; Lindsey, J. S. *Org. Lett.* **2000**, *2*, 2563.
110. Dubowchik, G. M.; Hamilton, A. D. *Chem. Commun.* **1986**, 1392.
111. Dubowchik, G. M.; Hamilton, A. D. *Chem. Commun.* **1986**, 665.
112. Dubowchik, G. M.; Hamilton, A. D. *Chem. Commun.* **1987**, 293.

113. Screen, T.E.O.; Thome, J.R.G.; Denning, R.G.; Bucknall, D.G.; Anderson, H.L. *J. Am. Chem. Soc.* **2002**, *124*, 9712.
114. Taylor, P. N.; Anderson, H. L. *J. Am. Chem. Soc.* **1999**, *121*, 11538
115. Anderson, H. L.; Hunter, C. A.; Sanders, J. K. M. *Chem. Commun.* **1989**, 226.
116. Anderson, H. L.; Hunter, C. A.; Meah, M. N.; Sanders, J. K. M. *J. Am. Chem. Soc.* **1990**, *7/2*, 5780.
117. Anderson, S.; Anderson, H. L.; Sanders, J. K. M. *Acc. Chem. Res.* **1993**, *26*, 469.
118. Vidal-Ferran, A.; Muuler, C. M.; Sanders, J. K. M. *Chem. Commun.* **1994**, 2657.
119. Mackay, L. G.; Wylie, R. S.; Sanders, J. K. M. *J. Am. Chem. Soc.* **1994**, *116*, 3141.
120. Anderson, S.; Anderson, H. L.; Bashall, A.; McPartlin, M.; Sanders, J. K. M. *Angew. Chem. Int. Ed. Engl.* **1995**, *34*, 1096.
121. Marty, M.; Clyde-Watson, Z.; Twyman, L. J.; Nakash, M.; Sanders, J. K. M., *Chem. Commun.* **1998**, 2265.
122. Mak, C. C; Bampos, N.; Sanders, J. K. M. *Angew. Chem. Int. Ed. Engl.* **1998**, *37*, 3020.
123. Wojaczynski, J.; Latoz-Grazynski, L. *Coord.Chem.Rev.* **2000**, *204*, 113.
124. Imamura, T.; Fukushima, K. *CoordChem. Rev.* **2000**, *198*, 133.
125. Drain, C. M.; Lehn, J. -M. *Chem. Commun.* **1994**, 2313.

126. Drain, C. M.; Nifiatis, F.; Vasenko, A.; Batteas, J. D. *Angew. Chem. Int. Ed. Engl.* **1998**, *37*, 2344.
127. Slone, R. V.; Hupp, J. T. *Inorg. Chem.* **1997**, *36*, 5422.
128. Kimura, A.; Funatsu, K.; Imamura, T.; Kido, H.; Sasaki, Y. *Chem. Lett.* 1995, 207.
129. Alessio, E.; Macchi, M.; Heath, S.; Marzilli, L. G. *Chem. Commun.* **1996**, 1411.
130. Yuan, H.; Thomas, L.; Woo, L. K. *Inorg. Chem.* **1996**, *35*, 2808.
131. Kariya, N.; Imamura, T.; Sasaki, Y. *Inorg. Chem.* **1997**, *36*, 833.
132. Alessio, E.; Macchi, M.; Heath, S. L.; Marzilli, L. G. *Inorg. Chem.* **1997**, *36*, 5614.
133. Funatsu, K.; Imamura, T.; Ichimura, A.; Sasaki, Y. *Inorg. Chem.* **1998**, *37*, 4986.
134. Funatsu, K.; Imamura, T.; Ichimura, A.; Sasaki, Y. *Inorg. Chem.* **1998**, *37*, 1798.
135. Kariya, N.; Imamura, T.; Sasaki, Y. *Inorg. Chem.* **1998**, *37*, 1658.
136. Gerasimchuk, N. N.; Mokhir, A. A.; Rodgers, K. R. *Inorg. Chem.* **1998**, *37*, 5641.
137. Abrahams, B. F.; Hoskins, B. F.; Robson, R. J. *Am. Chem. Soc.* **1991**, *113*, 3606.
138. Abrahams, B. F.; Hoskins, B. F.; Michail, D. M.; Robson, R. *Nature* **1994**, *369*, 727.

139. Sharma, C. V. K.; Broker, G. A.; Huddleston, J. G.; Baldwin, J. W.; Metzger, R. M.; Rogers, R. D. *J. Am. Chem. Soc.* **1999**, *121*, 1137.
140. Wojaczynski, J.; Latoz-Grazynski, L. *Inorg. Chem.* **1995**, *34*, 1044.
141. Wojaczynski, J.; Latoz-Grazynski, L. *Inorg. Chem.* **1995**, *34*, 1054.
142. Wojaczynski, J.; Latoz-Grazynski, L. *Inorg. Chem.* **1996**, *35*, 4812.
143. Hunter, C. A.; Tregonning, R. *Tetrahedron*, **2002**, *55*, 691.
144. Haycock, R. A.; Hunter, C. A.; James, D. A.; Michelsen, D.; Sutton, L. R. *Org. Lett.* **2000**, *2*, 2435.
145. Haycock, R. A.; Yartsev, A.; Michelsen, U.; Sundstrom, V.; Hunter, C. A. *Angew. Chem., Int. Ed. Engl.* **2000**, *39*, 3762.
146. Chi, X.; Guerin, A. J.; Haycock, R. A.; Hunter, C. A.; Sarson, L. D. *Chem. Commun.* **1995**, 2563.
147. Chi, X.; Guerin, A. J.; Haycock, R. A.; Hunter, C. A.; Sarson, L. D. *Chem. Commun.* **1995**, 2567.
148. McCallien, D. W. J. Sanders, J. K. M. *J. Am. Chem. Soc.* **1995**, *117*, 6611.
149. Tabushi, I.; Koga, N.; Yanagita, M. *Tetrahedron Lett.* **1979**, *29*, 257.
150. Ho, T. F.; McIntosh, A. R.; Bolton, J. R. *Nature*, **1980**, *286*, 254.
151. Kang, Y. K.; Rubtsov, I. V.; Iovine, P. M.; Chen, J.; Therein, M. J. *J. Am. Chem. Soc.* **2002**, *124*, 8275.
152. Hayashi, T.; Takimura, T.; Ohara, T.; Hitomi, Y.; Ogoshi, H. *Chem. Comm.* **1995**, 2503.

153. Gust, D.; Moore, T. A.; Moore, A. L.; Lee, S.; Bittersmann, E.; Luttrull, D. K.; Rehms, A. A.; Degraziano, J. M.; Ma, X. C.; Gao, F.; Belford, R. E.; Trier, T. T. *Science* **1990**, *24*, 199.
154. Hung, S.; Macpherson, A. N.; Lin, S.; Liddell, P. A.; Seely, G. R.; Moore, A. L.; Moore, T. A.; Gust, D. *J. Am. Chem. Soc.* **1995**, *117*, 1657. (and references therein)
155. Thanabal, V.; Krishnan, V. *J. Am. Chem. Soc.* **1982**, *104*, 3643.
156. Maiya, G. B.; Krishnan, V. *Inorg. Chem.* **1985**, *24*, 3253.
157. Chandrshekar, T. K.; van Willigen, H.; Ebersole, M. H. *J. Phys. Chem.* **1985**, *89*, 3453.
158. van Willigen, H.; Chandrashekar, T. K.; *J. Am. Chem. Soc.* **1986**, *108*, 709.
159. Lehn, J. -M. *Supramolecular Photochemistry*, Balzani, V.; Ed.; NATO ASI Ser. C, 1987, Vol. 24, p29f.
160. Sun, L.; van Gersdorff, J.; Niethammer, D.; Tian, P.; Kurreck, H. *Angew. Chem. Int. Ed Engl.* **1994**, *33*, 2318.
161. Lindsey, J. S.; Brown, P. A.; Siesel, D. A. *Tetrahedron* **1989**, *45*, 4845.
162. Brun, A. M.; Harriman, A. *J. Am. Chem. Soc.* **1994**, *116*, 10383.
163. Lehn, J. -M. *Chem. Commun.* **1994**, 2313.
164. Hunter, C. A. *Chem. Soc. Rev.* **1994**, 101.
165. Hunter, C. A.; Sarson, D. L. *Angew. Chem., Int. Ed. Engl.* **1994**, *33*, 2313.

166. Anderson, S.; Anderson, H. L.; Bashall, A.; McPartlin, M.; Sanders, J. K. *M. Angew. Chem., Int. Ed. Engl.* **1995**, *34*, 1096.
167. Imahori, H.; Yoshizawa, E.; Yamada, K.; Hagiwara, K.; Okada, T.; Sakata, Y. *Chem. Commun.* **1995**, 1133.
168. Arimori, S.; Murakami, H.; Takeuchi, M.; Shinkai, S. *Chem. Commun.* **1995**, 961.
169. Kuroda, Y.; Kato, Y.; Higashioji, T.; Hasegawa, J. Y.; Kawanami, S.; Takahashi, M.; Shiraishi, N.; Tanabe, K.; Ogoshi, H. *J. Am. Chem. Soc.* **1995**, *117*, 10950 and references therein.
170. Aoyama, Y.; Asakawa, M.; Matsui, Y.; Ogoshi, H. *J. Am. Chem. Soc.* **1991**, *113*, 6223.
171. Hayashi, T.; Asai, T.; Hokazono, H.; Ogoshi, H. *J. Am. Chem. Soc.* **1993**, *115*, 1220.
172. Hayashi, T.; Miyahara, Hashizume, N.; Ogoshi, H. *J. Am. Chem. Soc.* **1993**, *115*, 2049.
173. Hayashi, T.; Miyahara, T.; Aoyama, Y.; Nonoguchi, M.; Ogoshi, H. *Chem. Lett.* **1994**, 1749.
174. Hayashi, T.; Miyahara, T.; Aoyama, Y.; Kobayashi, M.; Ogoshi, H. *Pure and Appl. Chem.* **1994**, *66*, 797.
175. Mizutani, T.; Murakami, T.; Matsumi, N.; Kurahashi, T.; Ogoshi, H. *Chem. Commun.* **1995**, 1257.
176. Harriman, A.; Magda, D. J.; Sessler, J. L. *Chem. Commun.* **1991**, 345.

177. **Harriman**, A.; Magda, D. J.; Sessler, J. L. *J. Phys. Chem.* **1991**, *95*, 1530.
178. **Harriman**, A.; Kubo, Y.; Sessler, J. L. *J. Am. Chem. Soc.* **1992**, *114*, 388.
179. Sessler, J. L.; Wang, B.; **Harriman**, A. *J. Am. Chem. Soc.* **1993**, *115*, 10418.
180. D'Souza, F.; Deviprasad, G. R. *J. Org. Chem.* **2001**, *66*, 4601.
181. D'Souza, F. *J. Am. Chem. Soc.* **1996**, *118*, 923.
182. D'Souza, F.; Deviprasad, G. R.; Hsieh, Y. Y. *Chem. Commun.* **1996**, 533.
183. **Myles**, A.J.; **Branda**, N. J. *J. Am. Chem. Soc.* **2001**, *123*, 177.
184. **Lang**, K.; **Karl**, V.; **Kapusta**, P.; **Kubat**, P.; **Vasek**, P. *Tetrahedron Lett.* **2002**, *43*, 4919.
185. **Milbradt**, R.; **Weiss**, J. *Tetrahedron Lett.* **1995**, *35*, 1936.
186. **Arimura**, T.; **Brown**, C.T.; **Spring**, S. L.; **Sessler**, J. L. *Chem. Commun.* **1996**, 2293.
187. **Arimura**, T.; **Ide**, S.; **Sugihara**, H.; **Murata**, S.; **Sessler**, J. L. *New J. Chem.* **1999**, *23*, 977.
188. **Hoshino**, M.; **Ida**, H.; **Yasufuku**, K.; **Tanaka**, K. *J. Phys. Chem.* **1986**, *90*, 3984.
189. **Kadish**, K. M.; **Maiya**, B. G.; **Xu**, Q. Y. *Inorg. Chem.* **1989**, *28*, 2518.
190. **Segawa**, H.; **Kunimoto**, K.; **Nakamoto**, A.; **Shimidzu**, T. *J. Chem. Soc., Perkin Trans I.* **1982**, 939.
191. **Rao**, T. A.; **Maiya**, B. G. *Chem. Commun.* **1995**, 939.
192. **Rao**, T. A.; **Maiya**, B. G. *Inorg. Chem.* **1996**, *35*, 4829.

193. Reddy, D. R.; Maiya, B. G. *J. Phys. Chem. A* **2003**, *107*, 6326.
194. Reddy, D. R.; Maiya, B. G. *Chem. Commun.* 2001, 117.
195. Susumu, K.; Kunitomo, K.; Segawa, H.; Shimidzu, T. *J. Phys. Chem.* 1995, *99*, 29.
196. Segawa, H.; Kunitomo, K.; Susumu, K.; Taniguchi, M.; Shimidzu, T. *J. Am. Chem. Soc.* 1994, *116*, 11193.
197. Susumu, K.; Segawa, H.; Shimidzu, T. *Chem. Lett.* 1995, 929.
198. Susumu, K.; Tanaka, K.; Shimidzu, T.; Takeuchi, Y.; Segawa, H. *J. Chem. Soc. Perkin Trans 2*, **1999**, 1521.
199. Segawa, H.; Nakayama, N.; Shimidzu, T. *Chem. Commun.* 1992, 784.
200. Hunter, C.A.; Shannon, R.J. *Chem. Commun.* 1996, 1361.
201. Imahori, H.; Yoshizawa, E.; Yamad, K.; Hagiwara, T.; Okada, T.; Sakata, Y. *Chem. Commun.* 1995, 1133.
202. Imahori, H.; Yamad, K.; Yoshizawa, E.; Hagiwara, T.; Okada, T.; Sakata, Y.; J. *Porphyrins Phthalocyanines*, **1997**, *1*, 55.
203. Otuski, J.; Harada, K.; Toyama, K.; Hirose, Y.; Araki, K.; Seno, M.; Takatera, K.; Watanabe, T. *Chem. Commun.* 1998, 1515.
204. Flamigni, L.; Johnston, M.R.; *New J. Chem.* 2001, *25*, 1368.
205. Flamigni, L.; Johnston, M.R.; Giribabu, L. *Chem. Eur. J.* 2002, *8*, 3938.
206. D'Souza, F.; Deviprasad, G. R.; Zandler, M. E.; Honangm Vu. T.; Klykov, A.; Vanstipdonk, M.; Perera, A.; Khouly, M. E. El.; Fujitsuka, M.; Ito, O. *J. Phys. Chem. A* **2002**, *106*, 3243.

207. **D'Souza**, F.; Deviprasad, G. R.; Rahman, M. S.; Choi, J. *Inorg. Chem.* 1999,55,2157.
208. **D'Souza**, F.; Deviprasad, G. R.; Zandler, M. E.; Khouly, M. E. El.; Fujitsuka, M.; **Ito**, O. *J. Phys. Chem. A* **2003**, *106*, 4801.
209. Deviprasad, G. R.; **D'Souza**, F. *Chem. Commun.* **2000**, **1915**.
210. El-Khouly, M. E.; Gadde. S.; Deviprasad, G. R.; **Fujitsuka**, M.;**Ito**, O. *J. Porphyrins Phthalocyanines* **2003**, *7*,1.
211. El-Khouly, M. E.; Rogers, L. M.; Zandler, M. E.; Gadde, S.; **Fujitsuka**, M.; **Ito**, O.; **D'Souza**, F. *ChemPhysChem* **2003**, *4*, 474.
212. Yin, G.; Xu, D.; Xu, Z. *Chem. Phys. Lett.*, **2002**, *365*, 232.
213. Wilson, S. R.; MacMahon, S.; Tat, F. T.; Jarowski, P. D.; Schuster, D. I. *Chem. Commun.* **2003**, 226.
214. D'Souza, F.; Rath, N. P.; Deviprasad, G. R.; Zandler, M. E. *Chem. Commun.* **2001**, 267.
215. **Armaroli**, N.; Diederich, F.; Echegoyen, L.; Habicher, T.; **Flamigni**, L.; Marconi, G.; Nierengarten, J.-F. *New. J. Chem.* **1999**, *23*, 77.
216. Ros, D. T.; Prato, M.; **Guldi**, D. M.; Alessio, E.; Ruzzi, M.; Pasimeni, L. *Chem. Commun.* **1999**, 635.
217. D'Souza, F.; Deviprasad, G. R.; El-Khouly, M. E.; **Fujitsuka**, M.; **Ito**, O. *J. Am. Chem. Soc.* **2001**, *123*, 5277.
218. D'Souza, F.; Zandler, M. E.; Deviprasad, G. R.; **Kutner**, W. *J. Phys. Chem. A* **2000**, *104*, 6887.

CHAPTER 2

Materials and Methods

2. 1 Introduction

This chapter presents a listing of all the chemicals and other materials employed at various stages of the research work. Procedures followed for the purification of solvents and chemicals are also given here. Further, a brief discussion of the **physicochemical** techniques employed during the course of the investigation is presented.

2. 2 Materials

Pyrrole was obtained from Aldrich Chemicals (U.S.A.). It was distilled over **KOH** before use.

4-methlybenzaldehyde was purchased from Sisco **Chem** (India). It was distilled under vacuum before use. **4-hydroxybenzaldehyde** was procured from E.merck (India) and was used as such.

3,5-pyridine-dicarboxylic acid was purchased form Lancaster (U.K.)

4-tert-butylphenol was obtained from **Fluka** (U.S.A.).

Diphenylether was obtained from Spectro Chem. (India).

37% formaldehyde solution was purchased form E.merck (India)

Borontrifluoride diethyletherate was purchased from Aldrich Chemicals (U.S.A).

1,2-dibromoethane, 1,3-dibromoethane, were procured from Sisco Chem. (India) and were distilled under vacuum before use.

Tetrabutylammonium perchlorate was procured from Aldrich Chemicals (U.S.A.).

Tin(II) dichloride (dihydrate) was procured from B.D.H. (India). It was purified by stirring with acetic acid and acetic anhydride at room temperature under nitrogen for 4 h. The solid was filtered under nitrogen and washed with dry ether.¹

The various metal salts employed in the study were purchased from B.D.H. (India). These compounds are of AR grade and were used as such.

Calcium hydride was obtained from Spectro Chem. (India). The other drying agents used were calcium chloride, sodium sulfate and magnesium sulfate. These were purchased from B.D.H. (India) or from Qualigens (India) and were of LR grade.

The mineral acids such as hydrochloric acid, nitric acid and sulfuric acid were of AR grade and were obtained either from Ranbaxy (India) or from B.D.H. (India).

Potassium chloride, potassium hydroxide, potassium carbonate, aluminum chloride and sodium bicarbonate were of LR grade and were obtained from B.D.H. (India).

Aluminum oxide (basic and neutral) and silica gel for column chromatography were procured from Acme Synthetic Chemicals (India) and were used as such.

Nitrogen gas was obtained from Indian Oxygen Limited (India). It was further purified and dried by passing it through alkaline pyrogallol solution, sulfuric acid, and potassium hydroxide pellets.

Chlorine dioxide was produced by mixing 100 ml of 4% aqueous potassium persulfate and 50 ml of 16% aqueous sodium chlorite in a 250 ml three necked round-bottom flask. Nitrogen gas was bubbled through this solution and was allowed to pass through a series of flasks (equipped with gas bubbling frits) containing cold (0-5 °C) deionized water. The aqueous chlorine dioxide solutions ranging in concentration from ca. 30- 40% thus obtained were placed in amber glass bottles wrapped with aluminum foil and were stored in a refrigerator.²

2. 3 Solvents

The common solvents employed during the research work were purified according to the standard **procedures**.^{1,3}

Acetic acid, acetic anhydride and propanoic acid were purchased from Ranbaxy (India).

Pyridine was obtained from Ranbaxy (India). It was dried over potassium hydroxide pellets and distilled over calcium hydride under nitrogen before use.

Dimethylformamide and dimethyl sulphoxide were obtained from E-Merck (India). They were purified by flash vacuum distillation over calcium hydride.

Hexane was of recrystallisable grade from Ranbaxy (India). It was distilled over sodium and stored over sodium wire.

Chloroform, methylene chloride and **methanol** were of LR grade from B.D.H. (India) and were used for synthetic or chromatographic purposes. These solvents were extensively purified as described below, for spectroscopic purposes.

The LR grade methylene chloride was washed twice with sulfuric acid and then with water. This was followed by washing twice with sodium bicarbonate solution and then with water. The solvent was dried over calcium chloride and distilled over phosphorus pentoxide. It was stored over basic alumina until use. Chloroform (LR) was washed 3-4 times with water, stored over calcium chloride overnight and distilled over phosphorus pentoxide. It was stored in the dark over basic alumina.

Methanol (LR) was purified by distillation through an efficient fractionating column.

Acetone, ethanol and tetrahydrofuran were purified according to known procedures.^{1,3}

Deuterated chloroform (99. 8%) was obtained from Aldrich Chemicals (U.S.A.).

2. 4 Physical methods

The various porphyrins and other compounds synthesized in this study were characterized and investigated using elemental analysis, mass (FAB-MS or MALDI-TOF), infrared (IR), electronic absorption and emission, proton nuclear

magnetic resonance (^1H NMR) spectroscopies and electrochemical (cyclic- and differential pulse **voltammetry**) methods. These methods are briefly alluded to below.

The elemental analyses were done on a **Perkin-Elmer** model **240C-CHN** analyzer.

MALDI-TOF spectra were recorded on a **Kompact MALDI 4** mass spectrometer (**Kratos** Analytical Ltd). The instrument was operated in reflection time of flight mode with an accelerating potential of 20 **kV** and in the negative ion recording mode. The FAB mass spectra were recorded on a JEOL SX 102/DA-6000 mass spectrometer/data system using xenon (6 **kV**, 10 mA) as the FAB gas. The accelerating voltage was 10 **kV** and the spectra were recorded at room **temperature**. **m-nitrobenzyl** alcohol (NBA) was used as the matrix.

The **IR** spectra were recorded on a Jasco Model 5300 **FT-IR** spectrophotometer. The spectra of the solid samples were recorded by dispersing the sample in **Nujol** mull or as **KBr** wafers.

The **UV-visible** spectra were recorded with a Shimadzu Model UV-3101PC UV-vis spectrophotometer. A matched pair of quartz cuvettes were employed (path length = 1 cm each). Concentrations of the various investigated compounds employed for this purpose ranged from ca. 2×10^{-5} (porphyrin Soret bands) to 5×10^{-5} M (porphyrin Q- and other bands / bands due to other compounds).

Steady state fluorescence spectra were recorded either on a Spex Model **Fluoromax-3** or a Jasco Model FP 777 **spectrofluorometer** using a 1 cm quartz

cell. Right angle detection technique was employed for these measurements. The excitation and emission slit widths employed were either 2 or 5 nm. Concentration of the samples was adjusted such that the optical densities at the excitation wavelengths were less than ca. 0.2 for emission spectra and $\sim 1 \times 10^{-7}$ M (or the optical density at the emission wavelength, $\lambda_{em} < 0.2$) for excitation spectra. A Rhodamine 6G quantum counter was employed for spectral corrections at wavelengths < 600 nm. Fluorescence quantum yields (ϕ) were estimated by integrating the areas under the fluorescence curves using the expression of Austin and Gouterman.⁴

$$\phi_{\text{sample}} = \frac{\text{O.D.}_{\text{standard}} \times A_{\text{sample}}}{\text{O.D.}_{\text{sample}} \times A_{\text{standard}}} \times \phi_{\text{standard}} \quad (2.1)$$

Here, A is area under the emission spectral curve and O.D. is the optical density of the compound at the wavelength of exciting light. The fluorescence standards employed were either 5,10,15,20-tetra(4-methylphenyl)porphyrin (**H₂TTP**) or its zinc (II) complex (**[(TTP)Zn^{II}]**) ($\phi(\text{H}_2\text{TTP}) = 0.13$ and $\phi(\text{[(TTP)Zn}^{\text{II}}]) = 0.033$ in CH_2Cl_2)^{5,6} for excitation into the porphyrin absorption maxima of the free-base and zinc(II) porphyrin derivatives, respectively. 5,10,15,20-tetra (4-methylphenyl) porphyrinato tin(IV) dihydroxide (**[(TTP)Sn^{IV}(OH)₂]**) was the fluorescence standard employed for studies with the tin(IV) porphyrins. Refractive index corrections have been employed while estimating the ϕ values in various solvents.⁷

Fluorescence lifetimes were measured by the time correlated single photon counting (TCSPC) method, as described previously.^{8,9} Briefly, the samples were excited by 4 ps laser (Nd/YAG pumped Rhodamine 6G dye laser) pulses at a repetition rate of 800 kHz. The fluorescence was detected at the magic angle (54. 7°) with respect to polarization of the incident beam by a microchannel plate photomultiplier (MCP-PMT, R2809). The count rate

4 -1

employed was typically $2 \times 10^5 \text{ s}^{-1}$. The excitation wavelength was fixed at 575 nm and the fluorescence was collected at 650 nm. Deconvolution of the data was carried out by the method of iterative reconvolution of the instrument response function and the assumed decay function. The goodness of fit of the experimental data to the assumed decay function was judged by the standard statistical tests (i. e. random distribution of weighted residuals, the autocorrelation function and the values of reduced χ^2). The error estimates of the lifetimes, obtained by single/bi- exponential fits, were ~ 10%. Although no specific effort has been made here to estimate the error limit on the relative amplitudes (A_j), it is believed that they should be less than 2 - 3%.

¹H NMR spectra were recorded with either a Bruker NR-200 AF-FT or a Bruker DRX-400 spectrometer using CDCl_3 as the solvent and tetramethylsilane (TMS) as an internal standard. The sample concentration was typically $\sim 1 - 3 \times 10^{-3} \text{ M}$.

Cyclic- and differential pulse voltammetric experiments were performed on a CH Instruments model CHI 620A electrochemical analyzer. Tetrabutylammonium perchlorate (TBAP) was used as the supporting

electrolyte in all the cases. The working and the auxiliary (counter) electrodes employed were always platinum and the reference electrode chosen was a saturated calomel electrode (SCE). A salt bridge containing the same concentration of base electrolyte as that of the bulk solution was positioned between the nitrogen-purged bulk-test-solution and the reference electrode to reduce the effect due to liquid junction potentials. Ferrocene was chosen as the standard and it could be reversibly oxidized at 0.48 ± 0.03 V in CH_2Cl_2 , 0.1 M TBAP (vs. SCE) under these experimental conditions.

The geometry optimizations were carried out using Cerius² program (Accelrys). Structures were sketched using 3D-sketcher option available in this program on a Silicon Graphics Octane2 (6.5) workstation, and were minimized with the AM1 Hamiltonian in Mopac 93.

2. 4. 1 Absorption and fluorescence titrations

Absorption titration of a given porphyrin with a given ligand was carried out in the following way. CH_2Cl_2 solution containing the porphyrin ($\sim 3 - 5 \times 10^{-6}$ M) was taken in a cuvette and titrated with increasing volume of a concentrated solution of the ligand. The changes in absorbance at the Soret band maxima were measured. The ligand solutions also contained the porphyrin at its initial concentration so as to maintain the porphyrin concentration constant throughout the titration.

In an analogous manner, steady state fluorescence titrations were carried out by exciting the porphyrin solutions ($5 - 8 \times 10^{-6}$ M) with or without the added ligand. The excitation wavelength (λ_{exc}) was typically 530 nm (Q-band)

and the intensities were monitored at the emission maximum (λ_{em}) in each case. In the corresponding time-resolved fluorescence titrations, the concentration of the porphyrin used was typically 2.5×10^{-5} M, $\lambda_{exc} = 575$ nm and $\lambda_{em} = 650$ nm.

2. 4. 2 NMR titrations.

A solution of a given ligand was titrated against a given porphyrin ($3 - 5 \times 10^{-3}$ M) in $CDCl_3$. The [porphyrin] : [ligand] ratio was varied and, in doing so, initial concentration of the porphyrin was contained in all the ligand solutions to minimize the dilution effect.

2. 4. 3 Electrochemical titrations

In a typical experiment, a given ligand was titrated against a given porphyrin ($3 - 4 \times 10^{-3}$ M) and change in the redox potential was monitored by both cyclic- and differential-pulse voltammetric methods. Initial concentration of the porphyrin was contained in all the ligand solutions to minimize the dilution effect.

2. 5 General considerations

Error estimation of the data, reconstruction of various spectra, calculations of equilibrium constants, various regression analysis etc., that appear throughout this dissertation, have been carried out on an IBM compatible PC Pentium IV computer using the available in-house soft-ware/Origin 6. 0 software package.

At all times, care was taken to avoid the entry of direct, ambient light into the samples in the spectroscopic and electrochemical experiments. Unless otherwise specified, all experiments were carried out at the ambient temperature (ca. 293 ± 3 K).

All hazardous chemicals were handled with appropriate precaution. Protective gloves, goggles, and safety mask were employed to minimize exposure to obnoxious chemicals, ultraviolet light etc.

The following are the standard error limits involved in various measurements (unless otherwise stated):

λ_{\max}	± 1 nm
E	$\pm 10\%$
λ_{em}	± 1 nm
ϕ	$\pm 10\%$
τ	$\pm 10\%$
$E_{1/2}$	± 0.03 V
δ	± 0.1 ppm
J	± 1 Hz

2. 6 Summary

This chapter presents a brief account of various solvents and chemicals used in this study. A description of the spectroscopic and other physical methods employed during this study is also given.

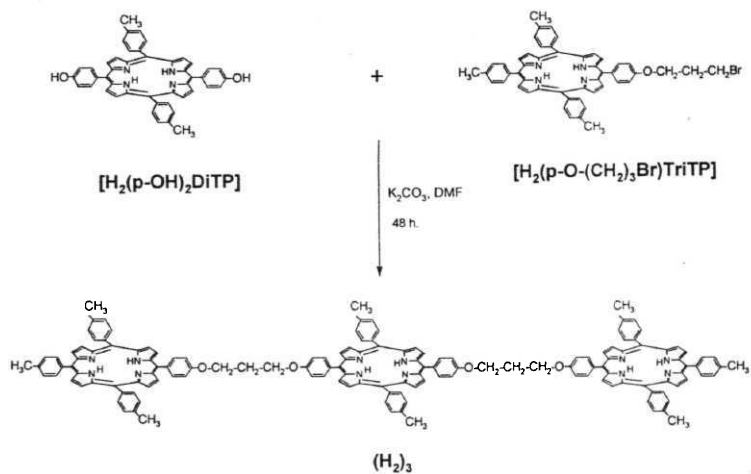
2. 7 References

1. *Vogel's Text Book of Practical Organic Chemistry* (Revised by Furniss, B. S.; Hannaford, A. J.; Smith, P. W. G.; Tatchell, A. R.), V Edn.; **Longmann** (ELBS): Essex (U.K.), 1991.
2. Nam, K. C; Kim, J. M. *Bull. Korean Chem. Soc.* **1994**, *15*, 268.
3. Perrin, D. D.; Armarego, W. L. F.; Perrin, D. R. *Purification of Laboratory Chemicals*, **Pergamon**: Oxford, 1980.
4. Austin, E.; Gouterman, M. *Bioinorg. Chem.* 1978, *9*, 281.
5. Quimby, D. J.; Longo, F. R. *J. Am. Chem. Soc.* **1975**, *97*, 5111.
6. Harriman, A.; Davila, J. *Tetrahedron* **1989**, *45*, 4737.
7. Lackowicz, J. R. *Principles of Fluorescence Spectroscopy*, Plenum: New York, 1983.
8. Maiya, B. G.; Doraisamy, S.; Periasamy, N.; Venkataraman, B. *J. Photochem. Photobiol. A: Chem.*, **1994**, *81*, 139
9. Sirish, M.; Maiya, B. G. *J. Photochem. Photobiol. A: Chem.*, **1994**, *77*, 189.

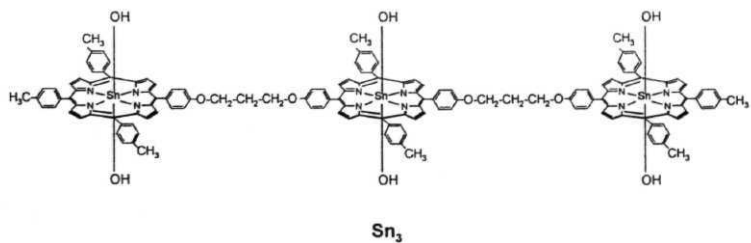
*A New **Nonameric** Array Based on Tin(IV) Porphyrin Scaffold*

3. 1 Introduction

Porphyrin arrays are useful in many research areas encompassing biomimetic photosynthesis, molecular electronics, molecular catalysis **etc.**¹⁻³ Most of the porphyrin arrays reported so far have been synthesized *via* typical organic reaction sequences carried out at the porphyrin peripheral (i.e. β - pyrrole or **meso**) position/s.⁴⁻²¹ In recent years, '**inorganic**' reactions that can be conducted at the axial sites of porphyrin-bound metal ions are also being employed for the construction of **metalloporphyrin arrays**.²²⁻³³ Adapting this latter 'axial-bonding' strategy and utilizing the well-known oxophilicity of metalloid ions, a series of **trimers** based on phosphorus(V), **tin(IV)** or germanium(IV) porphyrin scaffolds have been reported recently.^{34,35} During the course of the present investigations, it was realized that it should be possible to synthesize more elaborate hybrid-type porphyrin arrays having diverse structures and functions by utilizing the reactivities at both the peripheral and axial sites of a metalloid porphyrin species. Continued research efforts in this direction showed that the above concepts are readily achievable. Accordingly, a nonameric array - the structure of which is illustrated in the Fig 3. 1, was constructed. As seen in this figure, while a typical organic reaction {ether



$SnCl_2$, Pyridine
 aq. Ammonia



(continued)

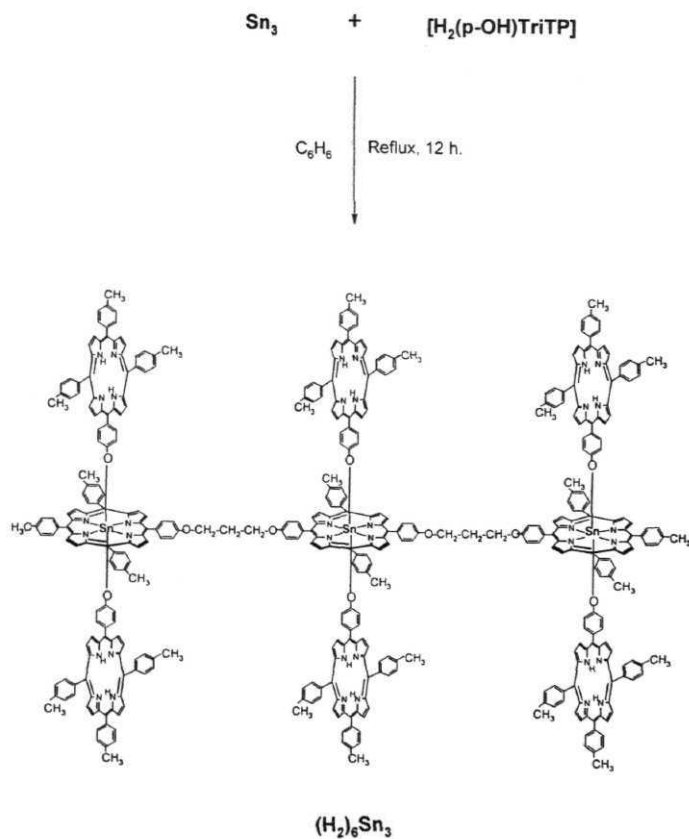


Fig. 3. 1 Scheme leading to the synthesis of $(\text{H}_2)_6(\text{Sn})_3$

formation) involving the porphyrin peripheral hydroxy group/s is employed for the propagation of this array in the lateral direction, oxophilic nature of the tin center has been advantageously utilized for its expansion in the axial direction. This Chapter provides details of design, construction, spectral characterization and redox as well as singlet state properties of this new nonameric array.

3. 2 Experimental details

3. 2. 1 Synthesis of 5-(4-hydroxyphenyl)10,15,20-tri(4-methylphenyl) porphyrin ([H₂(p-OH)TriTP])³⁶

4-hydroxybenzaldehyde (6. 1 g, 50 mmol) dissolved in 350 ml of propanoic acid was stirred at 120 °C for 10 min. To the resulting solution, 12. 0 g (100 mmol) of **p-tolualdehyde** followed by 10. 5 g (157 mmol) of pyrrole were added. The mixture was refluxed for 45 min., left overnight at 10 °C and then filtered. The black-violet residue obtained was washed several times with hot water, followed by methanol and purified by chromatography on a basic alumina column. Elution with CHCl₃ - CH₃OH (97 : 3, v/v) gave the desired product. Yield: **1. 25** g (5%).

3. 2. 2 Synthesis of 5-(4-methylphenyl)dipyrromethane³⁷

A solution of **4-methylbenzaldehyde** (0. 5 g, 4. 15 mmol) and pyrrole (2. 8 ml, 40 mmol) was degassed by bubbling nitrogen for 10 min. Trifluoroacetic acid (0. 08 ml, 0. 1 mmol) was then added to this deaerated solution and it was

stirred for 15 min. at room temperature, at which point no starting aldehyde was seen to be present (TLC analysis). The mixture was diluted with CH_2Cl_2 (50 ml), washed with 0.1 M aqueous NaOH and then with water and finally, dried over anhydrous Na_2SO_4 . The unreacted pyrrole was removed by vacuum distillation at room temperature. The resulting yellow amorphous solid was dissolved in minimal quantity of the CH_2Cl_2 and loaded onto a silica gel column. Elution with hexane - ethylacetate - triethylamine (80: 20: 1, v/v) gave pure sample of 5-(4-methylphenyl)dipyrromethane. Yield: 0.75 g (76%).

3. 2. 3 Synthesis of 5,15-bis(4-hydroxyphenyl)10, 20-bis(4-methylphenyl) porphyrin ($[\text{H}_2(\text{p-OH})_2\text{DiTP}]$)

This compound was synthesized according to a reported procedure. A solution containing 4-hydroxybenzaldehyde (0.24 g, 2 mmol) and 5-(4-methylphenyl)dipyrromethane (0.51 g, 2 mmol) in 250 ml of CHCl_3 was purged with nitrogen for 10 min. and then a catalytic amount of $\text{BF}_3\cdot\text{O}(\text{Et})_2$ was added. The resulting solution was stirred for 1 h. at room temperature and 2,3-dichloro-5,6-dicyano-1,4-benzoquinone (1.02 g, 4.5 mmol) was added. The mixture was stirred at room temperature for an additional hour and then the solvent was removed. The crude product was loaded onto a silica gel column. Elution with CHCl_3 - CH_3OH (98 : 2, v/v) gave pure sample of $[\text{H}_2(\text{p-OH})_2\text{DiTP}]$. Yield: 0.12 g (13%).

3. 2. 4 Synthesis of 5-(4-(3-bromo-1-propoxy)phenyl)-10,15,20-tri-(4-methylphenyl)porphyrin ($[\text{H}_2(\text{p-O}-(\text{CH}_2)_3\text{Br})\text{TriTP}]$)³⁸

A mixture of $[\text{H}_2(\text{p-OH})\text{TriTP}]$ (2. 0 g, 3 mmol), 1, 3-dibromopropane (4. 1 g, 22 mmol) and 3. 0 g of anhydrous K_2CO_3 was stirred magnetically in 50 ml of dimethylformamide for 48 h. at room temperature under the nitrogen atmosphere. The reaction mixture was then poured onto a solvent mixture containing 170 ml water and 30 ml methanol. The precipitated porphyrin was filtered off, washed successively with water and methanol and dried under vacuum. It was loaded onto a neutral alumina column. Elution with CHCl_3 gave $[\text{H}_2(\text{p-O}-(\text{CH}_2)_3\text{Br})\text{TriTP}]$. Yield: 2. 43 g (95%).

3. 2. 5 Synthesis of free-base trimer $(\text{H}_2)_3$

A mixture containing $[\text{H}_2(\text{p-OH})_2\text{DiTP}]$ (0. 20 g, 0. 30 mmol), $[\text{H}_2(\text{p-O}-(\text{CH}_2)_3\text{Br})\text{TriTP}]$ (2. 38 g, 3 mmol) and 0. 5 g of anhydrous K_2CO_3 in 50 ml of dimethylformamide was Stirred magnetically for 72 h. at room temperature under the nitrogen atmosphere. The product was precipitated by pouring the reaction mixture onto 100 ml of 10% aqueous methanolic solution. The precipitate obtained was filtered off and dried under vacuum. The solid was chromatographed on a neutral alumina column. Elution with CHCl_3 - hexane (1 : 1, v/v) gave unreacted $[\text{H}_2(\text{p-O}-(\text{CH}_2)_3\text{Br})\text{TriTP}]$, subsequent to which free-base trimer $(\text{H}_2)_3$ was eluted out. It was recrystallized from CH_2Cl_2 - hexane. Yield: 0. 29 g (46%).

3. 2. 6 Synthesis of tri-tin(IV) trimer Sn_3

A mixture containing $(\text{H}_2)_3$ (0. 21 g, 0.10 mmol) and SnCl_2 (0. 50 g, 2. 23 mmol) in pyridine (20 ml) was refluxed for 2 h., after which 10 ml aq. ammonia (25%, v/v) was added to it. The resulting solution was stirred for 1 h. at 50 °C. Solvent pyridine was removed under the reduced pressure. The solid obtained was taken up in CHCl_3 and washed several times with water. The organic layer was dried by passing through anhydrous Na_2SO_4 and chromatographed over basic alumina. Elution with CHCl_3 - CH_3OH (98 : 2, v/v) gave Sn_3 . The compound was recrystallized from CH_2Cl_2 - hexane. Yield: 0. 22 g (88%).

3. 2. 7 Synthesis of '(free-base porphyrin)₆ - (Sn (IV) porphyrin)₃' Nonamer $(\text{H}_2)_6\text{Sn}_3$

Trimer Sn_3 (0. 05 g, 0. 02 mmol) and monomer $[\text{H}_2(\text{p-OH})\text{TriTP}]$ (0. 20 g, 0. 30 mmol) were dissolved in dry C_6H_6 (20 ml) and the contents were refluxed for 12 h. under the nitrogen atmosphere. Evaporation of the solvent and purification of the residue by preparative TLC on neutral alumina (solvent: CHCl_3) afforded $(\text{H}_2)_6\text{Sn}_3$. It was recrystallized from CH_2Cl_2 - hexane. Yield: 0. 04 g (33%). Anal: Calcd. for: $\text{C}_{428}\text{H}_{318}\text{O}_{10}\text{N}_{36}\text{Sn}_3$: C, 79. 31; H, 4. 94; N, 7. 78. Found: C, 78. 71; H, 5. 06, N, 7. 34. Mass (MALDI-TOF): calcd: 6482, found: 6482.

Each investigated porphyrin was purified on a short alumina column before the spectral measurements were made. All the spectroscopic and electrochemical experiments have been carried out as described in Chapter 2.

3. 3 Results and discussion

3. 3. 1 Design and Synthesis

The majority of established methods that are available for the construction of porphyrin arrays involve *either* manipulation at the porphyrin peripheral position/s *or* axial ligation at the central metal/metalloid ion. In the present study, relying on a 'building block' approach, synthesis of $(\text{H}_2)_6\text{Sn}_3$ has been achieved by employing sequential 'organic' and 'inorganic' reactions. Indeed, from a retrosynthetic view point, whereas propagation of these 'branched-chain' type arrays in the lateral direction involves typical ether bond formation reaction, construction of the perpendicular 'branches' employs the 'axial-bonding' capability of the central oxophilic tin(IV) ion.³⁹ The precursor porphyrin building blocks necessary for the construction of nonamer $(\text{H}_2)_6\text{Sn}_3$ (i. e. $[\text{H}_2(\text{p-OH})_2\text{DiTP}]$ and $[\text{H}_2(\text{p-O}-(\text{CH}_2)_3\text{Br})\text{TriTP}]$) were prepared by closely following the corresponding methods reported in the literature.³⁶⁻³⁸ The nonamer was constructed in a step-wise manner starting from the trans-dihydroxy porphyrin $[\text{H}_2(\text{p-OH})_2\text{DiTP}]$ as the basic building block, Fig. 3. 1. Reaction of $[\text{H}_2(\text{p-OH})_2\text{DiTP}]$ with bromide $[\text{H}_2(\text{p-O}-(\text{CH}_2)_3\text{Br})\text{TriTP}]$ in $\text{K}_2\text{CO}_3/\text{DMF}$ milieu and purification afforded trimer $(\text{H}_2)_3$. The tri-tin(IV) trimer Sn_3 was

synthesized in high yield by reacting $(\text{H}_2)_3$ with SnCl_2 in refluxing pyridine for 2 h. followed by treatment with aq. ammonia. This trimer, with the two axial hydroxy ligands amenable for further reaction on each of its tin(IV) centers, reacted smoothly with excess $[\text{H}_2(\text{p-OH})\text{TriTP}]$ in refluxing dry C_6H_6 to afford the 'axial-bonding' type nonameric array $(\text{H}_2)_6\text{Sn}_3$ in good yield.

3. 3. 2 Ground state properties

Preliminary characterization of $(\text{H}_2)_6\text{Sn}_3$ was carried out by mass (MALDI-TOF) and UV-visible spectroscopic methods. MALDI-TOF spectra showed a peak at 6482 consistent with the calculated value. UV-visible data of $(\text{H}_2)_6\text{Sn}_3$ as well as those of the corresponding monomers $[\text{H}_2(\text{p-OH})\text{TriTP}]$, 5,10,15,20-tetra(4-methylphenyl) porphyrinato tin(IV) dihydroxide $[(\text{TTP})\text{Sn}^{\text{IV}}(\text{OH})_2]$ and trimers $(\text{H}_2)_3$ and Sn_3 are summarized in Table 3. 1. UV-visible spectrum of $(\text{H}_2)_6\text{Sn}_3$ is illustrated in Fig. 3. 2. A comparison of the data for $(\text{H}_2)_6\text{Sn}_3$ and that obtained for the spectrum of a solution containing 1 : 2 (mole/mole) equivalents of $[\text{H}_2(\text{p-OH})\text{TriTP}]$ and $[(\text{TTP})\text{Sn}^{\text{IV}}(\text{OH})_2]$ reveals that, within the experimental error, the peak maxima (λ_{max}) and also the molar absorptivities at the peak maxima ($\log \epsilon$) of this physical mixture and that of the nonamer are close to each other. This observation clearly indicates that there is minimal perturbation of the electronic structures of the individual macrocyclic *n*-systems in this array. Specifically, there exists no indication of the presence of

Table 3. 1 UV-visible data in CH_2Cl_2 ¹

Compound	λ_{max} nm (log ϵ)	
	Soret band	Q-bands
$[\text{H}_2(\text{p-OH})\text{TriTP}]$	418 (5.30)	5.16 (4.17) 551 (3.90) 592 (3.64) 650 (3.68)
$[\text{H}_2(\text{p-OH})_2\text{DiTP}]$	420 (5.16)	5.17 (4.23) 5.53 (4.00) 592 (3.70) 648 (3.68)
$[\text{H}_2(\text{p-O}-(\text{CH}_2)_3\text{Br})\text{TriTP}]$	420 (5.37)	5.17 (4.19) 553 (3.94) 594 (3.67) 649 (3.60)
$[(\text{TTP})\text{Sn}^{\text{IV}}(\text{OH})_2]$	428 (5.56)	5.24 (3.56) 563 (4.43) 603 (4.52)
$(\text{H}_2)_3$	420 (5.76)	5.17 (4.11) 553 (4.02) 592 (3.88) 648 (3.80)
Sn_3	430 (5.70)	5.23 (3.65) 5.64 (4.40) 6.05 (4.39)
$(\text{H}_2)_6\text{Sn}_3$	422 (5.99)	5.19 (4.69) 5.60 (4.70) 604 (4.52) 650 (4.27)

a) Error limits: $\lambda_{\text{max}} \pm 1$ nm; log ϵ , $\pm 10\%$

exciton coupling between the porphyrin rings (i. e. axial-axial, axial-basal or basal- basal).

Fig. 3. 3 illustrates the ^1H NMR spectrum of $(\text{H}_2)_6\text{Sn}_3$ along with the proton assignments, which are made on the basis of ^1H NMR data of the corresponding trimeric³⁵ and hexameric⁴⁰ arrays as well as on examination of the ^1H - ^1H COSY spectral features. **Table 3. 2** summarizes the ^1H NMR data of $(\text{H}_2)_6\text{Sn}_3$ along with that of relevant reference porphyrins. All the twenty four β -pyrrole protons present on the three tin(IV) porphyrins of the nonamer (protons of the type a, see Fig. 3. 3) resonate at 9.35 (m, 24H) ppm. On the

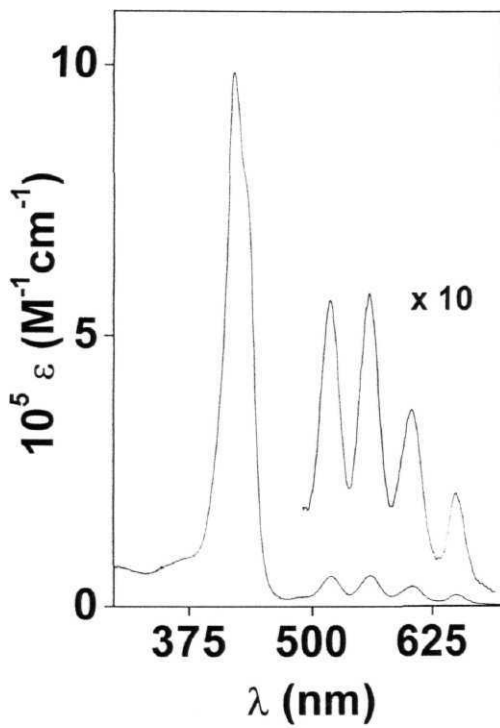


Fig. 3. 2 UV-visible spectrum of $(\text{H}_2)_6\text{Sn}_3$ in CH_2Cl_2 .

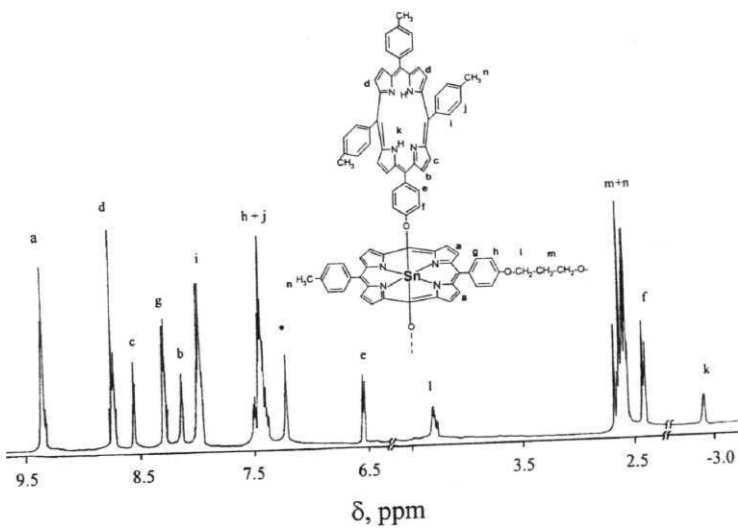


Fig. 3. 3 ^1H NMR spectrum of $(\text{CDCl}_3, \text{TMS})$ of $(\text{H}_2)_6\text{Sn}_3$.

Table 3. 2 ¹H NMR data (CDCl₃, TMS)^a

Compound	5, ppm [J _{HH}], Hz						
	P- pyrrole (central) (a)	P- pyrrole (axial) (d, c & b)	Axial Phenyl (e, f)	-NH (k)	Meso- tolyl (g, h, i & j)	Spacer -OCH ₂ (l)	-CH ₂ , -CH ₃ (m, n)
[H ₂ (p-OH)TriTP]	8.88 (s, 8H)	-	-	-2.73 (s, 2H)	8.18 (d, 8H) [8.4] 7.45 (d, 6H) [8.4] 7.22 (d, 2H) [8.4]	-	2.78 (s, 9H)
[H ₂ (p-OH) ₂ DiTP]	8.87 (s, 8H)	-	-	-2.72 (s, 2H)	8.15 (d, 8H) [8.6] 7.48 (d, 4H) [8.6] 7.21 (d, 4H) [8.6]	-	2.79 (s, 9H)
[H ₂ (p-O-(CH ₂) ₃ - Br)TriTP]	8.88 (s, 8H)	-	-	-2.73 (s, 2H)	8.18 (d, 8H) [8.2] 7.51 (d, 6H) [8.2] 7.31 (d, 2H) [8.2]	4.48, 4.36 (t, 4H)	2.78 (s, 9H) 2.79 (m, 2H)

(continued)

(H₂)₃	8.89 (m, 24H)			-2.72 (s, 6H)	8.12 (m, 24H) 7.48 (m, 24H)	4.63 (t, 8H)	2.78 (m, 28H)
Sn₃	9.15 (m, 24H)	-	-	-	8.23 (m, 24H) 7.55 (m, 24H)	4.65 (t, 8H)	2.69 (m, 28H)
(H₂)₆Sn₃	9.35 (m, 24H)	8.75 (m, 24H) 8.51 (d, 12H) [5.0] 8.15 (d, 12H) [5.0]	6.55 (d, 12H) [7.9] 2.40 (d, 12H) [7.9]	-2.90 (s, 12H)	8.30 (d, 24H) [7.0] 7.98 (m, 36H) 7.43 (m, 60H)	4.28 (m, 8H)	2.62 (m, 82H)

a) Error limits: 8, ± 0.01 ppm; J, ± 1 Hz

other hand, P-pyrrole proton signals of the axial free-base porphyrins are seen to be shifted to the upfield region (compared to those of **[H₂(p-OH)TriTP]**) and are also split into a multiplet (8. 75, m 24H) and a pair of doublets at 8. 51(d, 12H) and 8. 15 ppm (d, 12H). The resonances centered at 8. 75, 8. 51 and 8. 15 ppm are assigned to protons of the type d, c and b respectively, that are differently affected by the ring current of the central metalloid porphyrin.⁴¹ On the other hand, protons **meta**- (type e) and ortho- (type f) to the phenoxo groups of the free-base porphyrins, being affected by both the inherent deshielding

effect of the axial free-base porphyrin and the shielding effect of the basal porphyrin, resonate at 6.55 (d, 12H) and 2.40 ppm (d, 12H) respectively, as detected by the proton connectivity pattern in the corresponding ^1H - ^1H COSY spectrum. The inner imino protons of the axial free-base porphyrins (type k) of $(\text{H}_2)_6\text{Sn}_3$ are seen to experience the 'long range' shielding effect due to ring current of the basal tin(IV) porphyrin and resonate at -2.90 ppm (s, 12H) as against the corresponding -NH protons of $[\text{H}_2(\text{p-OH})\text{TriTP}]$ that appear at -2.73 ppm. The ortho- and meta- phenyl protons of the meso-tolyl groups (g and h, see: Fig. 3. 3) on the basal tin(rV)porphyrins, being located in a deshielding zone of each porphyrin ring current, resonate at 8.30 and 7.43 ppm, respectively. The corresponding protons of the axial free-base porphyrins (protons i and j) resonate as multiplets centered at 7.98 and 7.43 ppm, respectively (Table 3. 2). The terminal methylene protons of the spacer $-\text{O}-\text{CH}_2-\text{CH}_2-\text{CH}_2-\text{O}-$ (protons l) of the Sn_3 backbone in $(\text{H}_2)_6\text{Sn}_3$ resonate as a multiplet at 4.28 ppm, whereas the central methylene protons (m) resonate at 2.62 ppm - a region in which all the methyl protons (protons n) also resonate.

An additional concern with this class of octahedral tin(IV) complexes is lability of the axial bonds and, has indeed been investigated earlier by the NMR method for tin(IV) porphyrins having 'inorganic' or 'organic' ligands.⁴²⁻⁴⁴ Specifically, ^1H NMR studies carried out earlier on $\{(\text{P})\text{Sn}^{\text{IV}}(\text{OC}(\text{O})\text{A})_2\}$ (where P is a tetraryl porphyrin and $\text{OC}(\text{O})\text{A}$ is the axially ligated anthracene 9-carboxylate subunit), have revealed presence of the ligand on-off equilibrium, in

addition to the *n-n* interaction between the porphyrin and anthracene rings.⁴⁴ In contrast, neither the *n-n* interaction nor the ligand on-off equilibrium was discernable from the NMR data of **(H₂)₆Sn₃**, as is the case with its trimeric and hexameric predecessors.^{35,40} This observation indicates that, under the present set of experimental conditions, the two trans free-bases are strongly bound in a symmetric manner at each tin(IV) center in these tin(IV) porphyrin based arrays. In addition, the fact that resonance positions of the various protons of the axial free-base ligands present in **(H₂)₆Sn₃** are close to those of the corresponding protons of the **trimer/hexamer** suggests that the interaction between the axial rings bound at different tin(IV) centers are minimal in this higher array. However, it should be noted that free rotations about the axial Sn-O bonds can not be altogether neglected in this 'axial-bonding' type array. The issues concerning the axial bond rotation and the conformational equilibria that are possible in **(H₂)₆Sn₃** can be addressed with the help of variable temperature NMR data, but such experiments have not been carried out during the present study.

The electrochemical redox potentials, as measured from the cyclic- and differential pulse voltammetric measurements, also reveal the absence of electronic interaction between the various porphyrin rings in **(H₂)₆Sn₃**. Fig. 3. 4 illustrates the differential pulse voltammograms obtained during the cathodic scan and Table 3. 3 provides redox potential data of **(H₂)₆Sn₃** and the corresponding reference porphyrins. The nonameric array undergoes up to four

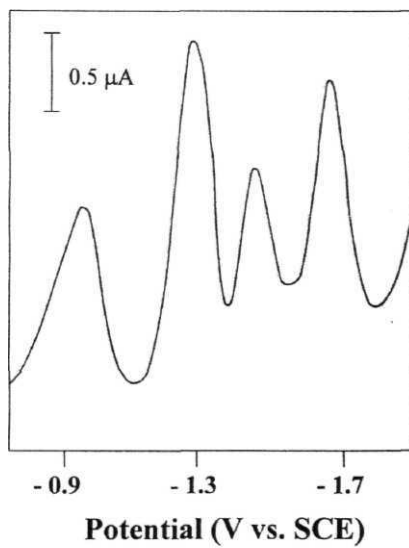


Fig. 3. 4 Differential pulse voltammogram of $(\text{H}_2)_6\text{Sn}_3$ in CH_2Cl_2 , 0.1M TBAP (scan rate 10 mV s^{-1}).

Table 3. 3 Redox potential data in CH_2Cl_2 , 0. 1 M TBAP ⁱ

Compound	Potential, V vs. SCE	
	Reduction	Oxidation
[H₂(p-OH)TriTP]	-1.24, -1.64	0. 94, 1.30 ^b
[H₂(p-OH)₂DiTP])	-1.20,-1.60	0.89,1.33"
[H₂(p-O-(CH₂)₃Br)TriTP]	-1. 12, -1.44	1. 02, 1. 28 ^b
[(TTP)Sn^{IV}(OH)₂]	-0.88,-1.02	1.39"
(H₂)₃	-1. 14,-1.45	1.02, 1. 39 ^b
Sn₃	-0.89,-1.27	1.44"
(H₂)₆Sn₃	-0.96, -1. 28, -1. 47 ^b , -1. 68	0.83,1.37"

a) Error limits: $E_{1/2} \pm 0.03$ V

b) Quasi-reversible/irreversible

reduction steps (Fig. 3. 4) and up to two oxidation steps in CH_2Cl_2 , 0.1 M TBAP. Wave-analysis of the corresponding cyclic voltammetric responses suggested that, in general, the first oxidation and also the first two reduction steps are reversible ($i_p/i_a = 0.9 - 1.0$ where i_p is the peak current) and diffusion controlled ($i_p/v = \text{constant}$ in the scan rate (v) range 50 - 500 mV s^{-1}) one-electron transfer ($\Delta E_p = 60\text{-}70$ mV where ΔE_p is the peak-to-peak potential difference; $\Delta E = 65 \pm 3$ mV for Fc/Fc⁺ couple) reactions.⁴⁵ The subsequent

steps are either quasi-reversible ($AE_p = 90 - 200 \text{ mV}$ and $i_{an}/i_{cat} = 0.5 - 0.8$ in the scan rate $100 - 500 \text{ mV s}^{-1}$) or totally irreversible.⁴⁵ Based on redox potential data of the individual monomers (i.e. $[H_2(p-OH)TriTP]$ and $[(TTP)Sn^{IV}(OH)_2]$) and also that of $[(TTP)Sn^{IV}(OPh)_2]$ (where OPh is the axially ligated phenoxy group),⁴⁶ the various midpoint potentials have been assigned to either the basal- or the axial porphyrins. Analysis of the data reveals that the redox potentials of the hybrid array are in the same range as those of the corresponding monomeric analogues or the precursor trimeric porphyrins.

Collectively, UV-visible, 1H NMR and redox potential data indicate that there exists a symmetric disposition of the two axial free-base porphyrins with respect to plane of the corresponding basal tin(IV) porphyrin in $(H_2)_6Sn_3$. These data also indicate that there is no specific interaction between the neighboring axial free-base porphyrins in this array. Notwithstanding this analysis, it needs to be emphasized that the structural drawing of $(H_2)_6Sn_3$ shown in Fig. 3. 1 does not necessarily convey the actual arrangement of the porphyrin rings. Specifically, the $Sn-O-C$ angles are not equal to 180° ; instead, it is likely that the free-base porphyrins might be somewhat diagonally disposed towards the tin(IV) porphyrins in this array as reported for $[(P)Sn^{IV}(ONap)_2]$ (where Nap is the axially ligated naphthyl subunit).⁴⁷ To date, attempts to grow single crystals of this large array for the possible determination of its structure by the X-ray crystallographic method have been unsuccessful.

3. 3. 3 Singlet State Properties

When excited at 445 nm, the **tri-tin(IV)trimer Sn₃** showed a typical two-banded fluorescence spectrum in CH₂Cl₂ with the emission maxima centered at 615 (band I) and 667 nm (band II). The quantum yield of fluorescence (ϕ) of this tin(IV) porphyrin precursor is found to be close to that of the reference porphyrin **[(TTP)Sn^{IV}(OH)₂]** ($\phi = 0.05$) as measured in the band I region. Excitation ($\lambda_{\text{exc}} = 405$ nm) of the precursor free-base porphyrins, **[H₂(p-OH)TriTP]** and **(H₂)₃** also resulted in a two-banded spectra; the emission maximum of the major band is located in the band II region (655 nm) mentioned above and the minor band is centered at ~ 720 nm (band III) in each case. The fluorescence quantum yield of **(H₂)₃** is found to be nearly equal to that of **[H₂(p-OH)TriTP]** ($\phi = 0.12$). These data of the **monomeric** and trimeric porphyrin precursors (Table 3. 4) indicate that it is possible to individually address the singlet state properties of the axial and basal porphyrins in **(H₂)₆Sn₃**. Thus, irradiation of this **nonameric** hybrid array at 405 nm should result in a predominant absorption by the axial free-base porphyrins and that at 445 nm excites the central tin(IV) porphyrins. Moreover, fluorescence due to the tin(IV) and free-base components of the array can be exclusively monitored at bands I and III respectively, with the band II being common to both. Armed with this information, fluorescence studies were carried out for **(H₂)₆Sn₃** and the results reveal that, unlike the case with the ground state properties, the singlet state activity of this array is quite different from the

corresponding activities of its precursor reference compounds, as described below.

3. 3. 3. 1 Excitation at 445 nm

Excitation of toluene, CH_2Cl_2 or dimethylformamide solutions of $(\text{H}_2)_6\text{Sn}_3$ at 445 nm was seen to result in strong quenching of its fluorescence with respect to fluorescence of $[(\text{TTP})\text{Sn}^{\text{IV}}(\text{OH})_2]$. In fact, the % quenching ($\%Q_1$, equn. 3. 1) is close to 100 in each investigated solvent, with the band I that is characteristic of the tin(IV) porphyrin emission being totally absent in the spectrum of this array (see: Fig. 3. 5 and Table 3. 4).

$$Q, = (\phi([(TTP)Sn^{\text{IV}}(OH)_2]) - \phi((H_2)_6Sn_3)) / \phi([(TTP)Sn^{\text{IV}}(OH)_2]) \quad (3.1)$$

This total quenching of emission observed for $(\text{H}_2)_6\text{Sn}_3$ is in contrast with the partial quenching observed when the trimer $(\text{H}_2)_2\text{Sn}$ was excited under the similar set of experimental conditions of excitation wavelength and solvent, Fig. 3. 5. Inspection of this figure reveals that while spectrum of the trimer shows the presence of band I along with bands II and HI, that of $(\text{H}_2)_6\text{Sn}_3$ is characterized by only bands II and III. It should be noted here that appearance of the bands II and III that are ascribable to the free-base porphyrin emission in the spectra of

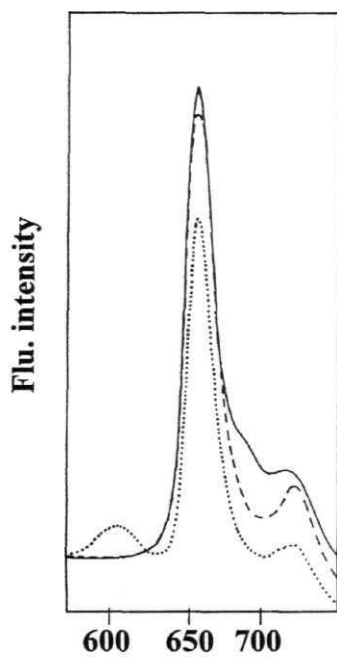


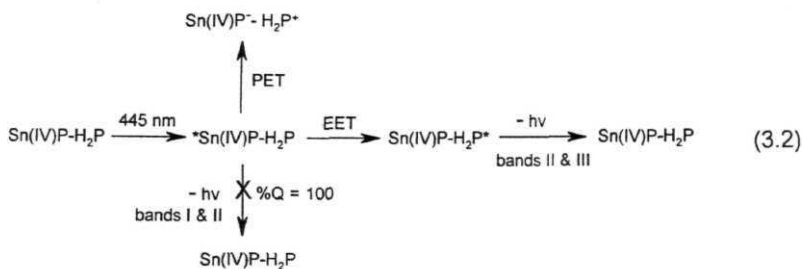
Fig. 3. 5 Fluorescence spectra of equi-absorbing (O. D. = 0.16) solutions of $(\text{H}_2)_6\text{Sn}_3$ (—), $(\text{H}_2)_4\text{Sn}_2$ (—) and $(\text{H}_2)_2\text{Sn}$ (.....) in toluene ($\lambda_{\text{exc}} = 445$ nm)

Table 3. 4 Fluorescence data^a

Compound	Toluene		CH ₂ Cl ₂		DMF	
	$\lambda_{em}, nm (\phi, \% Q)$		$\lambda_{em}, nm (\phi, \% Q)$		$\lambda_{em}, nm (\phi, \% Q)$	
	$\lambda_{ex} = 405\text{ nm}$	$\lambda_{ex} = 445\text{ nm}$	$\lambda_{ex} = 405\text{ nm}$	$\lambda_{ex} = 445\text{ nm}$	$\lambda_{ex} = 405\text{ nm}$	$\lambda_{ex} = 445\text{ nm}$
[H ₂ (p-OH)TriTP]	656.721 (0.11)		655.717 (0.12)		655.718 (0.11)	-
[H ₂ (p-OH) ₂ DiTP]	655.716 (0.10)	-	656.719 (0.10)	-	658.719 (0.11)	-
[H ₂ (p-O(CH ₂) ₃ Br)TriTP]	656.718 (0.11)		658.719 (0.10)	-	657.720 (0.11)	-
[(TTP)Sn ^{IV} (OH) ₂]	-	614, 660 (0.06)	-	614,667 (0.05)	-	615.665 (0.02)
(H ₂) ₃	655.720 (0.12)	-	658.719 (0.11)	-	655.718 (0.11)	-
Sn ₃		616, 667 (0.05)	-	615,665 (0.05)	-	616,666 (0.03)
(H ₂) ₆ Sn ₃	657.720 (0.010,97)	657, 719 (0.001, 100)	656.720 (0.006.94)	657,719 (0.001, 100)	658,719 (0.004, 94)	657.718 (0.001. 100)

a) Error limits: $\lambda_{em}, \pm 2\text{ nm}$; $\phi, \pm 10\%$

this **nonamer** when $\lambda_{exc} = 445\text{ nm}$ is not due to the direct excitation of its axial free-base components (Note, in this regard, that absorbance due to the free-base components of both **(H₂)₆Sn₃** and **(H₂)₂Sn** is minimum (<5%) at 445 nm) Rather, it is a consequence of the excitation energy transfer (EET) from the central metalloid porphyrin to the axial free-base porphyrin, as represented in equn. 3. 2.



In equn. 3. 2, Sn(IV)P and H_2P are the tin(IV)- and free-base porphyrin components present in the **nonameric** array, respectively and * represents the electronically excited singlet state. Such an intramolecular EET is a thermodynamically favored process in this array; singlet state energy of the tin(IV) porphyrin is higher (2.04 ± 0.03 eV) than that of the free-base analogue (1.94 ± 0.04 eV). Additionally, there is a considerable overlap of absorption by the free-base porphyrin and emission by the tin(IV) porphyrin in the 580 - 640 nm region. Indeed, estimation of the Forster overlap integral, J_{Forster} , by utilizing the emission spectrum of $[(\text{TTP})\text{Sn}^{\text{IV}}(\text{OH})_2]$ and absorption spectrum of H_2TTP gave a value that is as high as $1.40 \pm 0.2 \times 10^{14} \text{ cm}^6 \text{ mmol}^{-1}$ (equn. 3. 3)⁴⁸

$$J_{\text{forster}} = \frac{\int F(\bar{\nu}) \epsilon(\bar{\nu}) \nu^{-4} d\nu}{\int F(\bar{\nu}) d\nu} \quad (3.3)$$

where $F(\bar{\nu})$ is fluorescence intensity of $[(\text{TTP})\text{Sn}^{\text{IV}}(\text{OH})_2]$ at wavenumber ν (cm^{-1}), and ϵ is the molar extinction coefficient ($\text{mmol}^{-1} \text{cm}^{-1}$) of H_2TTP . Further support for the intramolecular energy transfer being the quenching mechanism comes from the excitation spectral measurements. Overlap of the normalized excitation spectrum (emission collected at 720 nm - where the emission is exclusively due to the free-base porphyrins) with the corresponding absorption spectrum of $(\text{H}_2)_6\text{Sn}_3$ revealed that efficiency of the intramolecular EET from the basal tin(IV) porphyrin to the axial free-base porphyrins in $(\text{H}_2)_6\text{Sn}_3$ is $\sim 85 \pm 10\%$ - a value close to that observed for the corresponding hexamer $(\text{H}_2)_4\text{Sn}_2$.⁴⁰ On the other hand, the reported EET efficiency for the lower homologue $(\text{H}_2)_2\text{Sn}$ is only $68 \pm 10\%$.³⁵ Interestingly, the higher fluorescence intensities observed for $(\text{H}_2)_6\text{Sn}_3$ compared to the trimer, under the similar set of experimental conditions (see Fig. 3. 5), is consistent with this variation of EET efficiency. The reason/s for the efficient EET observed for the higher homologues compared to the trimer in this class of 'axial-bonding' type hybrid arrays is still unclear. However, it should be noted that the number of acceptors (i. e. free-base porphyrins) in the neighborhood of a given donor (i. e. tin(IV) porphyrin) increases as one moves from the lower homologue to the

higher D-A ensembles in this series. Thus, unlike the case with the **trimer** where EET is from the basal tin(IV) porphyrin to its (own) two axial free-base acceptors, additional energy transfer from a given tin(IV) porphyrin to the free-bases ligated at the neighboring tin(IV) centers (i.e. 'trans-axial' energy transfer) is likely to occur in the higher arrays leading to more efficient quenching. Interestingly, the high efficiency of energy transfer from the basal tin(IV) porphyrin to the axial free-base acceptors observed here for the 'axial-bonding' type D-A array **(H₂)₆Sn₃** is in contrast with an inefficient flow of energy from a zinc(II) porphyrin to the axially ligated free-base porphyrin both of which are a part of an elegantly assembled 'wheel-and-spoke' array reported by Lindsey and co-workers.³³

As the quenching efficiency is **100%** but, the EET efficiency is ~ 85% for these arrays, it was found necessary to examine pathways other than the EET to explain the observed quantitative quenching. Among the various other mechanisms considered, a photoinduced electron transfer (PET) from the ground state free-base porphyrin to the singlet tin(IV) porphyrin seems to be more probable. This PET reaction in **(H₂)₆Sn₃** leads to a charge transfer state of the type **Sn(IV)P⁻ - H₂P⁺**, and involves free-energy change ($\Delta G_1(\text{PET})$) of **-0.25 ± 0.04 eV** (equn. 3.4).

$$\Delta G_1(\text{PET}) = E^{\text{ox}}(\text{H}_2\text{P}) - E^{\text{red}}(\text{Sn(IV)P}) - E_{0-0}(\text{Sn(IV)P}) \quad (3.4)$$

Where $E^{\text{ox}}(\text{H}_2\text{P})$ and $E^{\text{red}}(\text{Sn(IV)P})$ are the oxidation potential of the axial free-base porphyrin and the reduction potential of the basal **tin(IV)** porphyrin respectively, and $E_{0-0}(\text{Sn(IV)P})$ is singlet state energy of the tin(IV) porphyrin. Thus, the co-occurrence of an efficient EET and less prominent PET reactions as illustrated in equn. 3. 2 can rationalize the 100% fluorescence quenching observed for the tin(IV) porphyrins of this array.

3. 3. 3. 2 Excitation at 405 nm

Excitation of toluene, CH_2Cl_2 or dimethylformamide solutions containing **(H₂)₆Sn₃** at 405 nm resulted in a typical two-banded fluorescence spectrum in each case with emission maxima appearing at ~ 656 (band II) and ~ 718 (band III) nm. The quantum yields of fluorescence were measured based on the uncorrected fluorescence intensities in the band III region of the corresponding deconvoluted spectra using H2TPP as the standard, and were found to be much lower than those due to monomer [H₂(p-OH)TriTP] or trimer **(H₂)₃**. The %Q values (%Q₂, equn. 3. 5) for this array vary between 94 - 97.

$$Q_2 = (\phi([\text{H}_2(\text{p-OH})\text{TriTP}]) - \phi([\text{(H}_2)_6\text{Sn}_3])) / \phi([\text{H}_2(\text{p-OH})\text{TriTP}]) \quad (3. 5)$$

The Q_2 values thus evaluated for **(H₂)₆Sn₃** (see Table 3. 4) are quite close to the corresponding values of **(H₂)₄Sn₂** but are marginally higher than those reported for the trimeric homologue **(H₂)₂Sn**.^{35,40} As noted above, singlet state of the free-

base porphyrin lies at a lower energy than that of the **tin(IV)** derivative in these arrays and hence, an EET from the axial free-base porphyrins to the basal tin(IV) porphyrins can be safely ruled out as a quenching mechanism. On the other hand, a PET from singlet state of the axial free-base porphyrins to the tin(IV) macrocycle seems to be probable pathway of the observed quenching (see equn. 3.6).



Indeed, free-energy change for this PET ($\Delta G_2(\text{PET})$) is exoergic by 0.15 ± 0.03 eV for **(H₂)₆Sn₃** (equn. 3. 7).

$$\Delta G_2(\text{PET}) = E^{\text{ox}}(\text{H}_2\text{P}) - E^{\text{red}}(\text{Sn(IV)P}) - E_{0-0}(\text{H}_2\text{P}) \quad (3.7)$$

where $E_{0-0}(\text{H}_2\text{P})$ is singlet state energy of the free-base porphyrin. This interpretation is consistent with the similar interpretation made earlier for the trimeric and **hexmeric** species.^{35,40}

Overall, the above analysis reveals that singlet state dynamics of this nonamer involves: (i) EET from the basal **tin(IV)** porphyrin to the axial free-base porphyrin and PET from ground state of the free-base porphyrin to singlet state of the tin(IV) porphyrin (excitation at 445 nm) and (ii) PET from the singlet free-base porphyrin to the tin(IV) porphyrin (excitation at 405 nm), as illustrated

in Fig. 3. 6. While it was possible to experimentally verify the occurrence of EET reaction, PET has only been inferred based on the thermodynamic arguments.

3. 4 Summary

In summary, a new higher order array, $(\text{H}_2)_6\text{Sn}_3$, has been synthesized by adopting a hybrid 'organic - inorganic' protocol that involves synthetic manipulation at both the peripheral and axial sites of tin(IV) porphyrin scaffold. The array is highly soluble in various organic solvents and does not aggregate in solution as revealed by its spectral data. The structural features as probed, mainly, by the NMR method indicate unique 'axial-bonding' type architectural identity for this system. While the ground state properties of $(\text{H}_2)_6\text{Sn}_3$ are close to those of the corresponding reference compounds, the singlet state properties of it are quite different from those of the constituent monomers. Fluorescence quenching observed for the tin(IV)- and free-base porphyrin components of this **bichromophoric** system has been rationalized in terms of intra-array electron- and energy transfer reactions.

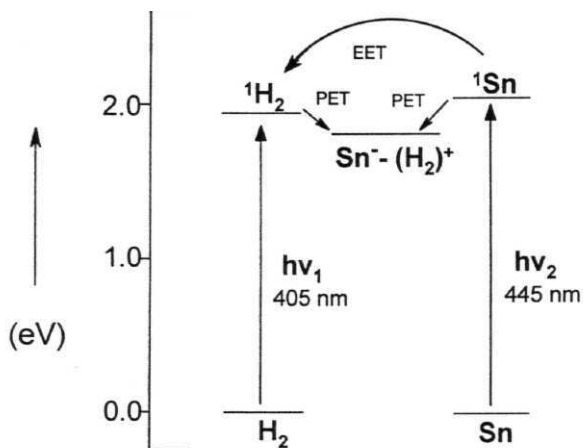


Fig. 3. 6 A generalized energy level diagram illustrating the singlet state dynamics of $(\mathbf{H}_2)_6\mathbf{Sn}_3$. The various energy levels were obtained by the absorption, emission, and redox data. EET = Excitation Energy Transfer and PET = Photoinduced Electron Transfer. \mathbf{H}_2 and Sn represent free-base and tin(IV) porphyrin components, respectively.

3. 5 References

1. Wojaczynski, J.; Latos-Grazynski, L. *Coord. Chem. Rev.* **2000**, *204*, 113.
2. Gust, D.; Moore, T. A. In *Hand book of porphyrins and related macrocycles*, Kadish, K. M.; Guillard, R.; Smith, K. M., Eds.; Academic Press: New York, 1999; Vol. 8, pp: 153 - 190.
3. Sanders, J. K. M. In *Hand book of porphyrins and related macrocycles*, Kadish, K. M.; Guillard, R.; Smith, K. M., Eds.; Academic Press: New York, 1999; Vol. 3, pp: 347-368.
4. Tsuda, A.; Nakamura, Y.; Osuka, A. *Chem. Commun.* **2003**, 1096.
5. Speckbacher, M.; Yu, L.; Lindsey, J. S. *Inorg. Chem.* **2003**, *43*, 4322.
6. Inomata, T.; Konish, K. *Chem. Commun.* **2003**, 1282.
7. Ballester, P.; Gomila, R. M.; Hunter, C. A.; King, S. H. M.; Twyman, L. *J. Chem. Commun.* **2003**, 39.
8. Ayabe, M.; Ikeda, A.; Kubo, Y.; Takeuchi, M.; Shinkai, S. *Angew. Chem. Int. Ed.* **2002**, *41*, 2190.
9. Lensen, M. C.; Castriano, M.; Coumans, R. E.; Foekema, J.; Rowan, A. L.; Scolaro, L. M.; Nolte, R. J. M. *Tetrahedron left.* **2002**, *43*, 9351.
10. Screen T. E. O.; Thorne, J. R. G.; Denning, R.; Bucknall, D. G.; Anderson, H. L. *J. Am. Chem. Soc.* **2002**, *124*, 9712.
11. Loewe, R. S.; Lammi, R. K.; Diers, J. R.; Kirmaier, C.; Bocian, D. F.; Holten, D.; Lindsey, J. S. *J. Mater. Chem.* **2002**, 1530.

12. Choi, M. S.; Aida, T.; Yamazaki, T.; Yamazaki, I. *Chem. Eur. J.* **2002**, *8*, 2668.
13. Higuchi, H.; Maeda, T.; Maiyabayashi, K.; Miyake, M.; Yamamoto, K. *Tetrahedron lett.* **2002**, *43*, 3097.
14. Susumu, K.; Therien, M. J. *Am. Chem. Soc.* **2002**, *124*, 8550.
15. Ambrosie, A.; Kirmier, C.; Wagner, R.; Loewe, R. S.; Bocian, D. F.; Lindsey, J. S. *J. Org. Chem.* **2002**, *67*, 3811.
16. Flamigni, L.; Marconi, G.; Dixon, I. M.; Collin, J. P.; Sauvage, J. P. *J. Phys. Chem. B.* **2002**, *106*, 6663.
17. Rucareanu, S.; Mongin, O.; Schuwey, A.; Hoyler, N.; Gossauer, A.; Amrein, W.; Hediger, H. U. *J. Org. Chem.* **2001**, *66*, 4973.
18. Maruyama, A.; Kobayashi, H.; Tanaka, H.; J. Mater. Chem., **2001**, 2262.
19. Promarak, V.; Burn, P. L. *J. Chem. Soc. Perkin Trans. I.* **2001**, 14.
20. Lammi, R. K.; Wagner, R. W.; Ambroise, A.; Bocain, D. F.; Holten, D.; Lindsey, J. S. *J. Phys. Chem. B.* **2001**, *105*, 5341.
21. Ikeda, C.; Tanaka, Y.; Fujihara, T.; Ishill, Y.; Ushiyama, T.; Yamamoto, K.; Yoshioka, N.; Inoue, H. *Inorg. Chem.* **2001**, *40*, 3395.
22. Takahashi, R.; Kobuke, Y. *J. Am. Chem. Soc.* **2003**, *125*, 2372.
23. Balaban, T. S.; Goddard, R.; Schaetzel, M. L.; Lehn, J. -M. *J. Am. Chem. Soc.* **2003**, *125*, 4233.

24. Redman, J. E.; Feeder, N.; **Teat**, S. J.; Sanders, J. K. M. *Inorg. Chem.* **2002**, *40*, 2486
25. Hunter, C. A.; Tregonning, R. *Tetrahedron* **2002**, *55*, 691.
26. Fallon, G. D.; Langford, S. L.; Lee, M. A. P.; Lygris, E. *Inorg. Chem. Commun.* **2002**, *5*, 715.
27. Lengo, E.; Zangrando, E.; Minaatel, R. Alessio, E. *J. Am. Chem. Soc.* **2002**, *124*, 1003.
28. **Tsuda**, A.; **Nakamura**, T.; Sakamoto, S.; Yamaguchi, K.; Osuka, A. *Angew. Chem. Int. Ed.* **2002**, *41*, 2817.
29. **Milic**, T. N.; Chi, N.; Yablon, D. G.; **Flynn**, G. W.; Batteas, J. D.; Drain, C. M. *Angew. Chem. Int. Ed.* **2002**, *41*, 2177.
30. **Barkigia**, K. ML; Battioni, P.; Riou, V.; Mansuy, D.; Fajer, J. *Chem. Commun.* **2002**, 956.
31. Yatskou, M. ML; Koehorst, R. B. M.; Donker, H.; **Schaafsma**, T. J. *J. Phys. Chem. A.* **2001**, *105*, 11425.
32. Mak, C. C; **Bampos**, N.; Darling, S. L.; Montaliti, M.; Prodi, L.; Sanders, J. K. M. *J. Org. Chem.* **2001**, *66*, 4476
33. **Ambroise**, A.; Li, J.; **Yu**, L.; Lindsey, J. S. *Org. Lett.* **2000**, *2*, 2563
34. Rao, T. A.; Maiya, B. G. *Chem. Commun.* **1995**, 939.
35. Giribabu, L.; Rao, T. A.; **Maiya**, B. G. *Inorg. Chem.* **1999**, *38*, 4971.
36. **Moghadam**, G. E.; Ding, L.; Tadj, F.; Meunier, B. *Tetrahedron* **1989**, *45*, 2641.

37. Lee, C. **H.**; Lindsey, J. S. *Tetrahedron* **1994**, *50*, 11427.
38. Little, R. G. *J. Heterocycl. Chem.* **1978**, *15*, 203.
39. Darling, S.; Mak, C. C; **Bampos**, N.; Feeder, N.; Teat, S. J.; Sanders, J. K. M. *New J. Chem.* **1999**, *23*, 359.
40. Kumar, A. A.; Giribabu, L.; Reddy, D. R.; Maiya. B. G. *Inorg. Chem.* **2001**, *40*, 6757.
41. Abraham, R. J.; Bedford, G. R.; McNeillie, D.; Wright, B. *Org. Magn. Reson.* **1980**, *14*, 418.
42. Kadish, K. M.; Xu, Q. Y.; Maiya, B. G.; Barbe, J. -M. Guillard, R. J. *Chem. Soc. Dalton Trans.* **1989**, 1531.
43. Hawley, J. C. *Ph. D. Thesis*, University of Cambridge, U.K., 1998.
44. Hawley, J. C; Bampos, N.; Abraham, R. J.; Sanders, J. K. M. *Chem. Commun.*, **1998**, 661.
45. Nicholson, R. S.; Shain, I. *Anal. Chem.* **1964**, *36*, 706.
46. Buchler, J. W.; Puppe, L.; Rohbock, K.; Schneehage, H. H, *Chem. Ber.* **1973**, *106*, 2710.
47. **Nimri**, S.; Keinan, E. *J. Am. Chem. Soc.* **1999**, *121*, 8978.
48. Forster, T. *Discuss. Faraday Soc.* **1959**, *27*, 7.

CHAPTER 4

A Photochemically-Active Supramolecular Array Assembled via the Complementary Binding Properties of Ruthenium (II) and Tin (IV) Porphyrins

4.1 Introduction

The recent resurgence in the coordination chemistry of metalloporphyrins is largely due to the realization that metal-ligand interactions provide a convenient means of constructing functional supramolecular arrays.¹ The available range of metals and porphyrin-based ligands and also the multitude of interactions between them has permitted what is otherwise a synthetically cumbersome modulation of the photophysical and electrochemical properties of the resulting supramolecular species.^{2,20} To this end, the well known binding of zinc(II) and ruthenium(II) to nitrogen and that of tin(IV) to oxygen has recently been employed to construct heterometallic porphyrin oligomers.²⁰ These oligomers were designed to exploit the complementary geometries and cooperative binding properties of the tailor-made metalloporphyrin building blocks. It is of interest to determine whether this theme can be 'amplified' to generate self-assembled, axially directed porphyrin arrays without relying on extended and inefficient syntheses of designed host and guest precursors. Research efforts made in this direction, during the present study, resulted in the design of a prototype trimeric array $(\text{Ru})_2\text{Sn}$, the

construction of which relies on the spontaneous self-assembly driven by independent coordination properties of the ruthenium(II) and tin(IV) centers (Fig. 4. 1). Unlike the case with the previously reported **heterometallic** porphyrins mentioned above, which are characterized by the nitrogen and oxygen donor functionalities built into their superstructures, the complementary binding achieved here is by an external, bifunctional ligand (i. e. pyridine-4-carboxylic acid) leading to the self-assembly of trimer **(Ru)₂Sn**. The design, construction and spectral characterization as well as the photophysical and electrochemical properties of this novel trimeric array are discussed in this Chapter.

4. 2 Experimental details

4. 2. 1 Synthesis of **5,10,15,20-tetra(3,5-di-tert-butylphenyl)porphyrinato ruthenium(II) carbonyl** $[(\text{DTPP})\text{Ru}^{\text{II}}(\text{CO})]$ ²¹

Tris-ruthenium dodecacarbonyl (0. 080 g, 0. 13 mmol) was added to a solution of 5,10,15,20-tetra(3,5-di-tert-butylphenyl) porphyrin (0. 033 g, 0. 024 mmol) in toluene (30 ml). The mixture was degassed by bubbling nitrogen for 10 **min.** and stirred at reflux for 18 h. It was allowed to cool, after which the solvent was removed and the residue was purified by silica gel column using hexane - ethylacetate (9 : 1 , v/v) as the eluent to give **[(DTPP)Ru^{II}(CO)]** as deep red solid. Yield: 0. 021 g (60 %)

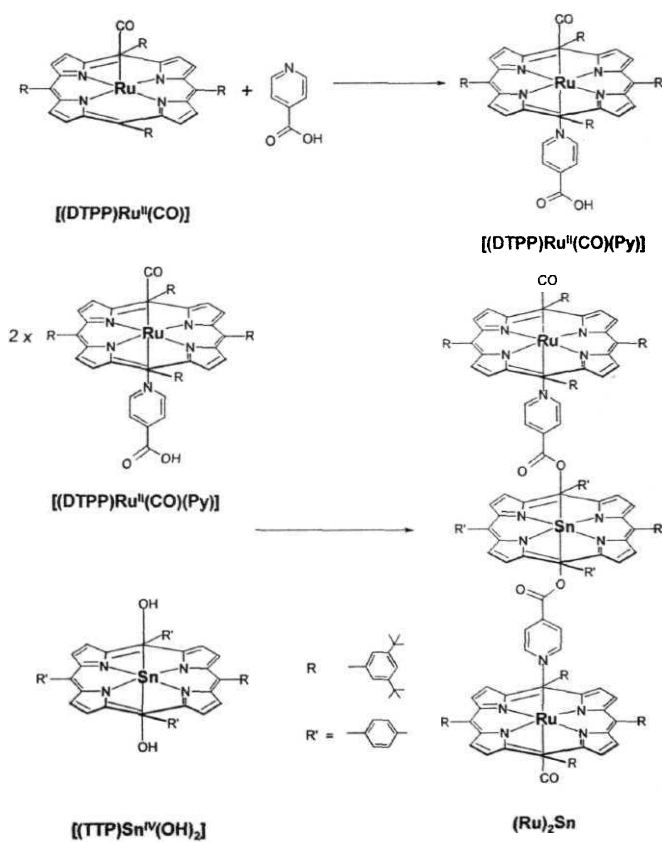


Fig. 4. 1 Scheme leading to the synthesis of $(Ru)_2Sn$.

4. 2. 2 Synthesis of 5,10,15,20-tetra(3,5-di-tert-butylphenyl)porphyrinato ruthenium(II) carbonyl pyridine carboxylic acid $[(\text{DTPP})\text{Ru}^{\text{II}}(\text{CO})(\text{Py})]$

$[(\text{DTPP})\text{Ru}^{\text{II}}(\text{CO})]$ (0. 003 g, 0. 013 mmol) was dissolved in 5 ml of CH_2Cl_2 . To this solution, 0. 0155 g (0. 126 mmol) of pyridine-4-carboxylic acid was added and the resulting mixture was sonicated and then heated at 40 °C for 5 min. The contents were passed through a pad of celite and the filtrate was evaporated to get the desired product in quantitative yield.

4. 2. 3 Synthesis of 5,10,15,20-tetra(4-methylphenyl)porphyrinato tin(IV) dihydroxide $[(\text{TTP})\text{Sn}^{\text{IV}}(\text{OH})_2]$ ²²

A mixture of 5,10,15,20-tetra(4-methylphenyl) porphyrin (2. 0 g, 3 mmol) and SnCl_2 (3. 0 g, 13 mmol) were dissolved in 50 ml of pyridine. The reaction mixture was then refluxed for 2 h., after which pyridine was removed under the reduced pressure. The solid obtained was taken up in CHCl_3 and washed several times with water. The organic layer was dried by passing through anhydrous Na_2SO_4 and chromatographed over basic alumina. Elution with CHCl_3 - CH_3OH (98 : 2, v/v) gave 5,10,15,20-tetra(4-methylphenyl)-porphyrinato tin(IV) dichloride $[(\text{TTP})\text{Sn}^{\text{IV}}\text{Cl}_2]$. To the CHCl_3 solution of $[(\text{TTP})\text{Sn}^{\text{IV}}\text{Cl}_2]$, 10% aqueous NaOH was added and the reaction mixture was stirred at room temperature for 2 h. The organic layer was separated and dried over anhydrous Na_2SO_4 to get violet solid of $[(\text{TTP})\text{Sn}^{\text{IV}}(\text{OH})_2]$, which was recrystallized from CH_2Cl_2 - hexane. Yield: 2. 43 g (90%)

4. 2.4 Synthesis of '(Ru (II) porphyrin)₂ - Sn(IV) porphyrin' ((Ru)₂Sn)

[(DTPP)Ru^{II}(CO)(Py)] (0.032 g, 0.024 mmol) was dissolved in 5 ml of CH₂Cl₂. To this, 0.010 g (0.012 mmol) of [(TTP)Sn^{IV}(OH)₂] was added and the resulting solution was sonicated for a few minutes. Evaporation of the solvent, first under a steady stream of nitrogen and then under vacuum, gave the desired product in quantitative yield.

All the spectroscopic and electrochemical experiments have been carried out as described in Chapter 2.

4. 3 Results and discussion

4. 3. 1 Design and synthesis

To achieve the construction of heterometallic trimer (Ru)₂Sn, ruthenium(II) and tin(IV) porphyrins are chosen in view of their contrasting coordination preferences. Ruthenium(II)(CO) porphyrins are known to adopt 6-coordinate geometry with an added nitrogen donor ligand and form stable and inert complexes.²³⁻²⁶ Tin(IV) porphyrins, on the other hand, prefer oxygen donor ligands, adopt 6-coordinate octahedral geometry and are also capable of exchanging the axial ligands.^{22,27} When complementary binding functions are introduced into appropriately designed ruthenium(II) and tin(IV) porphyrins, it becomes possible to assemble multiple components in a controlled manner; this has, indeed, been achieved earlier.^{6,20,28} In the present study, however, the complementary binding has been achieved by an external, bifunctional ligand

that incorporates both nitrogen and oxygen donor functionalities (i. e. pyridine-4-carboxylic acid) leading to the self-assembly of trimer **(Ru)₂Sn**.

The **monomeric** precursors employed during this study, viz: the five-coordinated **[(DTPP)Ru^{II}(CO)]** and the six-coordinated **[(TTP)Sn^{IV}(OH)₂]**, were prepared by closely following the known procedures.^{21,22} Trimer **(Ru)₂Sn** was constructed by both step-wise and one-pot methods. In the former method, the pyridine-bound ruthenium(II) porphyrin (**[(DTPP)Ru^{II}(CO)(Py)]**) was assembled first, by reacting together **[(DTPP)Ru^{II}(CO)]** and pyridine-4-carboxylic acid, with the 'pendant' carboxylic acid functionality being readily available for further coordination. The pyridine-acid itself is not soluble in organic solvents in which the porphyrin is soluble, but coordination by the ruthenium(II) porphyrin solubilizes this acid and allows one to obtain solutions of known concentration of **[(DTPP)Ru^{II}(CO)(Py)]**. Sonication of a solution containing **[(DTPP)Ru^{II}(CO)(Py)]** (2 equivalents) and **[(TTP)Sn^{IV}(OH)₂]** (1 equivalent) furnished **(Ru)₂Sn** in quantitative yield. The array was also prepared in one-pot by simply mixing **[(DTPP)Ru (CO)]**, **[(TTP)Sn^{IV}(OH)₂]** and pyridine-4-carboxylic acid in the appropriate stoichiometry.

4. 3. 2 Ground-state properties

Preliminary characterization of this new trimeic species was carried out by the UV-visible spectroscopic method. The wavelengths of maximum

absorption (λ_{max} , nm) and molar extinction coefficient (log ϵ) values of **(Ru)₂Sn** and those of its constituent individual compounds are summarized in Table. 4.

1. **UV-visible** spectra of the trimer and the monomers are illustrated in Fig. 4. 2. As seen, spectrum of the trimer is essentially a superposition of the spectra of its constituent components with the molar extinction coefficients at the peak maxima being close to those of **[(DTPP)Ru^{II}(CO)(Py)]** or **[(TTP)Sn^{IV}(OH)₂]**. This observation, coupled with the fact the λ_{max} values of **(Ru)₂Sn** are also similar to those of **[(DTPP)Ru^{II}(CO)(Py)]** and **[(TTP)Sn^{IV}(OH)₂]**, provides evidence for the absence of any electronic interaction between the porphyrin planes in this array. This is not surprising if one considers that the array has an 'axial-bonding' type architecture²⁹⁻³¹ and that the coordinated pyridine-acid spacer is dictating the separation distances between the porphyrin planes to be > 4 Å (CPK molecular model).

Table 4. 1 UV-visible data in CH₂Cl₂^a

Compound	λ_{max} , nm (log ϵ)	
	Soret band	Q-bands
[(TTP)Sn^{IV}(OH)₂]	427 (5.50)	561(4.15)601(3.92)
[(DTPP)Ru^{II}(CO)(Py)]	415(5.25)	532 (4.25)
(Ru)₂Sn	417(5.38)425(5.37)	532 (4.26) 562 (4.10) 602 (3.92)

a) Error limits: λ_{max} , ± 1 nm; ϵ , $\pm 10\%$

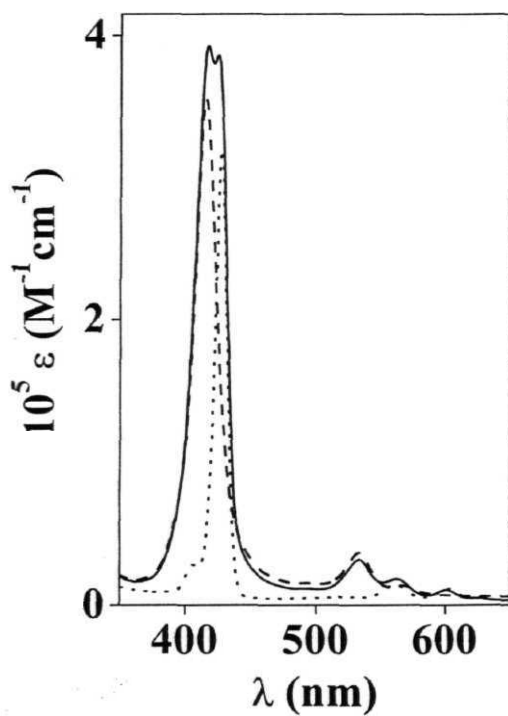


Fig. 4. 2 UV-visible spectra of $(\text{Ru})_2\text{Sn}$ (—), $[(\text{DTTP})\text{Ru}^{\text{II}}(\text{CO})(\text{Py})]$ (-----) and $[(\text{TTP})\text{Sn}^{\text{IV}}(\text{OH})_2]$ (.....).

Attempts were made to grow single crystals of **[(DTPP)Ru^{II}(CO)(Py)]** and **(Ru)₂Sn**. Crystals of **(Ru)₂Sn** suitable for X-ray diffraction could not be isolated, but complex **[(DTPP)Ru^{II}(CO)(Py)]** crystallized out in a P-1 space group. The crystallographic details are summarized in Table 4. 2.

Table 4. 2 Crystallographic data of **[(DTPP)Ru^{II}(CO)(Py)]**

Empirical formula	C ₈₉ H ₁₁₁ N ₅ O ₃ Ru
Formula weight	1399. 90
Temperature	180(2)
Wavelength	0. 71073 Å
Crystal system, space group	Triclinic, P-1
Unit cell dimensions	a = 13. 342 (2) Å a = 80.02(1) b = 16. 113 (2) Å β = 77.70(1) c = 25. 563 (2) Å γ = 69.65(1)
Volume	5004.6(10)
Z, Calculated density	2, 0. 929
Absorption coefficient	0. 197 mm ⁻¹
F (000)	1496
Crystal size	0. 20 x 0.15 x 0.10 mm
θ range for data collection	3. 52 to 27. 51°
Index ranges	-17 < h <17, -20 < k < 20, -33 < l < 33
Reflections collected / unique	22773/15643
Absorption correction (T _{min} , T _{max})	0. 9617, 0. 9806
Refinement method	Full-matrix least-squares on F ²
Data / restraints / parameters	15643/72/922
Goodness-of-parameters	1.055
Final R indices [I>2σ (I)]	R, = 0. 0779, wR ₂ = 0. 2352
R indices (all data)	R,=0. 1153, wR ₂ = 0.2640

Being too small in size for structural determination by normal laboratory X-ray methods, the crystal was subjected to high intensity synchrotron radiation source to obtain the structure. Fig. 4. 3 shows the structure of $[(\text{DTPP})\text{Ru}^{\text{II}}(\text{CO})(\text{Py})]$ thus obtained and it clearly shows the H-bonded dimeric nature of the complex with a O-H...O distance of 1. 843 Å. Therefore, self-assembly of array $(\text{Ru})_2\text{Sn}$ can be conceived to proceed with the breaking of these weak H-bonds prior to the competing 'ester' formation. It should be noted here that both the coordinated pyridyl ligand (Ru-N = 2. 201(3) Å) and CO (Ru-CO = 1. 839(4) Å) are near perpendicular to the porphyrin plane (dihedral angle approx 90°). Other details of the crystal structure data are summarized in the Appendix 1.

Structure of $(\text{Ru})_2\text{Sn}$ was probed in solution by the ^1H NMR spectroscopic method. The near perpendicular juxtaposition of the axial pyridine ligand with respect to the plane of the ruthenium porphyrin (*vide supra*), as evident in the crystal structure of $[(\text{DTPP})\text{Ru}^{\text{II}}(\text{CO})(\text{Py})]$, is expected to be retained in array $(\text{Ru})_2\text{Sn}$. Fig. 4. 4 compares the ^1H NMR spectra of $[(\text{DTPP})\text{Ru}^{\text{II}}(\text{CO})]$, $[(\text{DTPP})\text{Ru}^{\text{II}}(\text{CO})(\text{Py})]$ and $(\text{Ru})_2\text{Sn}$. Table 4. 3 summarizes the ^1H NMR data of $(\text{Ru})_2\text{Sn}$ along with that of relevant reference porphyrins. As seen from the Fig. 4. 4, α and β protons of the bound pyridine ligand in $[(\text{DTPP})\text{Ru}^{\text{II}}(\text{CO})(\text{Py})]$ are shielded by the porphyrin

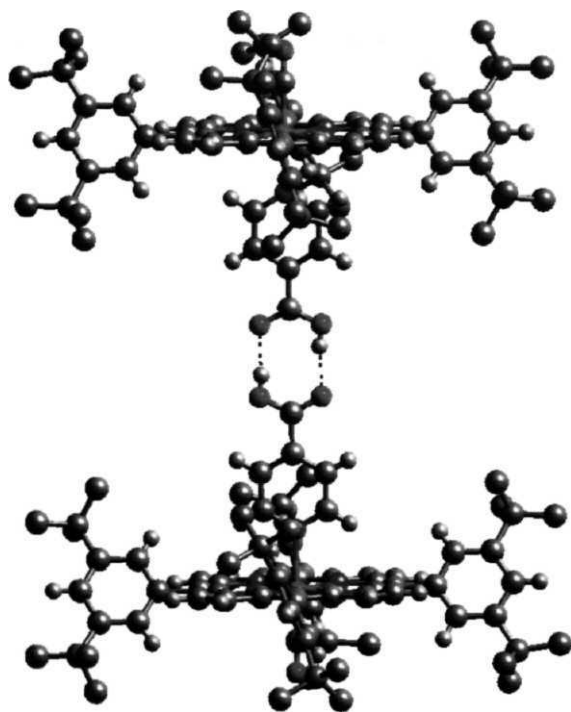


Fig. 4. 3 Crystal structure of $[(\text{DTPP})\text{Ru}^{\text{II}}(\text{CO})(\text{Py})]$. (color code: black, C, red, O; blue, N, purple, Ru).

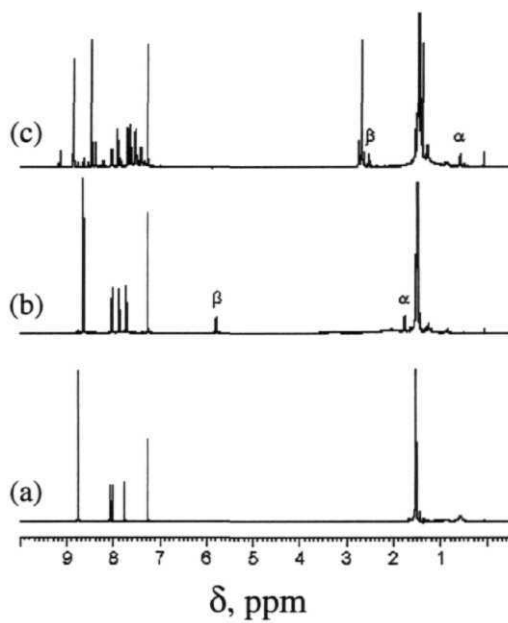


Fig. 4. ^1H NMR spectra (CDCl_3 , TMS) of (a) $[(\text{DTPP})\text{Ru}^{\text{II}}(\text{CO})]$ (b) $[(\text{DTPP})\text{Ru}^{\text{II}}(\text{CO})(\text{Py})]$ and (c) $(\text{Ru})_2\text{Sn}$. Peak at 7.26 ppm is due to the solvent.

Table. 4. 3 ^1H NMR data (CDCl_3 , TMS)^a

Compound	S, ppm $\{J_{\text{H-H}}\}$, Hz						
	β -pyrrole	α -phenyl	m-phenyl	p-phenyl	p & a Pyridyl	-CH ₃	t-butyl/hydroxy
$[(\text{TTP})\text{Sn}^{\text{IV}}(\text{OH})_2]$	9.15 (s, 8H)	8.22 (d, 8H) [7.8]	7.62 (d, 8H) [7.8]			2.74 (s, 9H)	-7.49 ^b (br, s, 2H)
$[(\text{DTPP})\text{Ru}^{\text{II}}(\text{CO})]$	8.76 (s, 8H)	8.04 (d, 8H) [8.4]		7.75 (s, 4H)			1.51 (s, 72H)
$[(\text{DTPP})\text{Ru}^{\text{II}}(\text{CO})(\text{Py})]$	8.68 (s, 8H)	8.0 (s, 4H) 7.8 (s, 8H)		7.65 (s, 4H)	5.81 (s, 2H) 1.77 (s, 2H)		1.51 (s, 72H)
$(\text{Ru})_2\text{Sn}^{\text{c}}$	8.94 (s, 8H) 8.31 (s, 16H)	7.45 (d, 8H) [7.9] 7.83 (s, 8H) 7.64 (s, 8H)	7.32 (d, 8H) [7.9]	7.49 (br s, 8H)	2.50 (d, 4H) [6.9] 0.57 (d, 4H) [6.9]	2.62 (s, 12H)	1.43 (s, 72H) 1.39 (s, 72H)

a) Error limits: δ , ± 0.01 ppm; J, + 1 Hz

b) Refer to the two axial hydroxy protons of this tin porphyrin

c) The 6 values are found to be the same for this array irrespective of the method
(i. e. step-wise/one-pot) utilized for its synthesis

ring-current³² and resonate at 1.77 and 5.81 ppm, respectively. The A8 ($\Delta\delta_1 =$

$\delta_{\text{pyridine-acid}} - \delta_{[(\text{DTPP})\text{Ru}^{\text{II}}(\text{CO})(\text{Py})]}$) values for the α and β protons are 7.03 and 2.

26 ppm, respectively. Resonances due to the same α and β protons in array **(Ru)₂Sn** are seen to be further shifted **upfield** to 0.57 and 2.50 ppm respectively (identified by ¹H - ¹H COSY see Fig. 4.5), due to the additional shielding effect exerted by the basal **tin(IV)** porphyrin. The corresponding $\Delta\delta_2 = \delta_{\text{pyridine-acid}} - \delta_{\text{(Ru)_2Sn}}$ values are 8.23 and 5.57 ppm respectively, thus providing evidence for the self-assembly of ruthenium(II) and tin(IV) porphyrins mediated by the pyridine-acid. Self-assembly of **(Ru)₂Sn** is also accompanied by disappearance of the axial hydroxy proton resonances (-7.49 ppm) of **[(TTP)Sn^{IV}(OH)₂]**.

The electrochemical redox potentials, as measured from the differential pulse voltammetric measurements, also reveal the absence of electronic interaction between the porphyrin rings in **(Ru)₂Sn**. Fig. 4.6 illustrates the differential pulse voltammograms obtained during the cathodic and anodic scans for this array and Table 4.4 summarizes redox potential data of **(Ru)₂Sn** and the corresponding monomeric porphyrins. The trimeric array undergoes up to four reduction steps (Fig. 4.6) and up to two oxidation steps in CH₂Cl₂, 0.1 M TBAP. Wave-analysis of the corresponding cyclic voltammetric responses suggested that while the first oxidation and also the first three reduction steps are reversible ($i_p/i_a = 0.9 - 1.0$ where i_p is the peak current) and diffusion controlled ($i_p/\nu = \text{constant}$ in the scan rate (ν) range 50 - 500 mV s⁻¹)

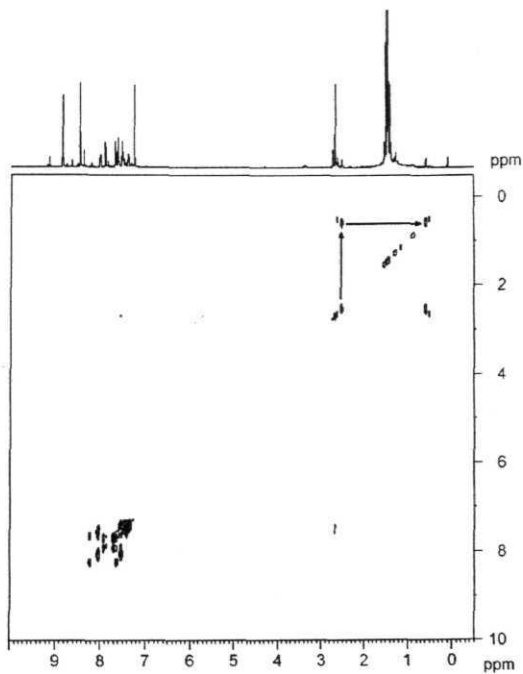


Fig. 4. 5 ^1H - ^1H COSY spectrum of **(Ru) $_2$ Sn** (CDCl_3 , TMS). The arrows indicate the presence of cross peaks for the pyridyl α and β protons.

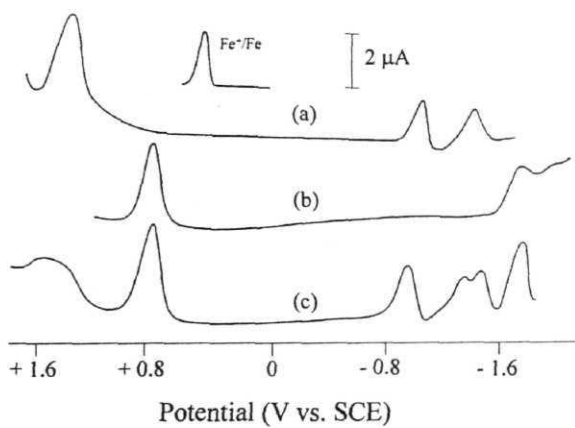


Fig. 4. 6 Differential pulse voltammograms of (a) $[(\text{TTP})\text{Sn}^{\text{IV}}(\text{OH})_2]$, (b) $[(\text{DTPP})\text{Ru}^{\text{II}}(\text{CO})(\text{Py})]$ and (c) $(\text{Ru})_2\text{Sn}$ in CH_2Cl_2 , 0.1 M TBAP (scan rate 10 mV s^{-1}).

Table 4. 4 Redox Potential data in CH_2Cl_2 , 0. 1 M TBAPⁱ

Compound	Potential, V vs. SCE	
	Oxidation	Reduction
$[(\text{TTP})\text{Sn}^{\text{IV}}(\text{OH})_2]$	1.41	-1.01,-1.41
$[(\text{DTPP})\text{Ru}^{\text{II}}(\text{CO})(\text{Py})]$	0.79	-1.76
$(\text{Ru})_2\text{Sn}$	0. 79, 1. 60 ^b	-0. 93, -1. 36, -1. 47, -1. 76 ^b

a) Error limits: $E_{1/2}, \pm 0.03 \text{ V}$

b) Quasi-reversible/irreversible

one-electron transfer ($\Delta E_p = 60 - 70 \text{ mV}$ where ΔE_p is the peak-to-peak: potential difference; $\Delta E_p = 65 \pm 3 \text{ mV}$ for Fc / Fc^+ couple) reactions, the subsequent steps are either quasi-reversible ($\Delta E_p = 90 - 200 \text{ mV}$ and $i_a / i_c = 0.5 - 0.8$ in the scan rate $100 - 500 \text{ mV s}^{-1}$) or totally irreversible.³³ The redox potentials of $(\text{Ru})_2\text{Sn}$ are found to be close to those of its monomeric components - $[(\text{DTPP})\text{Ru}^{\text{II}}(\text{CO})(\text{Py})]$ and $[(\text{TTP})\text{Sn}^{\text{IV}}(\text{OH})_2]$.

4. 3. 3 Singlet state properties

While the ruthenium(II) porphyrin component of this trimer was found to be non-fluorescent, as is the case with the monomeric porphyrins **[(DTPP)Ru^{II}(CO)]** and **[(DTPP)Ru^{II}(CO)(Py)]**, singlet state activity of the tin(IV) component of it was found to be quite different from that of **[(TTP)Sn^{IV}(OH)₂]**. A comparison of the UV-visible spectrum of **(Ru)₂Sn** with those of its two constituent monomeric porphyrin components suggests that photochemistry of the tin(IV) porphyrin in this trimer can be exclusively addressed by irradiating at 600 nm - a wavelength at which the ruthenium(II) porphyrin shows minimum absorption. Accordingly, a CH₂Cl₂ solution of the trimer was excited at 600 nm and it gave a fluorescence spectrum that is shown in Fig 4. 7. As seen in this figure, while the wavelength of maximum emission (λ_{em}) for the trimer is close to that of **[(TTP)Sn^{IV}(OH)₂]**, there is a quenching of fluorescence for the trimer. Fluorescence quantum yield (ϕ) of **(Ru)₂Sn** is evaluated to be nearly one third of the monomer, Table 4. 5. In addition, fluorescence lifetime (τ) of the trimer was found to be 0. 63±0.05 ns (92%; a long-lived component with a relative amplitude of 8% was also observed), while that of **[(TTP)Sn^{IV}(OH)₂]** is 1. 48±0.1 ns (see Fig. 4. 8 and Table 4. 5). This quenching of fluorescence observed for **(Ru)₂Sn** can be interpreted in terms of a photoinduced electron transfer (PET) from the axial ruthenium(II) porphyrin to the excited state of the basal tin(IV) porphyrin. Indeed, the free energy change for such a PET process (AGPET) is exoergic by 0. 32±0.04 eV, as

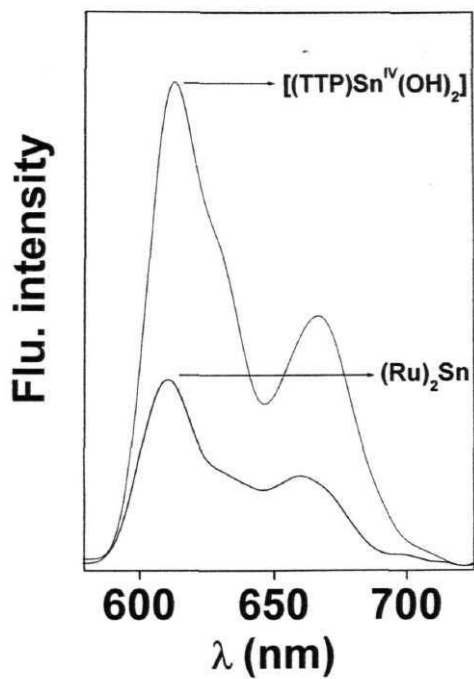


Fig. 4. 7 Fluorescence spectra of $[(\text{TTP})\text{Sn}^{\text{IV}}(\text{OH})_2]$ and $(\text{Ru})_2\text{Sn}$ in CH_2Cl_2 (λ_{exc} - 600 nm).

Table 4. 5. Fluorescence data in CH₂Cl₂

Compound	Steady state ^b λ_{em} , nm (ϕ)	Time-resolved ^c x (A %)
[(TTP)Sn^{IV}(OH)₂]	610, 665 (0. 024)	1.48±0.1 ns
(Ru)₂Sn	610, 660 (0. 007)	0. 63±0. 05 ns, (92%) 1.42±0. 01 ns,(8%)

a) Error limits: $\lambda_{em} + 2$ nm; ϕ , $\pm 10\%$.

b) $\lambda_{exc} = 600$ nm

c) $\lambda_{exc} = 440$ nm. Values in the parentheses refer to relative amplitudes of the respective decay components.

estimated from the redox potential data of the **trimer** and the singlet state energy of the **tin(IV)** porphyrin using equn. 4. 1.

$$= E^{ox}(\text{Ru(II)P}) - E^{red}(\text{Sn(IV)P}) - E_{0-0}(\text{Sn(IV)P}) \quad (4.1)$$

where $E^{ox}(\text{Ru(II)P})$ and $E^{red}(\text{Sn(IV)P})$ are the oxidation potential of the axial ruthenium(II) porphyrin and the reduction potential of the basal tin(IV) porphyrin, respectively (see: Table 4. 4) and $E_{0-0}(\text{Sn(IV)P})$ is the singlet state energy of the **tin(IV)** porphyrin (2. 04±0. 03 eV). Excitation energy transfer

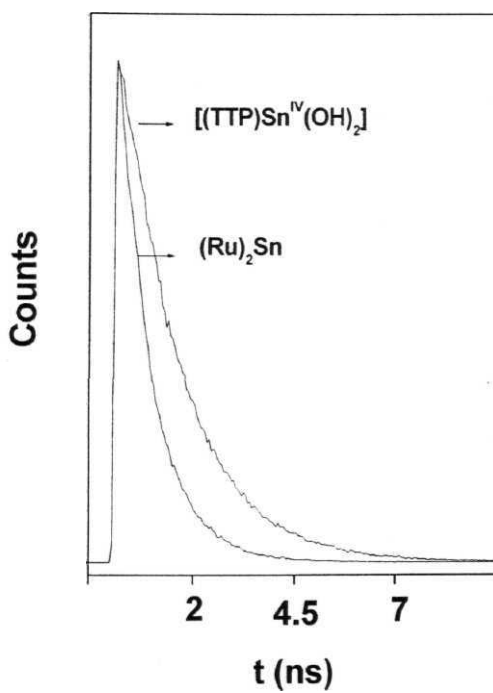


Fig. 4. 8 Time-resolved fluorescence decay of $[(\text{TTP})\text{Sn}^{\text{IV}}(\text{OH})_2]$ and $(\text{Ru})_2\text{Sn}$ in CH_2Cl_2 ($\lambda_{\text{exc}} = 440 \text{ nm}$).

between the two chromophores and heavy atom effect due to the ruthenium center are the other possible quenching mechanisms but, no direct/indirect evidence has been obtained for these processes to be operative in this system. Indeed, fluorescence due to $[(\text{TTP})\text{Sn}^{\text{IV}}(\text{OH})_2]$ was found to be unquenched in the presence of externally added $[(\text{DTPP})\text{Ru}^{\text{II}}(\text{CO})]$ (2 mole equivalents).

4. 4 Summary

In summary, a photochemically-functional, 'axial-bonding' type hybrid porphyrin trimer has been assembled by an advantageous utilization of the well known hard and soft acid-base (HSAB) principle and metal ion recognition by a ditopic ligand. While the ground state properties of the trimer are quite close to those of its constituent components, the singlet state properties are found to be quite different. The fluorescence quenching observed for the tin(IV) component of the trimer is rationalized in terms of a PET process. Clearly, the new strategy employed here for the construction of $(\text{Ru})_2\text{Sn}$ provides scope for building more elaborate arrays having interesting photochemical functions.

4. 5 References

1. Sanders, J. K. M.; Bampos, N.; Clyde-Watson, Z. W.; Darling, S. L.; Hawley, J. C; Kim, H. J.; Mak, C. C; Webb, S. J. In *Hand book of*

- porphyrins and related macrocydes*, Kadish, K. M.; Guillard, R.; Smith, K. M., Eds.; Academic Press: New York, 1999; Vol. 8, pp: 1 - 48.
2. Yin, J.; Guo, Q.; Palmer, R. E.; **Bambos**, N.; Sanders, J. K. M. *J. Phys. Chem. B.* **2003**, *103*, 209.
 3. Takahashi, R.; Kobuke, Y. *J. Am. Chem. Soc.* **2003**, *125*, 2372.
 4. Stulz, E.; Ng, Y. F.; Scott, S. M.; Sanders, J. K. M. *Chem. Commun.* **2002**, 524.
 5. Fallon, G. D.; Langford, S. L.; Lee, M. A. P.; Lygris, E. *Inorg. Chem. Commun.* 2002, *5*, 715.
 6. Redman, J. E.; Feeder, N.; Teat, S. J.; Sanders, J. K. M. *Inorg. Chem.* **2002**, *40*, 2486.
 7. Hunter, C. A.; Tregonning, R. *Tetrahedron* **2002**, *58*, 691.
 8. Tsuda, A.; **Nakamura**, T.; Sakamoto, S.; Yamaguchi, K.; Osuka, A. *Angew. Chem. Int. Ed.* **2002**, *41*, 2817.
 9. Mak, C. C; **Bambos**, N.; Darling, S. L.; Montaliti, M.; Prodi, L.; Sanders, J. K. M. *J. Org. Chem.* **2001**, *66*, 4476
 10. Ikeda, C; Tanaka, Y.; Fujihara, T.; Ishii, Y.; Ushiyama, T.; Yamamoto, K.; Yoshioka, N.; Inoue, H. *Inorg. Chem.* **2001**, *40*, 3395.
 11. Ogawa, K.; Kobuke, Y. *Angew. Chem. Int. Ed.* **2000**, *39*, 4070.
 12. Haycock, R. A.; Yartsev, A.; Michelsen, U.; Sundstrom, V.; Hunter, C. A. *Angew Chem. Int. Ed.* **2000**, *39*, 3616.
 13. Chichak, K.; Branda, N. R. *Chem. Comm.* **2000**, 1211.

14. Felluga, F.; Tecilla, P.; Hillier, L.; Hunter, C. A.; Licini, G.; Scrmin, P. *Chem. Commun.* **2000**, 1087.
15. Ikeda, C; Nagahara, N.; Yoshioka, N.; Inoue, H. *New J. Chem.* **2000**, 24, 897.
16. Darling, S. L. Stulz, E. Feeder, N. Bampos N. Sanders, J. K. M. *New J. Chem.* 2000,24,261.
17. Webb, S. J.; Sanders, J. K. M. *Inorg. Chem.* 2000, 39, 5912.
18. Alessio, E.; Geremia, S.; Mestroni, S.; Srnova, I.; Slouf, M.; Gianferrara, T.; Prodi, A. *Inorg. Chem.* **1999**, 38, 2527.
19. Darling, S. L.; Mak, C. C; Bampos, N.; Feeder, N.; Teat, S. J.; Sanders, J. K. M. *New J. Chem.* **1999**, 23, 359.
20. Kim, H. J.; Bampos, N.; Sanders, J. K. M. *J. Am. Chem. Soc.* **1999**, 727,8120.
21. Barley, M.; Becker, J. Y.; Domazetis, G.; Dolphin, D.; James, B. R. *Can. J. Chem.* **1983**, 61, 2389.
22. Kadish, K. M.; Xu, Q. Y.; Maiya, B. G.; Barbe, J. -M.; Guillard, R. J. *Chem. Soc. Dalton Trans.* **1989**, 1531.
23. Chow, B. C; Cohen, I. A. *Bioinorg. Chem.* **1971**, 7, 57.
24. Tsutsui, M.; Ostfeld, D.; Hoffman, L. M. *J. Am. Chem. Soc.* **1971**, 93, 1820.
25. Tsutsui, M.; Ostfeld, D.; Francis, J. N.; Hoffman, L. M. *J. Coord. Chem.* 1971,7, 115.

26. Bonnet, J. J.; Eaton, S. S.; Eaton, G. R.; Holm, R. H.; **Ibers**, J. A. *J. Am. Chem. Soc.* **1973**, *95*, 2141.
27. Hawley, J. C; **Bampos**, N.; Abraham, R. J.; Sanders, J. K. M. *Chem. Commun.* 1998,661.
28. Webb, S. J.; Sanders, J. K. M. *Inorg. Chem.*, **2000**, *39*, 5920.
29. Rao, T. A.; Maiya, B. G. *Chem. Commun.* **1995**, 939.
30. Giribabu, L.; Rao, T. A.; Maiya, B. G. *Inorg. Chem.* **1999**, *38*, 4971.
31. Kumar, A. A.; Giribabu, L.; Reddy, D.R.; **Maiya**, B. G. *Inorg. Chem.* **2001**, *40*, 6757.
32. Abraham, R. J.; Bedford, G. R.; McNeillie, D.; Wright, B. *Org. Magn. Reson.* **1980**, *14*, 418.
33. Nicholson, R. S.; **Shain**, I. *Anal. Chem.* **1964**, *36*, 706.

CHAPTER 5

A New ‘Axial-Bonding’ Type Donor-Acceptor System Assembled via Coordination of Zinc(II)Porphyrin with Pyridine-Linked Calix[4]diquinone

5. 1 Introduction

Numerous porphyrin-based donor-acceptor (D-A) systems have been developed and electronic energy transfer (EET) and photoinduced electron transfer (PET) reactions occurring in them have been **elucidated**.¹⁻⁷ The majority of such studies have been carried out on those D-A systems in which the donor or the acceptor subunits are linked, either covalently or **non-covalently**, at the porphyrin peripheral positions (i. e. **β -pyrrole and/or meso**).¹⁻²² On the other hand, relatively few studies have concentrated on the so-called ‘**axial-bonding**’ type D-A systems in which one or more donor/acceptor subunits are axially linked onto the metal ion of a given **porphyrin**.²³⁻³⁹ With the above considerations in mind, studies were initiated to construct a new ‘axial-bonding’ type metalloporphyrin-based D-A system in which a zinc(II) porphyrin has been axially coordinated to a pyridine linked calix[4]diquinone, Fig. 5. 1. This chapter presents the design, synthesis, spectroscopy and singlet state properties of this new D-A species.

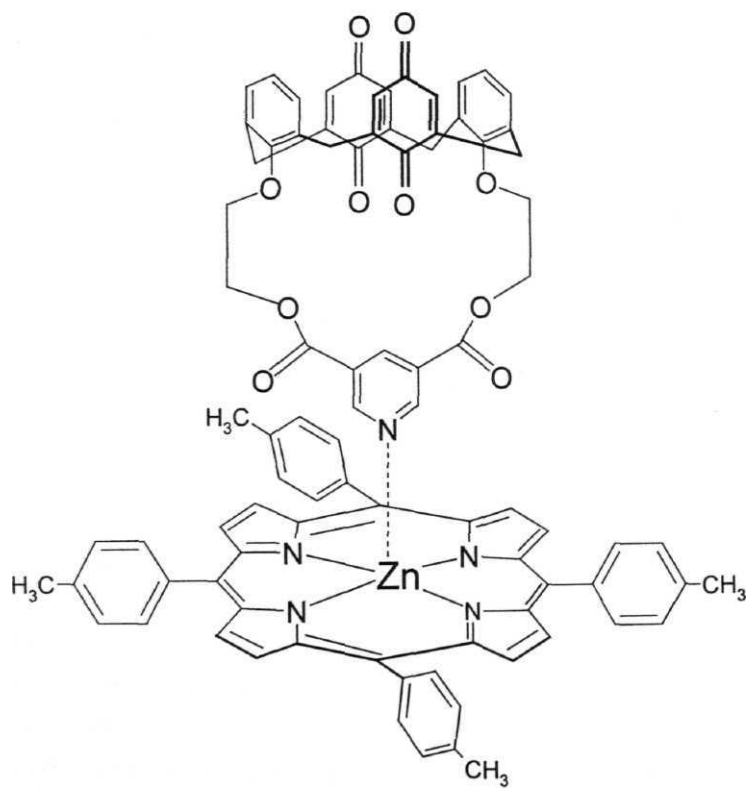


Fig. 5. 1 Structure of the D-A system investigated in this study.

5. 2 Experimental details

5. 2. 1 Synthesis of 5,10,15,20-tetra(4-methylphenyl) porphyrin (H_2TTP)⁴⁰

A solution of 4-methylbenzaldehyde (12. 0 g, 100 mmol) in propanoic acid (200 ml) was warmed to 120 °C with vigorous stirring for 30 min. Pyrrole (6. 9 ml, 100 mmol) was added and the resulting mixture was refluxed for 1 h. The solution was then cooled and allowed to stand overnight at the room temperature. The residue was filtered off, washed with methanol and dried. The solid obtained was dissolved in $CHCl_3$ and subjected to column chromatography on a basic alumina column with $CHCl_3$ as the eluent. The fast moving first fraction was collected and the solvent was evaporated to get H_2TTP . Yield = 1. 53 g (10%).

5. 2. 2 Synthesis of 5,10,15,20-tetra(4-methylphenyl) porphyrinato zinc(II) ($[TTP)Zn^{II}]$)⁴¹

H_2TTP (0. 10 g, 0. 15 mmol) was dissolved in 15 ml of $CHCl_3$. To this, a solution of 0. 16 g (0. 74 mmol) of zinc(II) acetate hydrate dissolved in a minimum amount of methanol was added. The resulting solution was stirred under reflux for 1 h. The solvent was evaporated and the solid obtained was dissolved in CH_2Cl_2 and then filtered. Evaporation of the solvent gave a solid residue which was recrystallized from CH_2Cl_2 - hexane to obtain $[TTP)Zn^{II}]$. Yield = 0. 13 g (95%).

5. 2. 3 Synthesis of bis-cesium 3,5-pyridine dicarboxylate (Py-Cs)⁴²

To a solution of pyridine-3,5-dicarboxylic acid (1. 67 g, 10 mmol) in dry dimethylformamide, 3. 25 g (10 mmol) of cesium carbonate was added. The contents were stirred at room temperature for 12 h. and the solvent was evaporated under the reduced pressure. White solid of cesium salt obtained was dried in a desicator. Yield = 4. 60 g (96%).

5. 2. 4 Synthesis of 4-tert-butylcalix[4]arene (t-but-Calix)⁴³

4-tert-butylphenol (10. 0 g, 66. 5 mmol) was mixed with 10 ml of 3N NaOH and 6. 23 ml (83. 5 mmol) of 37% formaldehyde solution. The mixture was heated at 50 - 55 °C for 45 min. and then at 110 - 120 °C for 2 h. to give a yellow solid. This was stirred with 1N HCl (100 ml) for 1 h. to neutralize the base. The solid was removed by filtration, washed with water and dried in an oven at 110 - 120 °C for 30 min. The material thus obtained was mixed with 120 ml of diphenylether and heated to 210 - 220 °C for 2 h. in an atmosphere of nitrogen (Note: vigorous frothing commenced at ca. 130 °C and subsided after ca. 0. 5 h.). The reaction mixture was cooled, treated with 150 ml of ethylacetate and filtered to give t-but-Calix. Yield = 5. 47 g (58%).

5. 2. 5 Synthesis of 25, 26, 27, 28- tetrahydroxy calix[4]arene (Calix)⁴⁴

A hot solution of t-but-Calix (5. 0 g, 6. 75 mmol) in 250ml toluene was placed in a 500 ml three-necked, round-bottom flask fitted with a mechanical

stirrer and a gas inlet tube. The solution was heated to 50 - 55 °C, treated with 5.0 g (37.0 mmol) of anhydrous AlCl_3 and stirred for 2 h. in an inert atmosphere. The mixture was cooled in an ice bath and stirred with 125 ml of 1N HCl for 30 min. The organic phase was separated, washed with water, dried over anhydrous Na_2SO_4 and finally evaporated to leave a yellow residue. This was triturated with 500 ml of ether and the insoluble material was recrystallized from CHCl_3 - CH_3OH mixture to give **Calix** as off-white micro crystals. Yield = 1.93 g (66%).

5. 2. 6 **Synthesis of 25, 27-bis-(2-bromoethoxy)-26, 28-dihydroxy calix[4]arene (**Calix-Br₂**)**⁴⁵

A mixture of **Calix** (1.00 g, 2.36 mmol), 1, 2-dibromoethane (8.24 g, 44 mmol) and finely ground anhydrous K_2CO_3 (0.33 g, 2.36 mmol) were refluxed in CH_3CN (50 ml) for 24 h. under the nitrogen atmosphere while being stirred magnetically. The solvent was evaporated and the crude residue was taken up in CHCl_3 and washed with aqueous HCl (10%, v/v) and then with water. The organic layer was dried by passing through anhydrous Na_2SO_4 and chromatographed on a silica gel column. Elution with CHCl_3 - hexane (9:1, v/v) and evaporation of the solvent gave the desired product. Yield = 1.07 g (71%).

5. 2. 7 Synthesis of Cyclo-25, 27-bis-(2-ethoxy)-26,28-dihydroxycalix[4]arene 3,5-pyridine dicarboxylate (Calix-py)

Calix-Br₂ (0. 64 g, 1 mmol) and Py-Cs (0. 43 g, 1 mmol) were taken in a 25 ml round-bottom flask, and 20 ml of dry dimethylformamide was added to this mixture. The contents were stirred under nitrogen at 80 - 90 °C for 24 h. The solvent was evaporated under the reduced pressure and the crude residue obtained was taken up in CHCl₃ and washed with water. The organic layer was dried by passing through anhydrous Na₂SO₄ and chromatographed on a silica gel column. The desired product was eluted using CHCl₃ - CH₃OH (98 : 2, v/v). The solvents were evaporated to get the desired product. Yield: 0. 50 g (78%). UV-visible (CH₂Cl₂): λ_{max} , nm (log e): 281 (3. 83); IR (KBr pellets): 1730, 3364 cm⁻¹; FAB-MS: m/z = 643.

5. 2. 8 Synthesis of Cyclo-25, 27-bis-(2-ethoxy)-26,28-calix[4]diquinone 3,5-pyridine dicarboxylate (CalixQ-py)

To a solution of **Calix-py** (0. 64 g, 1 mmol) dissolved in 100 ml acetone and 25 ml phosphate buffer (pH = 7), 50 ml of aqueous, yellowish ClO₂ (15 - 20 %) was added and the reaction mixture was stirred at room temperature for 12 h. The solvent was evaporated under the reduced pressure and the residue was treated with water to give a pale yellow solid, which was filtered and dried. The crude residue was loaded onto a silica gel column; elution with CHCl₃ - CH₃OH (98 : 2, v/v) gave the desired product. The compound was

recrystallized from CHCl_3 - hexane. Yield = 0.32 g (48 %). UV-visible (CH_2Cl_2): λ_{max} , nm (log ϵ): 256 (3.67); IR (KBr pellets): 1726, 1655 cm^{-1} ; FAB-MS: $m/z \approx 673$.

All the spectroscopic and electrochemical experiments have been carried out as described in Chapter 2.

5.3 Results and discussion

5.3.1 Synthesis and characterization of Calix-py and CalixQ-py

CalixQ-py was synthesized in three steps: (i) selective alkylation of **Calix** with 1,2-dibromoethane to yield **Calix-Br₂** (ii) cyclization of **Calix-Br₂** with bis-cesium-3,5-pyridine dicarboxylate to give **Calix-py** and (iii) mild oxidation of **Calix-py** with aqueous chlorine dioxide to obtain **CalixQ-py** (Fig. 5.2.). Preliminary characterization of **Calix-py** and **CalixQ-py** was carried out by the IR, mass (FAB), UV-visible and $^1\text{H-NMR}$ spectroscopies and electrochemical methods.

In the IR spectra, hydroxyl groups of **Calix-py** showed a peak centered at 3364 cm^{-1} due to the strong intramolecular hydrogen bonding. **CalixQ-py** shows a strong quinone (C=O) stretching vibration at 1655 cm^{-1} , as expected. FAB-MS spectra showed prominent peaks at $m/z = 643$ and 673 for **Calix-py** and **CalixQ-py** respectively, due to their M^+ fragments. UV-visible spectra of

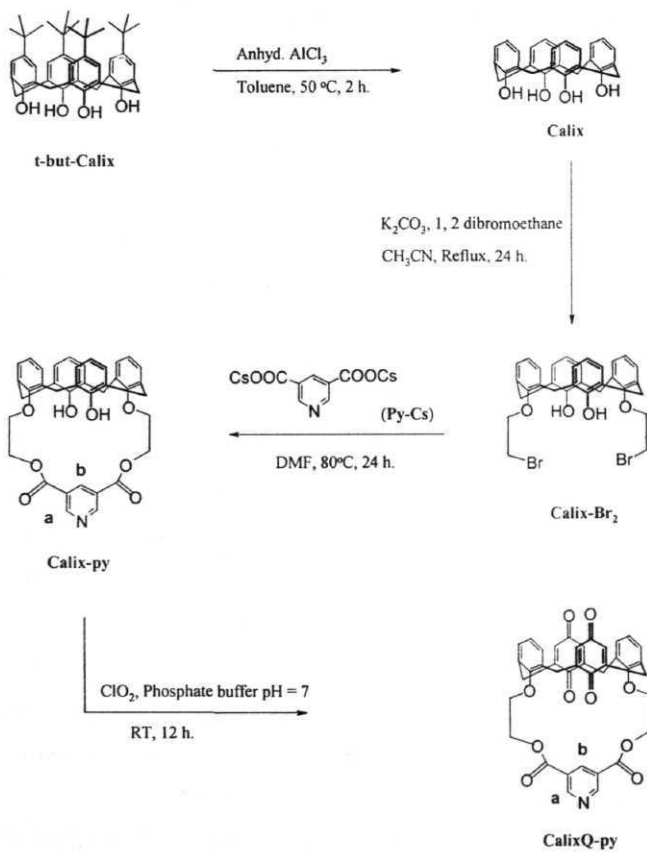


Fig. 5. 2 Scheme leading to the synthesis of **CalixQ-Py**.

Calix-py and **CalixQ-py** show bands in the UV region with the absorption peak maxima (λ_{max}) at 281 and 257 nm respectively, revealing the presence hydroxy/quinone **auxochrome** in these ligands.

^1H NMR spectra (CDCl_3 , TMS) of **Calix-py** and **CalixQ-py** are displayed in the Fig. 5.3. Relevant data are summarized along with that of their precursors in the Table 5. 1. These spectra show characteristic resonances, and the peak positions as well as their integrated intensities are consistent with the proposed structures for the new compounds. The resonances due to protons **a** (see: Fig. 5. 2 for proton identification) of the pyridyl groups on **Calix-py** and **CalixQ-py** appear at 9. 44 and 9. 31 ppm (d, 2H, $^3\text{J}_{\text{H-H}} = 1. 8/2. 0$ Hz), respectively. The resonance due to proton b of the pyridyl group in **Calix-py** is located at 9. 58 ppm (t, 1H), whereas the corresponding peak on **CalixQ-py** is shielded and appears at 8. 79 ppm (t, 1H). While aromatic protons of the two 'unalkylated' rings of **Calix-py** resonate as a doublet at 7. 05 ppm (4H, $^3\text{J}_{\text{H-H}} = 7. 8$ Hz) and a triplet at 6. 78 ppm (2H), the corresponding protons of the two rings that are substituted with the ethoxyester limbs (alkylated) resonate at 6. 94 (d, 4H, $^3\text{J}_{\text{H-H}} = 7. 8$ Hz) and 6. 66 ppm (t, 2H). In the case of **CalixQ-py**, the aromatic protons of the two alkylated rings resonate as a doublet and a triplet at 6. 85 (4H, $^3\text{J}_{\text{H-H}} = 7. 8$ Hz) and 6. 69 ppm (2H), respectively. The four protons present on the two quinone rings resonate as a singlet at 6. 60 ppm. Due to the strong intramolecular hydrogen bonding, hydroxyl protons of **Calix-py** resonate as a singlet at 7. 83 ppm. The **-O-CH₂-CH₂-O-** protons of the spacer

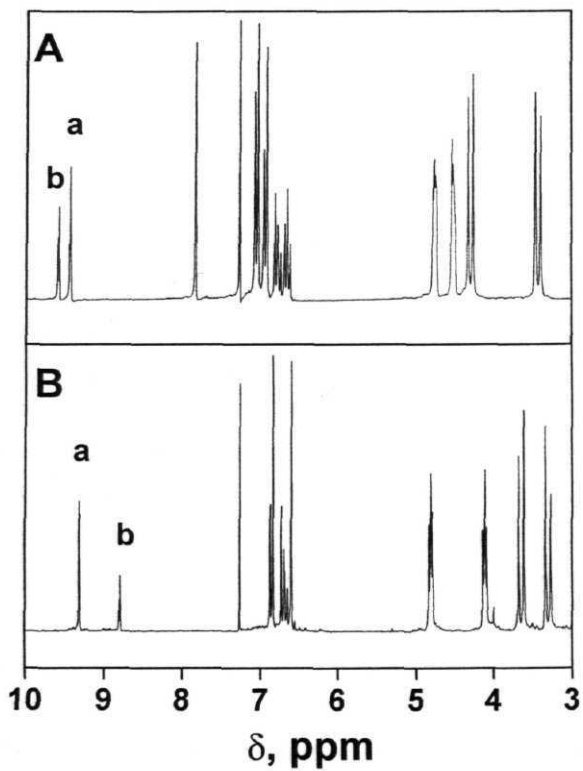


Fig. 5. ^1H NMR spectra (CDCl_3 , TMS) of (A) Calix-py and (B) CalixQ-py. Peak at 7.26 ppm is due to solvent.

Table 4. 1 ^1H NMR data (CDCl_3 , TMS)^a

Compound	δ , ppm $[J_{\text{HH}}]$, Hz					
	Pyridyl	Hydroxyl	Phenyl	Quinone	-OCH ₂ CH ₂ -	ArCH ₂ Ar
Py-Cs	9.24 (br, s, 2H) 8.64 (br, s, 1H)	-	-	-	-	-
Calix	-	10.19 (s, 4H)	7.28 6.68 (d, 8H) (t, 4H) [7.8]	-	-	3.63 (d, 4H) [12.8] 3.48 (d, 4H) [12.8]
Calix-Br ₂	-	7.58 (s, 2H)	7.08 6.92 (d, 2H) (d, 2H) [7.3] [7.3]	-	4.36 (t, 4H) 3.92 (t, 4H)	4.23 (d, 4H) [13.1] 3.42 (d, 4H) [13.1]
Calix-py	9.58 (t, 1H) 9.44 (d, 2H) [1.8]	7.83 (s, 2H)	7.05 6.94 (d, 4H) (d, 4H) [7.8] [7.8] 6.78 6.66 (t, 2H) (t, 2H)	-	4.76 (t, 4H) 4.53 (t, 4H)	4.28 (d, 4H) [13.6] 3.43 (d, 4H) [13.6]
CalixQ-py	9.31 (d, 2H) [2.0] 8.79 (t, 1H)	-	6.85 6.69 (d, 4H) (t, 2H) [7.8]	6.60 (s, 4H)	4.81 (t, 4H) 4.10 (t, 4H)	3.65 (d, 4H) [13.6] 3.30 (d, 4H) [13.6]

a) Error limits: δ , ± 0.01 ppm; J, ± 1 Hz.

ethoxyester moiety resonate as a pair of triplets in the aliphatic region at **4. 76** and **4. 53 ppm** in **Calix-py** and at **4. 81** and **4. 10 ppm** in **CalixQ-py**. The Ar-CH₂-Ar protons resonate as pair of doublets at **4. 28** and **3. 43 ppm** for **Calix-py** and at **3. 65** and **3. 30 ppm** in **CalixQ-py** with the geminal coupling constants of **13. 6 Hz** in each case. This suggests that the calixarene/calixquinone moieties are present in their cone conformation in these compounds.⁴⁶

Redox potentials of **Calix-py** and **CalixQ-py** have been measured in CH₂Cl₂, 0. 1 M TBAP by both cyclic- and differential pulse voltammetric methods. **Calix-py** showed an irreversible peak at +1. 32 V for the oxidation of phenolic moieties. No cathodic response was observed for this calixarene under our experimental conditions. On the other hand, **CalixQ-py** showed three cathodic responses when the potential was scanned between 0 and -1. 8 V, as illustrated in Fig. 5. 4. The first two reduction peaks observed at -0. 63 and -0. 76 V are found to be reversible ($i_p/i_r = 0. 9 - 1. 0$ where i_p is the peak current) and diffusion controlled ($i_p/v = \text{constant}$ in the scan rate (v) range 50 - 500 mV s⁻¹) one-electron transfer ($\Delta E_p = 60-70$ mV where ΔE_p is the peak-to-peak potential difference; $\Delta E = 65 \pm 3$ mV for Fc /Fc couple) reactions. On the other hand, the subsequent peak seen at -1. 38 V is totally irreversible. Calix[4]diquinones can, in principle, accept a total of four electrons to generate the corresponding tetraanion.⁴⁸ For such species, three successive reduction

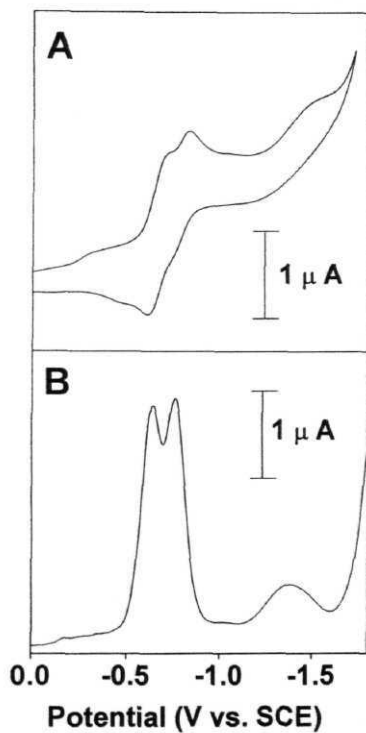


Fig. 5. 4 Cyclic- (A) and differential-pulse (B) voltammograms of **CalixQ-py**. The scan rates employed are 100 and 10 mV s^{-1} for (A) and (B), respectively.

processes are generally observed in the cyclic- and differential-pulse voltammograms. Based on this knowledge, the first two peaks appearing at -0.63 and -0.76 V for **CalixQ-py** are assigned to successive one-electron reductions of the quinone units, giving the semiquinone species in each case. The third cathodic response at more negative potential is believed to be due to simultaneous one-electron transfer to both the semiquinones that results in the generation of a tetraanionic species.⁴⁸

5. 3. 2 **Complexation** studies

It is well known that zinc(II) porphyrins form pentacoordinated complexes with coordinating ligands and that this complexation can be conveniently monitored by the UV-visible spectroscopy.^{49,53} Complexation of zinc(II) porphyrins with an axial ligand generally results in two effects, often seen in the UV-visible spectrum. These are: (i) a red shift of the entire spectrum relative to that of the corresponding tetracoordinated, square planar zinc(II) porphyrin and (ii) an increase in the $\epsilon_{\alpha}/\epsilon_{\beta}$ ratio of the two visible (Q) bands.⁵⁴ These spectral features have been utilized in the present study to examine the complexation behavior of **Calix-py** and **CalixQ-py** with $[(TTP)Zn^{II}]$. Addition of increasing concentrations of **Calix-py** or **CalixQ-py** ($0 - 3.8 \times 10^{-4}$ M) to a solution containing a constant concentration of $[(TTP)Zn^{II}]$ (3.11×10^{-6} M) resulted in a red shift of 8 nm for both the Soret- (420 to 428 nm) and Q- bands (548 to 556 nm), suggesting complexation of the appended pyridine

subunit at the zinc(II) center in each case. The ratio $\epsilon_{\alpha}/\epsilon_{\beta}$ also increased from 0.24 to 0.55 during these titrations. Fig. 5. 5. illustrates spectral changes observed during the titration of **Calix-py** with $[(TTP)Zn^{II}]$, and similar changes were noticed when **CalixQ-py** was titrated with this metalloporphyrin. Changes observed in the UV-visible spectra were treated using eqn. 5. 1.⁵⁵

$$\Delta A/b = (Q_t K \Delta \epsilon [L]) / (1 + K [L]) \quad (5.1)$$

Here, ΔA refers to the change in absorbance from initial value at the required wavelength (420 nm), b is cuvette path length (in cm), Q_t is total concentration of $[(TTP)Zn^{II}]$, K is the apparent binding constant, $\Delta \epsilon$ is change in extinction coefficient between free and bound $[(TTP)Zn^{II}]$ and $[L]$ is concentration of the titrated ligand. K values evaluated are 1685 ± 200 and $2101 \pm 220 \text{ M}^{-1}$ for the binding of $[(TTP)Zn^{II}]$ by **CalixQ-py** and **Calix-py**, respectively.

1H NMR titrations have also been carried out using various concentrations of **CalixQ-py** or **Calix-py** ($0 - 9.77 \times 10^{-3} \text{ M}$) and a constant concentration of $[(TTP)Zn^{II}]$ ($3.76 \times 10^{-3} \text{ M}$). The results are shown for the titration with **CalixQ-py** in Fig.5. 6. As seen in this Figure, addition of 0.4 equivalents of **CalixQ-py** to a $CDCl_3$ solution of $[(TTP)Zn^{II}]$ induced large upfield shifts for protons **a** of the pyridine in **CalixQ-py** ($\Delta \delta = \delta_{\text{CalixQ-py}}$

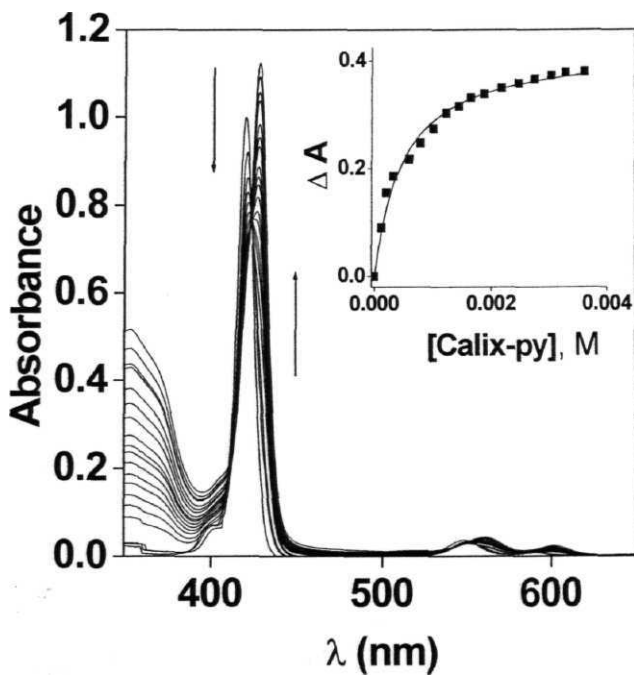


Fig. 5. 5 UV-visible titration of $[(TTP)Zn^{II}]$ (3.11×10^{-6} M) with various concentrations ($0 - 3.8 \times 10^{-3}$ M) of Calix-py. The inset shows a fit to equn. 3. 1.

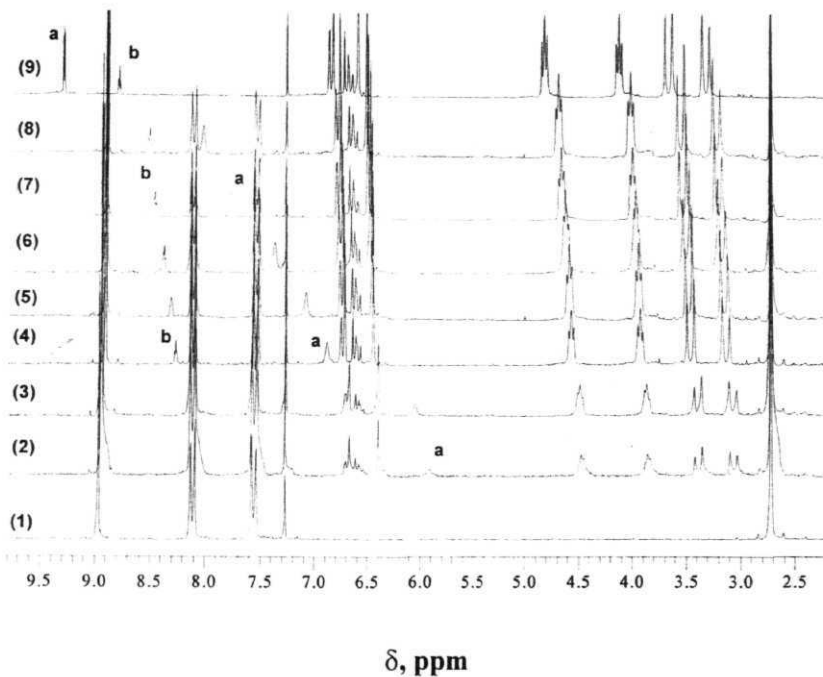


Fig. 5. 6 ^1H NMR spectra of $[(\text{TTP})\text{Zn}^{\text{II}}]$ (3.76×10^{-3} M) in CDCl_3 upon addition of (1) 0, (2) 0.4, (3) 1.0, (4) 1.3, (5) 1.7, (6) 2.1, (7) 2.4 and (8) 2.6 equivalents of **CalixQ-py**. Spectrum (9) is the ^1H NMR spectrum of uncomplexed **CalixQ-py** in CDCl_3 shown for comparison. Singlet seen at 7.26 ppm is due to the solvent.

$-\delta_{\text{complex}} = 3.38$ ppm; see spectrum number 2 in Fig. 5. 6). Resonance due to proton b is also upfield shifted, albeit, to a lesser extent ($\Delta\delta = 0.68$ ppm) than that experienced by protons a. Upfield shifts for the pyridyl protons have been noticed earlier during the NMR titrations of various substituted pyridines with zinc(II) porphyrins, and have been interpreted in terms of the strong ring current effect exerted by the porphyrin upon complexation of the ligand.⁵⁶⁻⁵⁸ Based on this fact, it is suggested that upfield shifts noticed for protons **a** and **b** of **CalixQ-py** indicate complexation of this pyridyl ligand with $[(\text{TTP})\text{Zn}^{\text{II}}]$. This complexation, however, does not seem to have any influence on the macrocyclic ring protons of $[(\text{TTP})\text{Zn}^{\text{II}}]$ in the aromatic region, which are found to be rather insensitive to the addition of **CalixQ-py**. On the other hand, minor shifts were noticed for the various aliphatic and aromatic protons on **CalixQ-py** in the presence of the porphyrin. As the ratio $[\text{CalixQ-py}]/[(\text{TTP})\text{Zn}^{\text{II}}]$ is varied from 2.6 to 0.4 during the titration (i.e. spectrum number 8 to 2) all the signals of **CalixQ-py** were seen to shift towards the downfield region. Similar changes in the ^1H NMR spectra were noticed during the titration of **Calix-py** with $[(\text{TTP})\text{Zn}^{\text{II}}]$.

Electrochemical techniques have been employed earlier to monitor the binding of pyridine ligands with zinc(II) porphyrins.^{59,60} In the present case, complexation of **CalixQ-py** with $[(\text{TTP})\text{Zn}^{\text{II}}]$ has been monitored by both cyclic- and differential-pulse voltammetric methods. The titration results are shown in Fig. 5. 7. $[(\text{TTP})\text{Zn}^{\text{II}}]$ shows two successive, reversible, one-electron

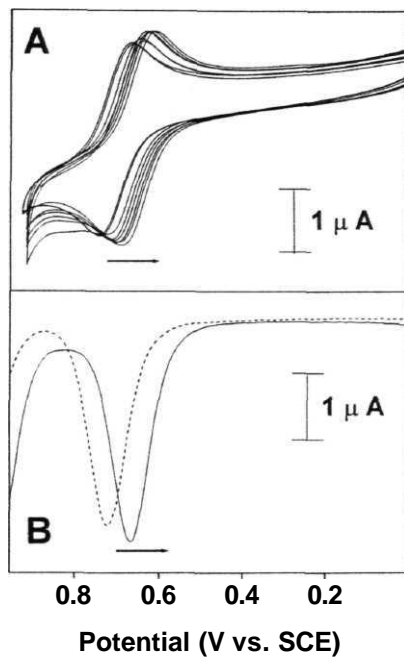
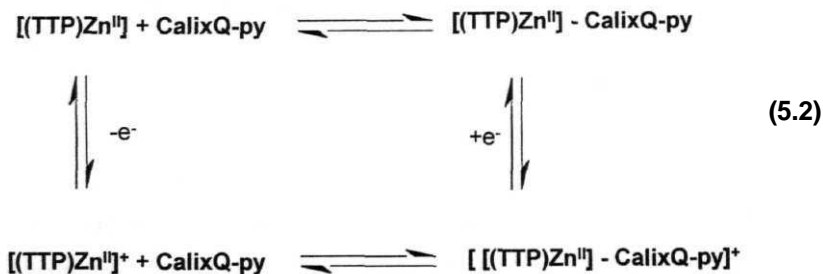


Fig. 5. 7 (A) Cyclic voltammograms of $[(TTP)Zn^{II}] < 3.12 \times 10^{-3} \text{ M}$ with various added concentrations (0 - $18.3 \times 10^{-3} \text{ M}$) of **CalixQ-py**. (B) The corresponding differential-pulse voltammograms in the absence (—) and presence (---) of ($18.3 \times 10^{-3} \text{ M}$) of CalixQ-py. The scan rates employed are 100 and 10 mV s^{-1} for (A) and (B), respectively.

oxidation peaks at 0.72 and 1.05 V producing mono and dications, respectively.⁴⁷ The binding ability of **CalixQ-py** with $[(TTP)Zn^{II}]$ was monitored at the first oxidation peak of the porphyrin. Upon addition of increasing concentrations of **CalixQ-py** ($0 - 18.3 \times 10^{-3}$ M) to a solution of $[(TTP)Zn^{II}]$ (3.12×10^{-3} M), oxidation peak of the porphyrin was found to successively shift to less anodic region suggesting facile electron abstraction from the ring due to complexation. The maximum shift observed at the end of the titration is 56 mV (to a more cathodic region) and is in good agreement with the previously reported data for axial coordination of zinc(II) porphyrins with pyridyl ligands.^{59,60} The overall electrochemistry of the $[(TTP)Zn^{II}]$ - **CalixQ-py** system is illustrated in eqn. 5.2.



The above equation suggests that the redox data can be treated according to eqn. 5.3.⁶¹

$$E_0^b - E_0^f = RT/nF \log (K([(\text{TTP})\text{Zn}^{\text{II}}])/K([(\text{TTP})\text{Zn}^{\text{II}}]^+)) \quad (5.3)$$

Here, E_0^b and E_0^f are the thermodynamic redox potentials for the bound and free complexes respectively, n is the number of electrons transferred, $K([(\text{TTP})\text{Zn}^{\text{II}}])/K([(\text{TTP})\text{Zn}^{\text{II}}]^+)$ is the ratio of binding constants for $[(\text{TTP})\text{Zn}^{\text{II}}]$ and its oxidized species and other parameters have their usual meaning. Substitution of appropriate values to suit the electrochemistry of $[(\text{TTP})\text{Zn}^{\text{II}}]$ in the presence of **CalixQ-py** and from a limiting shift of -56 mV, $K([(\text{TTP})\text{Zn}^{\text{II}}]^+)/K([(\text{TTP})\text{Zn}^{\text{II}}])$ was calculated to be ≈ 250 . Thus, $[(\text{TTP})\text{Zn}^{\text{II}}]$ binds to CalixQ-py less strongly than its one-electron oxidized form. This result is in agreement with the reported data for binding of various substituted pyridines with zinc(H) porphyrins and their one-electron oxidized products.⁵

5. 3. 3 Singlet State properties

When excited at 530 nm in dry CH_2Cl_2 , steady state fluorescence spectrum of $[(\text{TTP})\text{Zn}^{\text{II}}]$ exhibited two emission bands located at 600 and 647 nm. The emission intensities of these bands did not appreciably change during the titration of $[(\text{TTP})\text{Zn}^{\text{II}}]$ (8.31×10^{-6} M) with **Calix-py** ($0 - 3.6 \times 10^{-3}$ M). In contrast, significant quenching of fluorescence due to $[(\text{TTP})\text{Zn}^{\text{II}}]$ was observed upon successive addition of **CalixQ-py** ($0 - 3.6 \times 10^{-3}$ M), Fig. 5. 8. At the limit of complete complexation, the fluorescence intensity is nearly 25%

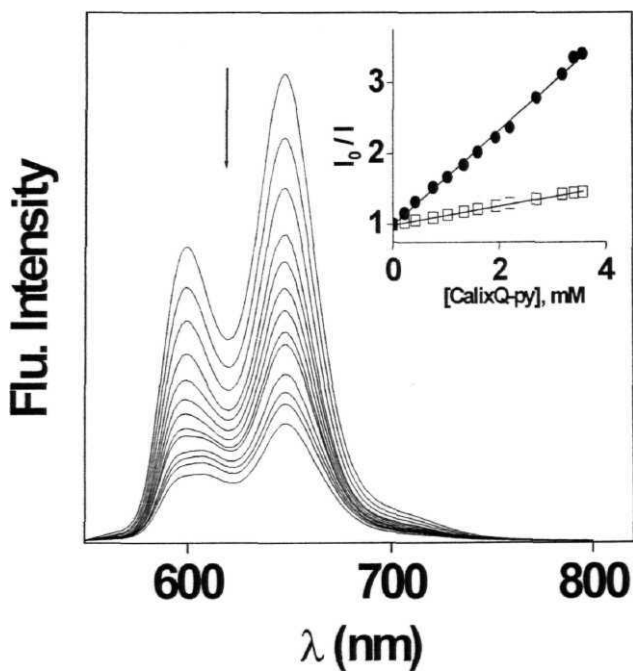


Fig. 5. 8. Fluorescence spectra ($\lambda_{\text{exc}} = 530 \text{ nm}$, CH_2Cl_2) of $[(\text{TTP})\text{Zn}^{\text{II}}]$ (top curve) in the presence of increasing concentrations of CalixQ-py ($0 - 3.6 \times 10^{-4} \text{ M}$, subsequent curves). Inset shows Stern-Volmer plots for the quenching of $[(\text{TTP})\text{Zn}^{\text{II}}]$ by CalixQ-py (●) and Calix-py (○).

less than that of uncoordinated $[(TTP)Zn^{II}]$. Inset to Fig. 5. 8 shows the Stern-Volmer plots for the quenching of $[(TTP)Zn^{II}]$ fluorescence by **Calix-py** and **CalixQ-py**. While both the plots are linear, the Ksv (Stern-Volmer quenching constant) values are found to be different.

$$I_0/I = 1 + K_{sv} [Q] \quad (5. 4)$$

where I_0 and I represent fluorescence intensities of the porphyrin in the absence and the presence of quencher Q (**CalixQ-py/Calix-py**), respectively.⁶² Analysis of the data using equn. 5. 4 gave Ksv values of 132 and 661 M^{-1} for the quenching of $[(TTP)Zn^{II}]$ fluorescence by **Calix-py** and **CalixQ-py**, respectively.

In the time-resolved fluorescence experiments ($\lambda_{exc} = 575$ nm and $\lambda_{em} = 650$ nm), the fluorescence intensity decay profile ($I_f(t)$) of $[(TTP)Zn^{II}]$ (2.5×10^{-5} M, CH_2Cl_2) could be fit to a single exponential function, equn. 5.5.

$$I_f(t) = A \exp(-t/\tau) \quad (5.5)$$

The fit gave a lifetime (τ_1) of 1. 61 ns for the uncomplexed $[(TTP)Zn^{II}]$. Upon addition of increasing concentrations of **Calix-py** or **CalixQ-py** ($0 - 15 \times 10^{-3}$ M) to $[(TTP)Zn^{II}]$ solutions, fluorescence lifetimes (τ_2) were found to decrease and reached the minimum of 1. 40 ns in the case of **Calix-py** and 0. 61

ns in the case of **CalixQ-py**. Again, these decays could be fit to a monoexponential function, equn. 5. 5. The quenching rate constant (k_q), obtained from these dynamic quenching experiments, (Fig. 5. 9) are found to be 6. 64 x 10⁹ M⁻¹ s⁻¹ for **Calix-py** and 6. 22 x 10¹⁰ M⁻¹ s⁻¹ for **CalixQ-py**, equn. 5. 6.

$$\tau_1/\tau_2 = 1 + k_q \tau_1 [Q] \quad (5. 6)$$

These rates suggest that the quenching reactions are nearly diffusion controlled processes.

Several reports exist in the literature on the quenching of fluorescence due to zinc(II) porphyrins by intramolecular PET to the covalently/non-covalently bound quinones.^{2,4,5} Among these, those that describe the D-A systems in which a monomeric or a dimeric zinc(II) porphyrin is bound to a pyridine-appended quinone/diimide acceptor are of relevance to the present work.^{23,24,30,33} In these latter supramolecular D-A compounds, PET between the zinc(II) porphyrin and the quinone/diimide has been implicated based on thermodynamic data and results of control experiments. In the present case also, the thermodynamic data suggests the possibility of a PET between singlet porphyrin and **CalixQ-py**. The free energy change for this electron transfer (AGPET) has been calculated using equn. 5. 7.⁶³

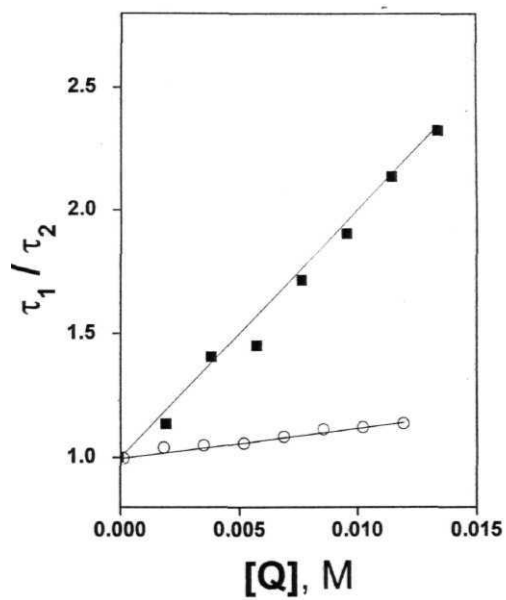


Fig. 5. 9 Dynamic Stern-Volmer plots for the quenching of $[(TTP)Zn^{II}]$ by **CalixQ-py** (\bullet) and **Calix-py** (\circ).

$$\Delta G_{\text{PET}} = E_{1/2}(\text{ox}) - E_{1/2}(\text{red}) - E_{0-0} \quad (5.7)$$

where $E_{1/2}(\text{ox})$ and $E_{1/2}(\text{red})$ are the potentials for one-electron oxidation of the donor ($[(\text{TTP})\text{Zn}^{\text{II}}]$) in the presence of **CalixQ-py**, 0.66 V and one-electron reduction of the acceptor (**CalixQ-py**, -0.63 V) respectively, and E_{0-0} is the singlet state energy of $[(\text{TTP})\text{Zn}^{\text{II}}]$ (2.07±0.03 eV) obtained by overlapping the absorption and fluorescence spectra of the fluorophore. The value of ΔG_{PET} evaluated using equn. 5.7 is exoergic by 0.78±0.04 eV. In addition, quenching of fluorescence due to $[(\text{TTP})\text{Zn}^{\text{II}}]$ by **Calix-py** is an order of magnitude lower than that by **CalixQ-py** by both the steady state and time resolved methods. Put together, this analysis suggests that strong quenching of fluorescence due to $[(\text{TTP})\text{Zn}^{\text{II}}]$ in the presence of **CalixQ-py** is a consequence of a PET between singlet $[(\text{TTP})\text{Zn}^{\text{II}}]$ and the quinone moieties on this ligand. The rate constant for this PET (k_{PET}) can be calculated using equn. 5.8.

$$k_{\text{PET}} = 1/\tau_{2(\text{lim})} - 1/\tau_{1(\text{lim})} \quad (5.8)$$

where $1/\tau_{2(\text{lim})}$ and $1/\tau_{1(\text{lim})}$ refer to the limiting life times of $[(\text{TTP})\text{Zn}^{\text{II}}]$ obtained during its titrations with **CalixQ-Py** (0.61 ns) and **Calix-Py** (1.40 ns), respectively. The k_{PET} thus calculated is $\sim 1 \times 10^9 \text{ s}^{-1}$. This value is low compared to that obtained for the PET between the quinone and zinc(II)

porphyrin in a compactly assembled diporphyrin - dipyridyl (quinone) D-A system ($k_{\text{PET}} = 1.6 \times 10^{10} \text{ s}^{-1}$) reported by Imahori et al.^{24,30} However, it is close to the k_{PET} values reported for several zinc(II) porphyrin - pyridyl (or imide) systems reported by Hunter et al.²³ and Otsuki et al.³³

Finally, recall that $K ([(\text{TTP})\text{Zn}^{\text{II}}]^+) / K ([(\text{TTP})\text{Zn}^{\text{II}}])$ is ≈ 250 as revealed by the electrochemical data (*vide infra*). Thus, the reduced calix[4]diquinone does not dissociate itself from the PET product, namely, $[(\text{TTP})\text{Zn}^{\text{II}}]^+ - \text{CalixQ-py}^{\text{---}}$; instead, it is expected to be more strongly bound at the zinc(II) center in this state.

5. 4 Summary

In summary, the present investigation demonstrates the self-assembly of a $[(\text{TTP})\text{Zn}^{\text{II}}]$ -calix[4]diquinone D-A pair *via* the axial **ligation** method. The UV-visible and ^1H NMR studies reveal that the complex formed between $[(\text{TTP})\text{Zn}^{\text{II}}]$ and CalixQ-py is a stable species. Fluorescence studies show efficient quenching of the excited zinc(II) porphyrin upon axial **ligation** by CalixQ-py. On the basis of free energy calculations and control experiments, fluorescence quenching observed for the $[(\text{TTP})\text{Zn}^{\text{II}}] - \text{CalixQ-py}$ system has been assigned to the occurrence of a PET from the singlet $[(\text{TTP})\text{Zn}^{\text{II}}]$ to the axially positioned calix[4]diquinone. The electron transfer rate in this system is close to that reported for the analogous zinc(II) porphyrin based, 'vertically linked' D-A pairs.

5. 5 References

1. Gust, D.; Moore, T. A. *Top. Curr. Chem.* **1991**, *159*, 103.
2. Wasielewski, M. R. *Chem. Rev.* **1992**, *92*, 435.
3. Speiser, S. *Chem. Rev.* **1996**, *96*, 1953.
4. Ward, M. D. *Chem. Soc. Rev.* **1997**, *26*, 365.
5. Hayashi, T.; Ogoshi, H. *Chem. Soc. Rev.* **1997**, *26*, 355.
6. Connolly, J. S.; Bolton, J. R. In *Photoinduced Electron Transfer (Part D)*; Fox, M. A., Channon, M., Eds.; Elsevier: Amsterdam, 1988.
7. Holten, D.; Bocian, D. F.; Lindsey, J. S. *Acc. Chem. Res.* **2002**, *35*, 57.
8. Hayashi, T.; Takimura, T.; Ohara, T.; Hitomi, Y.; Ogoshi, H. *Chem. Comm.* **1995**, 2503.
9. Osuka, A.; Yamada, H.; Maruyama, K.; Takeshi, O.; Nozaki, K.; Okada, T.; Tanaka, Y.; Mataga, N. *Chem. Lett.* **1995**, 591.
10. Imahori, H.; Hasegawa, M.; Taniguchi, S.; Aoki, M. Okada, T.; Sakata, Y. *Chem. Lett.* **1998**, 721.
11. Higashida, S.; Imahori, H.; Kaneda, T.; Sakata, Y. *Chem. Lett.* **1998**, 605.
12. Cheng, P.; Wilson, S. R.; Schuster, D. I. *Chem. Commun.* **1999**, 89.
13. Taylor, P. N. Wylie, A. P.; Huuskonen, Anderson, H. L. *Angew. Chem. Int. Ed. Engl.* **1998**, *37*, 986.
14. Tamaki, K.; Imahori, H.; Nishimura, Y.; Yamazaki, I.; Sakata, Y. *Chem. Commun.* **1999**, 625.

15. Tsuchiya, S. *J. Am. Chem. Soc.* **1999**, *121*, 48.
16. Harriman, A.; Hissler, M.; Trompette, O.; Ziessel, R. *J. Am. Chem. Soc.* **1999**, *727*, 2281.
17. Iovine, P. M.; Kellett, M. A.; Redmore, N. P.; Therien, M. J. *J. Am. Chem. Soc.* **2000**, *122*, 8717.
18. Rajesh, C. S.; Capitosti, G. J.; Cramer, S. J.; Modarelli, D. A. *J. Phys. Chem. B.* **2001**, *105*, 10175.
19. Capitosti, G. J.; Cramer, S. J.; Rajesh, C. S.; Modarelli, D. A. *Org. Lett.* **2001**, *3*, 1645.
20. D'Souza, F.; Deviprasad, G. R. *J. Org. Chem.* **2001**, *66*, 4601.
21. Imahori, H.; Tamaki, K.; Araki, Y.; Sekiguchi, Y.; Ito, O.; Sakata, Y.; Fukuzami, S. *J. Am. Chem. Soc.* **2002**, *124*, 5165.
22. Mori, Y.; Sakaguchi, Y.; Hayashi, H.; *J. Phys. Chem. A* **2002**, *106*, 4453.
23. Hunter, C. A.; Sanders, J. K. M.; Beddard, G.; Evans, S. *Chem. Commun.* **1989**, 1765.
24. Imahori, H.; Yoshizawa, E.; Yamad, K.; Hagiwara, T.; Okada, T.; Sakata, Y. *Chem. Commun.* **1995**, 1133.
25. Susumu, K.; Kunitomo, K.; Segawa, H.; Shimidzu, T. *J. Phys. Chem.* **1995**, *99*, 29.
26. Segawa, H.; Kunitomo, K.; Taniguchi, M.; Shimidzu, T. *J. Am. Chem. Soc.* **1994**, *116*, 11193.

27. Rao, T. A.; Maiya, B. G. *Chem. Commun.*, **1995**, 939.
28. Hunter, C. A.; Shannon, R. J. *Chem. Commun.* **1996**, 1361.
29. Rao, T. A.; Maiya, B. G. *Inorg. Chem.* **1996**, **35**, 4829.
30. Imahori, H.; Yamad, K.; Yoshizawa, E.; Hagiwara, T.; Okada, T.; Sakata, Y. *J. Porphyrins Phthalocyanines* **1997**, **1**, 55.
31. Maruyama, H.; Fujiwara, M.; Tanaka, K. *Chem. Lett.* **1998**, 805.
32. Hawley, J. C.; Bampos, N.; Abraham, R. J.; Sanders, J. K. M. *Chem. Commun.* 1998,661.
33. Otsuki, J.; Harada, K.; Toyama, K.; Hirose, Y.; Araki, K.; Takatera, K.; Watanabe, T. *Chem. Commun.* **1998**, 1515.
34. Chichak, K.; Branda, N. *Chem. Lett.* **1999**, 523.
35. Hirakawa, K.; Segawa, H. *J. Photochem. Photobiol., A:Chem.* **1999**, **123**, 67.
36. Giribabu, L.; Maiya, B.G. Kumar, A. A.; Neeraja, V. *Angew. Chem. Int. Ed. Engl.* **2001**, **40**, 3621.
37. Flamigni, L.; Johnston, M. R. *New J. Chem.* **2001**, **25**, 1368.
38. Reddy, D. R.; Maiya, B. G. *J. Porphyrins Phthalocyanines* **2002**, **6**, 1.
39. Flamigni, L.; Johnston, M. R.; Giribabu, L. *Chem. Eur. J.* **2002**, **8**, 3938.
40. Alder, A. D.; Longo, F. R.; Finarelli, J. D.; Goldmacher, J.; Assour, J.; Korsakoff, L. *J. Org. Chem.* **1967**, **32**, 476
41. Fuhrhop, J. -H; Smith, K. M. In *Porphyrins and Metalloporphyrins*; Smith, K. M., Ed.; Elsevier : Amsterdam, 1975; p. 769.

42. Pandey, P. S.; Rai, R.; Singh, R. B. *Tetrahedron* **2002**, 55, 355.
- 43. Gutsche, C. D.; Dhawan, B.; Muthukrishnan, R. *J. Am. Chem. Soc.* **1981**, 103, 3782.
44. Gutsche, C. D.; Levine, J. A.; Sujeeth. P. K. *J. Org. Chem.* **1985**, 50, 5802.
45. Li, Z. T.; Ji, G.Z.; Zhao, C. X.; Yuan, S. D.; Ding, H.; Huang, C; Diu, A. L.; Wei. M. *J. Org. Chem.* **1999**, 64, 3572.
46. Gutsche, C. D. In *Calixarenes, Monographs in Supramolecular Chemistry, Vol. 1*; Stoddart, J. F., Eds.; The Royal Society of Chemistry: London; 1989.
47. Nicholson, R. S.; Shain, I. *Anal. Chem.* **1964**, 36, 706.
48. Webber, P. R. A.; Beer, P. D.; Chen, C. Z.; Felix, V.; Drew, M. G. B. *J. Am. Chem. Soc.* **2003**, 125, 57 A.
49. Nappa, M.; Valentine, J. S. *J. Am. Chem. Soc.* **1978**, 100, 5075.
50. Vogel, G. C; Stahlbush, J. R. *Inorg. Chem.* **1977**, 16, 950.
51. Kolling, O. W. *Inorg. Chem.* **1979**, 18, 1175.
52. Drago, R. S.; Kroeger, M. K.; Stahlbush, J. R. *Inorg. Chem.* **1981**, 20, 307.
53. Cole, J.; Curthoys, G. C; Magnusson, E. A.; Phillips, J. N. *Inorg. Chem.* **1977**, 11, 1024.
54. D'Souza, F.; Hsieh, Y.-Y.; Deviprasad, G. R. *Inorg. Chem.* **1996**, 35, 5747.

55. Connors, K. A. *Binding Constants: The Measurements of Molecular Complex Stability*; John Wiley & Sons: New York. **1987**.
56. Abraham, R. J.; Bedford, G. R.; McNeillie, D. Wright, B. *Org. Magn. Reson.* **1980**, *14*, 418.
57. Abraham, R. J.; Fell, S. C. M.; Smith, K. M. *Org. Magn. Reson.* **1977**, *9*, 367.
58. Chachaty, C; Gust, D.; Moore, T. A.; Nemeth. G. A.; Liddell, P. A.; Moore, A. L. *Org. Magn. Reson.* **1984**, *22*, 39.
59. Kadish, K. M.; Shiue, L. R. Rhodes, R. K. Bottomley, L. A. *Inorg. Chem.* **1981**, *20*, 1277.
60. Lin, C. L.; Fang, M. Y.; Cheng, S. H. *J. Electroanal. Chem.* **2002**, *531*, 155.
61. Carter, M. T.; Bard, A. J. *J. Am. Chem. Soc.* **1987**, *109*, 7528.
62. Lakowicz, J. R. *Principles of Fluorescence Spectroscopy* (2nd ed.); Kluwer/Plenum: New York, **1983**.
63. Rehm, D.; Weller, A. *Isr. J. Chem.* **1970**, *8*, 529.

CHAPTER 6

***'Intra-Complex**Electron Transfer in a Series ofQuinone-Bound Isomeric Porphyrin-Calix[4]arene Conjugates*

6. 1 Introduction

Calixarenes, a well known family of **macrocyclic** oligophenols, play an important role in modern **supramolecular chemistry**.¹ Because of their unique three dimensional shape and good complexation ability, calixarenes have found many applications in the design of synthetic **receptors** and sophisticated molecular **assemblies**.^{2, 3} Likewise, porphyrins - the tetrapyrrolic class of macrocyclic compounds - are known to be one of the support pillars of supramolecular chemistry. Having been endowed with attractive photoactive and electroactive properties, porphyrins are suitable for the construction of molecular devices, photosynthetic model systems, **photodynamic** therapeutic agents **etc.**⁴⁻⁸ The above considerations suggest that porphyrin-calixarene (**P-Calix**) conjugates are appealing receptors with multipoint recognition ability towards guest molecules and that the host-guest interactions in such systems can be conveniently detected by optical spectroscopic and electrochemical methods. Indeed, a great variety of **P-Calix** conjugates have been built for potential use in various applications including binding as well as sensing

various cations, anions and other small molecules of biological interest, templating **supramolecular** ensembles, supramolecular electron transfer **etc.**⁹⁻²⁶

Among the many **P-Calix** systems reported so far, those in which a quinone moiety can be housed inside the calixarene that, in turn, is covalently linked to the porphyrin are of relevance to the present work.^{24,26} It has been established, in these novel donor-acceptor (D-A) systems that a quinone acceptor binds to the calixarene *via* supramolecular contacts. Fluorescence studies have revealed the occurrence of intramolecular photoinduced electron transfer (PET) from singlet porphyrin to the calixarene-bound quinone. In two such **P-Calix** systems, rate constants for electron transfer reactions have been estimated using the time-resolved fluorescence method, but no other details of these supramolecular PET reactions are available to date.

In the present study, a series of isomeric **P-Calix** conjugates have been synthesized in which a calix[4]arene subunit is covalently linked, at o-, m- or p-position of one of the **aryl** groups of a tetra(aryl) porphyrin, Fig. 6. 1. This isomeric nature coupled with flexibility of the **-O-(CH₂)₂-O-** spacer separating the two subunits in these conjugates has resulted in interesting differences in their spectroscopic properties. Rates of photoinduced electron transfer (**k_{PET}**) reactions occurring from the singlet porphyrin to calixarene-bound quinone in these isomeric, D-A systems have been measured in both hydrophobic- (**CH₂Cl₂** solutions, where the calixarene-quinone interaction is *via* H-bonding) and hydrophilic (**water/THF, 9 : 1 v/v**, where the quinone is expected to be

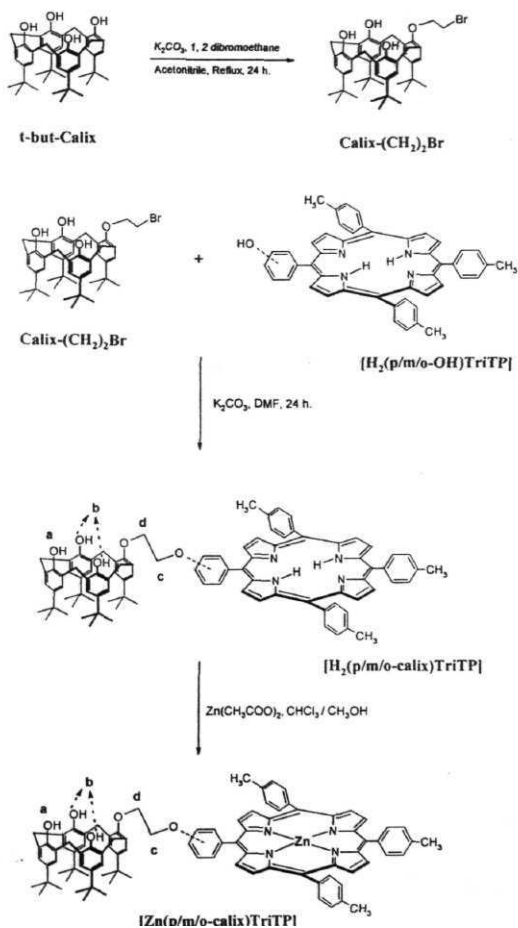


Fig. 6. 1 Scheme leading to the synthesis of isomeric **P-Calix** conjugates.

encapsulated within the calixarene cavity) environments. The results indicate the **presence** of distance and orientation dependence of electron transfer reactions in these supramolecular D-A ensembles, as is the case with analogous **covalently** linked porphyrin-quinone systems.

6. 2 Experimental details

5,10,15,20-tetra(4-methyl-phenyl)porphyrin (**H₂TTP**)²⁷ and its zinc(II) analogue(**[(TTP)Zn^{II}]**)²⁸ and also 4-tert-butylcalix[4]arene (**t-but-Calix**)²⁹ were synthesized by the reported procedures, as described in Chapter 5 (see sections 5. 2. 1 , 5. 2. 2 and 5. 2. 4, respectively)

6. 2. 1 Synthesis of 5-(4/3/2-hydroxyphenyl) 10,15,20-tri(4-methylphenyl) porphyrin (**[H₂(p/m/o-OH)TriTP]**)³⁰

4-, 3- or 2-hydroxybenzaldehyde (6. 1 g, 50 mmol) dissolved in 350 ml of propanoic acid was stirred at 120 °C for 10 min. in each case. To the resulting solution, 12. 0 g (100 mmol) of **4-methylbenzaldehyde** followed by 10. 5 g (157 mmol) of pyrrole were added. The mixture was refluxed for 45 **min.**, left overnight at 10 °C and then filtered. The **black-violet** residue obtained was washed several times with hot water, followed by methanol and purified by **chromatography** on a basic alumina column. Elution with CHCl₃ - CH₃OH (97 : 3, v/v) gave the desired product in each case. Yield: ~ 1. 25 g, (5%).

6. 2. 2 Synthesis of 25-(2-bromoethoxy) 26, 27, 28-tri(hydroxy)-4-tert-butyl calix [4] arene (Calix-(CH₂)₂Br)³¹

1, 2-dibromoethane (3. 53 g, 18. 8 mmol) and finely ground anhydrous K₂CO₃ (0. 17 g, 1. 18 mmol) were added to a suspension of **t-but-Calix** (1. 00 g, 2. 36 mmol) in CH₃CN (50 ml) The reaction mixture was stirred and refluxed for 24 h. under the nitrogen atmosphere. The solvent was evaporated and the crude residue was taken up in CHCl₃ and washed with aqueous HCl (10%, v/v) and water. The organic layer was dried by passing through anhydrous Na₂SO₄ and chromatographed on a silica gel column. The desired product was eluted using CHCl₃ - hexane (9 : 1 , v/v). The solvents were evaporated to get the desired product. Yield = 1. 07 g (71%).

6. 2. 3 Synthesis of 5-((4-phenoxy)-(25-ethoxy)-26, 27, 28-tri(hydroxy)-4-tert-butyl calix[4]arene) 10,15,20-tri(4-methylphenyl) porphyrin ([H₂(p-calix)TriTP])

A mixture of [H₂(p-OH)TriTP] (0. 25 g, 0. 37 mmol), **Calix-(CH₂)₂Br** (0. 32 g, 0. 42 mmol) and 0. 5 g of finely ground anhydrous K₂CO₃ was stirred magnetically in 15 ml of dry dimethylformamide for 24 h. at room temperature under the nitrogen atmosphere. The solvent was evaporated to dryness under the reduced pressure. The residue, dissolved in ca. 50 ml of CHCl₃, was washed repeatedly with water. The CHCl₃ solution was dried over anhydrous Na₂SO₄, after which it was evaporated to 5 ml. This solution was applied onto a silica

gel column. The desired product was eluted using CHCl_3 - hexane (1 : 1, v/v) mixture. Solvents were evaporated and the product was recrystallized in CH_2Cl_2 - hexane mixture. Yield = 0. 44 g (88 %).

6. 2. 4 Synthesis of 5-((4-phenoxy)-(25-ethoxy)-26, 27, 28-tri(hydroxy)-4-tert-butyl calix[4]arene) 10,15,20-tri(4-methylphenyl) porphyrinato zinc(II) ($[\text{Zn}(\text{p-calix})\text{TriTP}]$)

$[\text{H}_2(\text{p-calix})\text{TriTP}]$ (0. 1 g, 0. 07 mmol) was dissolved in 15 ml of CHCl_3 . To this, a solution of 0. 16 g (0. 74 mmol) of zinc(II) acetate hydrate dissolved in a minimum amount of methanol was added. The resulting solution was stirred under reflux for 1 h. The solvent was evaporated and the solid obtained was dissolved in CH_2Cl_2 and then filtered. Evaporation of the solvent gave a solid residue that was purified by column chromatography (silica gel, CHCl_3) and recrystallization (CH_2Cl_2 - hexane). Yield = 0. 16 g (95%).

6. 2. 5 Synthesis of 5-((3-phenoxy)-(25-ethoxy)-26, 27, 28-tri(hydroxy)-4-tert-butyl calix[4]arene) 10,15,20-tri(4-methylphenyl) porphyrin ($[\text{H}_2(\text{m-calix})\text{TriTP}]$)

A mixture of $[\text{H}_2(\text{m-OH})\text{TriTP}]$ (0. 25 g, 0. 37 mmol), **Calix- $(\text{CH}_2)_2\text{Br}$** (0. 32 g, 0. 42 mmol) and 0. 5 g of finely ground anhydrous K_2CO_3 was stirred magnetically in 15 ml of dry dimethylformamide for 24 h. at room temperature under the nitrogen atmosphere. The solvent was evaporated to

dryness under the reduced pressure. The residue was worked up as described above for **[H₂(p-calix)TriTP]** to yield the desired product. Yield = 0.45 g (85%).

6. 2. 6 Synthesis of 5-((3-phenoxy)-(25-ethoxy)-26, 27, 28-tri(hydroxy)-4-tert-butyl calix[4]arene) 10,15,20-tri(4-methylphenyl) porphyrinato zinc(II) ([Zn(m-calix)TriTP])

A 0.1 g (0.07 mmol) of the above compound was dissolved in 15 ml of CHCl₃. To this, a solution of 0.16 g (0.74 mmol) of zinc(II) acetate hydrate dissolved in a minimum amount of methanol was added. The resulting solution was stirred under reflux for 1 h. The solvent was evaporated and the solid obtained was worked up as described above for **[Zn(p-calix)TriTP]**. Yield = 0.16 g (95%).

6. 2. 7 Synthesis of 5-((2-phenoxy)-(25-ethoxy)-26, 27, 28-tri(hydroxy)-4-tert-butyl calix[4]arene) 10,15,20-tri(4-methylphenyl) porphyrin ([H₂(o-calix)TriTP])

A mixture of **[H₂(o-OH)TriTP]** (0.25 g, 0.37 mmol), **Calix-(CH₂)₂Br** (0.32 g, 0.42 mmol) and 0.5 g of finely ground anhydrous K₂CO₃ were stirred magnetically in 15 ml of dry dimethylformamide for 24 h. at room temperature under the nitrogen atmosphere. The solvent was evaporated to dryness and the

residue was worked up as described above for [H2(p-calix)TriTP] to yield the desired product. Yield = 0. 44 g (81 %).

6. 2. 8 Synthesis of 5-((2-phenoxy)-(25-ethoxy)-26, 27, 28-tri(hydroxy)-4-tert-butyl calix[4]arene) 10,15,20-tri(4-methylphenyl) porphyrinato Zinc (II) ([Zn(o-calix)TriTP])

A 0. 1 g (0. 07 mmol) of the above compound was dissolved in 15 ml of CHCl_3 . To this, a solution of 0. 16 g (0. 74 mmol) of zinc(II) acetate hydrate dissolved in a minimum amount of methanol was added. The resulting solution was stirred under reflux for 1 h. The solvent was evaporated and the solid obtained was worked up as described above for the other two zinc(II) complexes. Yield = 0. 14 g (83%).

Each investigated compound was purified on a short alumina column before spectral measurements were made. All the spectroscopic and electrochemical experiments have been carried out as described in Chapter 2.

6. 3 Results and discussion

6. 3. 1 Design and synthesis

Although a great variety of covalently linked porphyrin-quinone systems are reported in the literature,^{5-7, 32-35} relatively less attention has been paid towards the construction of analogous **non-covalent** D-A systems. Previously reported non-covalent porphyrin-quinone assemblies have been built by using nucleic acid base-pairing, coordinate binding, H-bonding,

quinhydrone interactions etc.³⁶⁻⁵⁰ More recently, a few **P-Calix** systems in which 1,4-benzoquinone (BQ) is **supramolecularly** bound at the calixarene part of the ensemble have been reported.²⁴⁻²⁶ In all these **non-covalent** systems, **supramolecular** PET from singlet state of the porphyrin to ground state of quinone has been implicated.

The present work has been undertaken to extend the scope of **P-Calix** systems in understanding the details of supramolecular PET reactions and, this Chapter provides the synthesis, characterization and fluorescence studies of a series of new **P-Calix** systems shown in Fig. 6. 1. The structural features of these new **P-Calix** systems somewhat differ from those of the previously reported systems wherein supramolecular PET has been established.^{24,26} While two of the previously reported such **P-Calix** systems are characterized by a meso-diphenyl porphyrin being connected *via* ether linkages to two calixarene **subunits**,^{24, 25} there is a direct C-C bond between the calixarene and **meso** position of the porphyrin in the other **P-calix** system.²⁶ On the other hand, a calix[4]arene subunit is covalently linked, at o-, m- or p- position of one of the **aryl** groups of a tetra(aryl) porphyrin *via* an **-O-(CH₂)₂-O-** spacer, in the presently investigated conjugates. In addition, these new conjugates are readily synthesized by reacting together **isomeric** mono(hydroxyphenyl) porphyrins and **Calix-(CH₂)₂Br** in K₂CO₃/DMF milieu in > 80% yields in each case. In contrast, the previously reported **P-Calix** systems have been prepared either by reacting together the bis(bromoalkyl)diphenyl porphyrin and the parent

calix[4]arene^{24, 25} or by the mixed - aldehyde condensation of dipyrromethane with benzaldehyde and calixarene aldehyde²⁶ in not more than 52% yields.

6.3.2 Ground state properties

MALDI-TOF spectra of the isomeric zinc(II)porphyrin-calix[4]arene conjugates showed the molecular ion peak at $m/z = 1409$ in each case. UV-visible spectral data of the isomeric free-base and zinc(II) derivatives of **P-Calix** conjugates investigated during this study and also that of their constituent individual components (i. e. **Calix(CH₂)₂Br**, **H₂TTP** and **[(TTP)Zn^{II}]**) are summarized in the Table 6. 1. Fig.6. 2 illustrates UV-visible spectra of the p- and o- isomers of zinc(II)porphyrin-calixarene conjugates. As seen from Fig. 6. 2 and Table 6. 1, spectra of the **P-Calix** conjugates show bands due to calix[4]arene subunit's absorption between 250 and 300 nm and those due to porphyrin absorption between 400 and 700 nm. Data given in Table 6. 1 also suggests that, except for o- isomer of the zinc(II)porphyrin-calixarene conjugate, wavelengths at the maximum absorption (λ_{max}) values of these **P-Calix** systems are within the same range as those of the individual components . As seen in Fig. 6. 2, in comparison with its p- analogue, **[Zn(o-calix)TriTP]** experiences a red shift of 7 nm (280 to 287 nm) for its calix[4]arene band. The porphyrin Soret and Q- bands are also similarly red shifted by 5 (421 to 426 nm) and 6 (549 to 555 nm; 589 to 595 nm) respectively, for this isomer. The close proximity between the calixarene and porphyrin subunits in

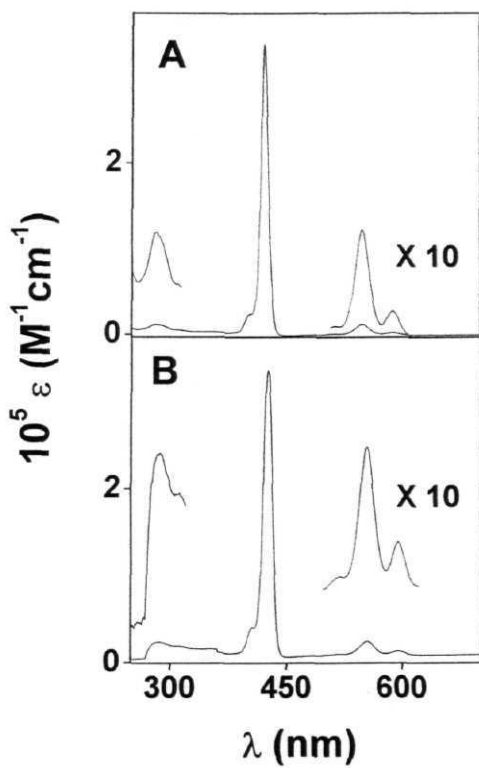


Fig. 6. 2 UV-visible spectra of (A) $[\text{Zn(p-calix)TriTP}]$ and (B) $[\text{Zn(o-calix)TriTP}]$ in CH_2Cl_2 .

Table 6. 1 UV-visible data of **P-Calix** conjugates in CH_2Cl_2 ^a

Compound	λ_{max} , nm (log e)		
	Calixarene band	Soret band	Q-bands
Calix-(CH₂)₂Br	279 (3. 98)	-	-
H₂TTP	-	418(5.30)	516 (4. 17) 551 (3. 90) 592 (3. 64) 650 (3. 76)
[(TTP)Zn^{II}]	-	420 (5. 55)	549(4.12)587(3.49)
[H₂(p-calix)TriTP]	280(4.10)	419(5.44)	515 (4. 02) 550 (3. 79) 593 (3. 45) 649 (3.40)
[Zn(p-calix)TriTP]	280 (4. 08)	421(5.51)	549 (4. 08) 589 (3. 48)
[H₂(m-calix)TriTP]	280(4. 10)	418(5.41)	514 (4. 07) 549 (3. 73) 592 (3. 52) 648 (3. 39)
[Zn(m-calix)TriTP]	281 (4.04)	421 (5.49)	549 (4. 05) 589 (3. 40)
[H₂(o-calix)TriTP]	280 (4. 35)	419(5.46)	515 (4. 15) 550 (3. 87) 593 (3. 69) 649 (3.57)
[Zn(o-calix)TriTP]	287 (4. 38)	426 (5. 52)	555(4.39)595(4.14)

a) Error limits: $\lambda_{\text{max}} \pm 1$ nm; log E, $\pm 10\%$

[Zn(o-calix)TriTP] can lead to either π - π interaction between the porphyrin and calixarene aryl groups or an intramolecular coordination between zinc(II) center of the porphyrin and one of the hydroxyl group of calix[4]arene moiety.

Literature data suggests that a red shift of the Soret and Q- bands of the porphyrin chromophore is expected to occur in either case.^{49,50} However, the fact that red-shifts are seen only in the spectrum of [**Zn(o-calix)TriTP**] and not in the spectrum of its free-base analogue, [**H₂(o-calix)TriTP**], favours an intramolecular coordination of the hydroxyl group at the zinc(II) center. In order to probe this aspect further, detailed ¹H NMR investigations were carried out, the results of which are discussed below.

The ¹H NMR (CDCl₃, TMS) spectra of {**Zn(p-calix)TriTPJ**} and [**Zn(o-calix)TriTP**] are compared in Fig. 6. 3. NMR data of all the new porphyrins investigated in this study along with the data on **Calix(CH₂)₂Br**, **H₂TTP** and [**(TTP)Zn^{II}**] are summarized in Tables 6. 2a and 6. 2b. ¹H NMR features of each new **P-Calix** conjugate are highly characteristic with the integrated intensities of the proton resonances in the 1D spectrum and also the ¹H - ¹H coupling patterns observed in the 2D (¹H - ¹H COSY) spectra being in conformity with the proposed structure. Interestingly, while ¹H NMR spectral features of the p- and m- isomers of these conjugates are similar to those of the corresponding reference compounds, spectra of the o- isomers are found to be quite different. Therefore, spectral features of the o- isomers are discussed separately.

The β-pyrrole protons of [**H₂(p, m-calix)TriTP**] resonate at 8. 84 ppm as a **multiplet** due, mainly, to **unsymmetric** substitution at the **macrocyclic** periphery in contrast with the singlet seen at 8. 85 ppm for the corresponding

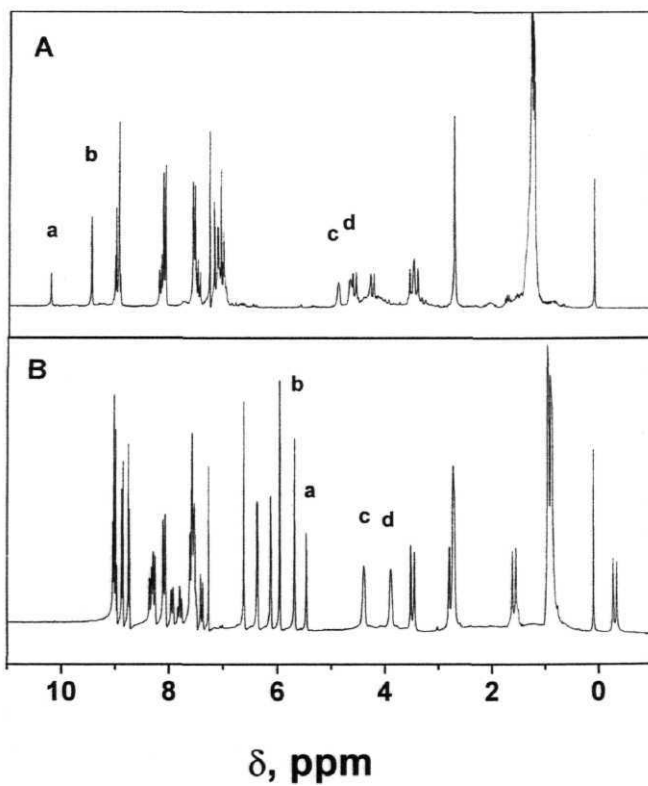


Fig. 6. ^1H NMR spectra (CDCl_3 , TMS) of (A) $[\text{Zn}(\text{p-calix})\text{TriTP}]$ and (B) $[\text{Zn}(\text{o-calix})\text{TriTP}]$. Peak at 7.26 ppm is due to solvent.

Table 6. 2a ¹H-NMR data of free-base derivatives of the **P-Calix** conjugates

Compound →	S, ppm [J _{HH}], Hz				
	Calix-(CH₂)₂Br	H,TTP	[H ₂ (p-calix)TriTP]	[H ₂ (m-calix)TriTP]	[H ₂ (o-calix)TriTP]
Porphyrin H_p		8 85 (s, 8H)	8. 84 (m, 8H)	8.85 (m, 8H)	8.77 (m, 8H)
Porphyrin H_o	-	8. 10 (d, 8H) [7. 81]	8. 17 8. 09 (d, 6H)(d,2H) [8. 81 [8. 8]	8.10 7.99 7.87 (d, 6H)(s, 1H)(d, 1H) [8.0] [8.0]	8.06 7.97 7.85 (d,6H)(d, 1H)(m, 1H) [8. 81 [8. 8]
Porphyrin H_m	-	7. 55 (d, 8H) [7. 8]	7. 54 7. 46 (d, 6H)(d, 2H) [7. 8] [7. 8]	7. 70 7. 54 (m, 2H)(d, 6H) [7.81]	7.68 7.54 7.41 (d, 1H)(d, 6H)(m, 1H) [7.8] [7.8]
Porphyrin CH₃		2. 71 (9, 9H)	2. 70 (s, 9H)	2.69 (s, 9H)	2.70 (s, 9H)
Porphyrin NH		-2. 76 (s, 2H)	-2. 76 (s, 2H)	-2.78 (s, 2H)	-2.80 (s, 2H)
Spacer-O-CH₂-CH₂-O-	4. 51 4. 00 (t, 2H)(t, 2H)	-	4.89 4.71 (t, 2H)(t,2H)	4. 80 4. 62 (t, 2H)(t, 2H)	4 48 3. 61 (l,211)(l,21l)
Calix OH	10. 19 9. 31 (s, 1H)(s, 2H)	-	10.32 9.57 (s, 1H)(s, 2H)	10.26 9.49 (s, 1H)(s, 2H)	9. 62 9. 61 (s, 2H)(s, 1H)
Calix Phenyl	7. 06 (m, 8H)	-	7. 18 7. 13 (s, 2H)(s, 2H) 7. 07 7. 03 (s, 2H)(s, 2H)	7. 09 7. 02 6. 92 (s, 2H)(s, 4H)(s, 2H)	6. 84 6. 64 (s, 2H)(s, 2H) 6. 50 6. 36 (s, 2H)(s, 2H)
Calix ArCH₂Ar	4. 35 (m, 4H) 3. 42 (d,4H) [13. 6]	-	4. 64 4. 55 (d,2H)(d, 2H) [13.6] [13. 6] 3.47 3.35 (d, 2H)(d, 2H) [13. 6] [13. 6]	4. 53 4. 22 (d, 2H)(d, 2H) [13.6] [13.6] 3. 43 3. 30 (d, 2H)(d, 2H) [13.6] [13.6]	3.72 3.47 (d, 2H)(d, 2H) [13.6] [13.6] 3. 05 2. 37 (d, 2H)(d, 2H) [13.6] [13.6]
Calix (-Butyl	1. 20 (s, 36H)		1. 24 (s, 36H)	1. 23 1. 15 (s, 9H)(s, 27H)	1.25 1.14 0.93 0. 86 (s,9H) (s, 9H) (s,9H) (s,9H)

a) Error limits: 8, ± 0.01 ppm; J, ± 1 Hz

Table 6. 2b ^1H -NMR data of zinc(II) derivatives of the **P-Calix** conjugates

Compound →	δ , ppm $[J_{\text{HH}}]$, Hz				
	Calix-(CH ₂) ₂ Br	[(TTP)Zn ^{II}]	[Zn(p-calix)TriTP]	[Zn(m-calix)TriTP]	[Zn(o-calix)TriTP]
Porphyrin H_p	-	8.85 (s, 8H)	8.85 (m, 8H)	8.97 (m, 8H)	9.01 8.86 8.74 (m, 6H) (d, 2H) (d, 2H) [4. 8] [4. 8]
Porphyrin H_m	-	8.10 (d, 8H) [7. 8]	8.19 8.10 (d, 2H) (d, 2H) [8. 8] [8. 8]	8.12 8.00 7.91 (d, 6H) (s, 1H) (d, 1H) [8. 0] [8. 0]	8.30 8.09 7.94 7.80 (m, 3H) (d, 3H) (d, 1H) (m, 1H) [8. 0] [8. 0]
Porphyrin H_m	-	7.55 (d, 8H) [7.81]	7.54 7.46 (d, 6H) (d, 2H) [8. 81] [8. 81]	7.70 7.54 (m, 2H) (d, 6H) [7. 8]	7.80 7.56 7.39 (m, 1H) (m, 6H) (d, 1H) [7.8]
Porphyrin CH₃		2.72 (s, 9H)	2.72 (s, 9H)	2.72 (s, 9H)	2.73 (s, 9H)
Spacer -O-CH ₂ -CH ₂ -O-	4.51 4.00 (t, 2H) (t, 2H)	-	4.89 4.68 (t, 2H) (t, 2H)	4.76 4.52 (t, 2H) (t, 2H)	4.40 3.89 (t, 2H) (t, 2H)
Calix OH	10.19 9.31 (s, 1H) (s, 2H)		10.23 9.47 (s, 1H) (s, 2H)	10.13 9.34 (s, 1H) (s, 2H)	5.69 5.47 (s, 2H) (s, 1H)
Calix Phenyl	7.06 (m, 8H)	-	7.18 7.12 (s, 2H) (s, 2H) 7.06 7.01 (s, 2H) (s, 2H)	7.10 7.02 (s, 2H) (s, 4H) 6.92 (s, 2H)	6.62 6.37 (s, 2H) (s, 2H) 6.13 5.96 (s, 2H) (s, 2H)
Calix ArCH ₂ Ar	4.35 3.42 (m, 4H) (d, 4H) [13.6]	-	4.61 4.27 (d, 2H) (d, 2H) [13.6] [13.6] 3.52 3.44 (d, 2H) (d, 2H) [13. 6] [13.6]	4.44 4.10 (d, 2H) (d, 2H) [13.6] [13.6] 3.40 3.29 (d, 2H) (d, 2H) [13.61] [13. 6]	3.48 2.78 (d, 2H) (d, 2H) [13.6] [13. 6] 1.59 -0.30 (d, 2H) (d, 2H) [13.61] [13. 6]
Calix (-Bun l	1.20 (s, 36H)	-	1.26 (s, 36H)	1.26 1.22 (s, 9H) (s, 27H)	0.94 0.87 (s, 18H) (s, 18H)

a) Error limits: 8, ± 0.01 ppm; J, ± 1 Hz

protons of the symmetrically substituted **H₂TTP**. The eight β -pyrrole proton resonances of **[Zn(p-calix)TriTP]** (see: Fig. 6. 3) and **[Zn(m-calix)TriTP]** also resonate as a multiplet at 8. 85 and 8. 97 ppm, respectively. Phenyl protons of the **meso-tolyl** groups of these isomeric free-base and zinc(II) conjugates resonate between 8. 19 - 7. 87 ppm (protons o- to the porphyrin ring) and between 7. 70 - 7. 46 ppm (protons m- to porphyrin ring), as expected. Similarly, the methyl groups of **[H₂/Zn(p, m-calix)TriTP]** resonate as a singlet in the aliphatic region between 2. 69 - 2. 72 ppm, quite close to the methyl group resonance positions of the control systems, viz. **H₂TTP/[(TTP)Zn^{II}]**. The spacer **-O(CH₂)₂-O-** protons (protons c and d, see: Fig. 6. 1 for proton identification) appear as a pair of triplets in the 4. 89 - 4. 52 ppm range for these p- and m- isomers. Due to the strong intramolecular hydrogen **bonding**,¹ the calixarene **subunit's** hydroxyl protons of the p- and m- isomers appear as two separate singlets in the range 10. 32 - 10. 13 (protons a) ppm and 9. 57 - 9. 34 ppm (proton b) with the proton integration ratio of 1 : 2 in each case. Aromatic protons of the porphyrin-bound calix[4]arene subunit resonate as four separate singlets between 7. 18 and 7. 01 ppm for the p- isomers. The corresponding protons of the m- analogues resonate as three singlets in the ratio of 1: 2: 1 between 7. 09 and 6. 92 ppm. However, **methylene** protons on the calixarene subunits resonate as 'two pairs of doublets' between 4. 64 - 3. 29 ppm for both p- and m- isomers with the geminal coupling constant of 13. 6 Hz. in each case. This observation is suggestive of the fact that the

calix[4]arene ring is present in its partial cone conformation in these **isomeric conjugates**.¹ Finally, the **tert-butyl** groups of each calixarene subunit resonate in the region 1.26 - 1.15 ppm, as expected.

The ¹H NMR spectra of both the free-base and zinc(II) derivatives of the o- analogues showed several interesting features, as detailed below:

- (i) The p-pyrrole protons of [**H2(o-calix)TriTP**] resonate as a multiplet (8.77 ppm, m, 8H), as is the case with the corresponding p- and m- analogues. On the other hand, resonances due to P-pyrrole protons of [**Zn(o-calix)TriTP**] (see: Fig.6. 3(B)) are split and appear at 9.01 (**m**, 6H), 8.86 (d, 1H) and 8.74 (d, 1H) ppm, unlike the case with the corresponding proton resonances of [**Zn(p, m-calix)TriTP**] that appear as a single set of multiplet (see: Fig.6. 3(A)).
- (ii) The spacer $\text{--O(CH}_2\text{)}_2\text{--O}$ - protons (protons **c** and **d**) of [**H₂/Zn(o-calix)TriTP**] are shifted upfield, compared to the resonance positions of protons **c** and **d** of the corresponding p- and m- analogues, and appear between 4.48 and 3.61 ppm as a pair of triplets.
- (iii) More dramatic upfield shifts are noticed for the calixarene's hydroxyl protons of both these o- derivatives in comparison with those of the p- and m- analogues. While the resonances due to hydroxyl protons **a** and **b** for [**H2(o-calix)TriTP**] appear as closely separated singlets at 9.62 (s, 2H) and 9.61 ppm (s, 1H) respectively,

those of **[Zn(o-calix)TriTP]** are more severely shielded and resonate at 5.69 (s, 2H) and 5.47 (s, 1H) ppm, respectively.

- (iv) As far as resonances due to protons on the calix[4]arene rings are concerned, the aromatic protons of these o-isomers resonate as four separate singlets between 6.84 and 5.96 ppm, shifted upfield in comparison with the corresponding protons of the p- and m- isomers that resonate in the region 7.18 - 6.92 ppm. Similarly, the methylene protons are also shifted upfield and appear as two pairs of doublets for both the free-base (3.72 - 2.37 ppm) and the zinc(II) (3.48 - 2.30 ppm) derivatives, with the geminal coupling constant of 13.6 Hz in each case. Thus, as is the case with **[H₂/Zn(p, m -calix)TriTP]**, the calix[4]arene subunit is present in a partial cone conformation in these o- isomers.¹

The ¹H NMR spectral data presented above reveals that there is a close proximity between the calixarene and porphyrin subunits in **[H₂(o-calix)TriTP]** and **[Zn(o-calix)TriTP]**; the latter conjugate showing porphyrin ring-current induced,⁵¹ dramatic differences in the resonance positions of various protons in comparison with its p- or m- analogues. Specifically, observations that resonances due to the calix[4]arene's aryl, methylene and, more importantly, the hydroxyl protons are shielded in **[Zn(o-calix)TriTP]** are in conformity with the UV-visible data presented above for this conjugate.

Thus, close proximity of the two subunits in [Zn(o-calix)TriTP] can lead to an intramolecular coordination between zinc(II) **center** of the porphyrin and hydroxyl group of the calix[4]arene moiety. The multiplet pattern observed for the β -pyrrole resonances of this zinc(II) **isomer** is also consistent with the axial coordination at the metal center that renders the local porphyrin structure quite 'asymmetric'. Finally, intramolecular *n-n* interaction between the porphyrin and calixarene subunits can explain the less dramatic shielding effects observed for the various protons on [H2(o-calix)TriTP].

Interestingly, except for a marginal broadening of the peaks, resonances due to hydroxyl protons of the calixarene subunit of each P-Calix conjugate investigated here were found to be insensitive to the presence of even excess BQ during the ^1H NMR titration experiments carried out under the present set of experimental conditions (200 MHz, CDCl_3). This observation is in contrast with the behavior of the previously reported P-Calix compounds wherein it was possible to estimate the binding constant for the calixarene-quinone interaction by monitoring the calixarene hydroxyl protons. The BQ binding constants for the present series of isomeric P-Calix systems could, however, be obtained by the time-resolved fluorescence method as will be discussed in a later section of this Chapter.

Table 6. 3 summarizes redox potential data of the **P-Claix** conjugates along with the data of their constituent components, as obtained from the

differential pulse voltammetric experiments. Fig. 6. 4 illustrates a representative differential pulse voltammogram. Each investigated porphyrin

Table 6. 3 Redox potential data of **P-Calix** conjugates (CH_2Cl_2 , 0. 1 M TBAP)^a

Compound	Potential, V vs. SCE		ΔG_{PET} (eV)
	Reduction	Oxidation	
Calix-(CH₂)₂Br	-	1.33	-
H₂TTP	-1.24,-1.53	0.97, 1.21	-
[(TTP)Zn^{II}]	-1.40,-1.79	0.74, 1.032	-
BQ	-0.46	-	-
[H₂(p-calix)TriTP]	-1. 15	0.94, 1.33 ^b	-0.54
[H₂(m-calix)TriTP]	-1. 19	0.93, 1. 31 ^b	-0.55
[H₂(o-calix)TriTP]	-1. 17	0.90, 1.33 ^b	-0.58
[Zn(p-calix)TriTP]	-1.37,-1.75	0.75, 1.06, 1.39 ^b	-0.86
[Zn(m-calix)TriTP]	-1.39.-1.74	0.77,1.07, 1. 38 ^b	-0.84
[Zn(o-calix)TriTP]	-1.39.-1.78	0.76, 1.09, 1. 39 ^b	-0.85

a) Error limits: $E_{1/2} \pm 0. 03 \text{ V}$

b) Quasi-reversible/irreversible

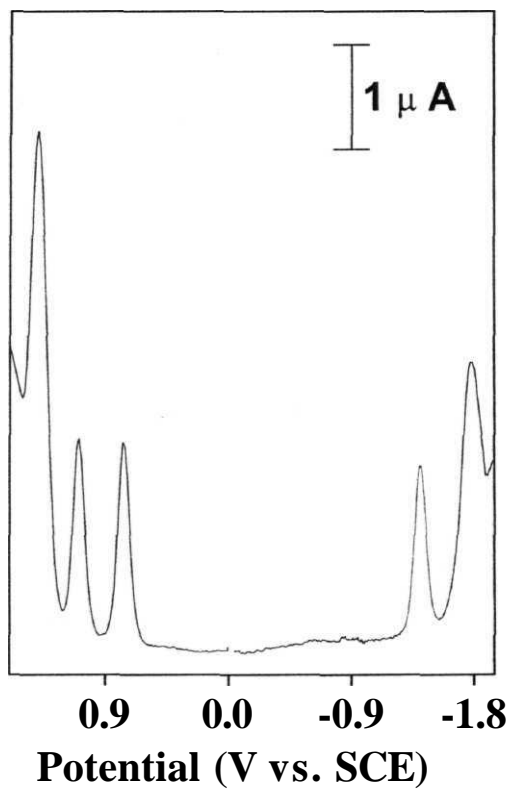


Fig. 6. 4 Differential pulse voltammogram of $[\text{Zn}(\text{o-calix})\text{TriTP}]$ in CH_2Cl_2 , 0.1 M TBAP (scan rate = 10 mV s^{-1}).

was found to undergo up to two successive reduction reactions and up to three successive oxidation reactions in CH_2Cl_2 , 0.1 M TBAP. Wave-analysis of the corresponding cyclic voltammetric responses suggested that the two reduction- and also the first oxidation steps are all reversible ($i_{\text{c}}/i_{\text{a}} = 0.9 - 1.0$ where i is the peak current) and diffusion controlled ($i/v = \text{constant}$ in the scan rate (v) range 50 - 500 mV s^{-1}) one-electron transfer ($\Delta E_{\text{p}} = 60 - 70 \text{ mV}$ where ΔE_{p} is the peak-to-peak potential difference; $\Delta E_{\text{p}} = 65 \pm 3 \text{ mV}$ for Fc/Fc⁺ couple) reactions.⁵² On the other hand, the second and the third oxidation steps of these complexes are found to be either quasi-reversible ($\Delta E_{\text{p}} = 90 - 200 \text{ mV}$ and $i_{\text{pc}}/i_{\text{pa}} = 0.5 - 0.8$ in the scan rate 100 - 500 mV s^{-1}) or totally irreversible. Thus, the zinc(II) conjugates showed two anodic responses, one between 0.75 and 0.77 V and the other between 1.06 and 1.09 V, corresponding to first and second one-electron abstractions from the porphyrin moiety, respectively. These oxidation peaks are close to those of $[(\text{TTP})\text{Zn}^{\text{II}}]$. The third, irreversible voltammetric response seen at +1.39 V can thus be attributed to oxidation of the appended calix[4]arene subunit. During the cathodic scan, these zinc(II) porphyrins showed two reversible peaks ($-1.38 \pm 0.01 \text{ V}$ and $\sim -1.76 \text{ V}$) corresponding to successive one-electron additions to the porphyrin ring. In the case of free-base analogues, each compound showed only one cathodic and two anodic responses under our experimental conditions. Based on the data of H_2TTP , the first anodic (0.90 - 0.94 V) and the first cathodic ($-1.15 - -1.19$

V) responses are ascribed to one-electron addition and one-electron abstraction reactions involving the porphyrin ring. The peak appearing at ~ 1.32 V, in each case, is found to be irreversible and, in addition, showed higher current values in comparison with the corresponding first one-electron oxidation responses. This observation and the fact that phenolic groups of the calix[4]arene subunit in the zinc(II) systems discussed above are oxidized at $+1.39$ V, together suggest that the second oxidation responses seen at ~ 1.32 V for the free-base **P-Calix** derivatives represent simultaneous electron abstractions from the porphyrin and calixarene moieties. Finally, BQ could be reduced at -0.46 V under the similar set of experimental conditions employed to probe redox characteristics of the **P-Calix** conjugates.

6.3.3 Singlet state properties

When excited at 530 nm in CH_2Cl_2 or $\text{H}_2\text{O}/\text{THF}$ (9:1, v/v) medium, steady state fluorescence spectrum of each isomeric **P-Calix** conjugate showed two emission bands. These bands are located at 656 ± 2 and 718 ± 2 nm for the free-base conjugates and at 610 ± 2 and 656 ± 2 nm for the zinc(II) conjugates in CH_2Cl_2 . The corresponding bands in $\text{H}_2\text{O}/\text{THF}$ (9:1, v/v) medium are at 656 ± 2 and 718 ± 2 nm (free-bases) and at 606 ± 2 and 657 ± 2 nm (zinc(II) conjugates) respectively. The singlet state energies (E_{0-0}), estimated by overlapping the absorption and fluorescence spectra, are 1.91 ± 0.01 and 2.00 ± 0.01 eV for the p-, m- and o- isomers of the free-base and zinc(II)

conjugates, respectively. The fluorescence quantum yields (ϕ) of **p-, m-** and **o-isomers** of the free-base and zinc(II) derivatives are ($\pm 10\%$): 0. 098, 0. 103 and 0. 089 (free-base) and 0. 030, 0. 030 and 0. 027 (**zinc(II)** porphyrins), respectively. Thus, the wavelengths of maximum emission (λ_{em}), singlet state energies and ϕ values of these isomeric free-base and zinc(II) conjugates are close to those of the reference porphyrins, viz **H₂TTP** and **[(TTP)Zn^{II}]**. Excitation at 290 nm (predominantly calixarene absorption band) did not show any fluorescence in the UV region suggesting that the linked calixarene subunit of these conjugates is photochemically inactive under the present set of experimental conditions.

Quenching of porphyrin fluorescence by quinone under intermolecular situations and also in covalently linked intramolecular porphyrin-quinone compounds is long known in the literature.⁵³⁻⁵⁵ Both steady state and time-resolved **emission/absorption** studies have confirmed that electron transfer from the photoexcited porphyrin to the quinone is mainly responsible for this **quenching**.^{5-7, 32-35} By using a variety of covalently linked porphyrin-quinone dyads, the optimal D - A distance and mutual orientation factors for realizing an efficient electron transfer have been evaluated by several research groups. On the other hand, relatively few such studies have been carried out using non-covalent porphyrin-quinone **complexes**.³⁶⁻⁴⁸ The series of isomeric **P-Calix** systems being investigated here provide an opportunity to evaluate the

geometric details of supramolecular PET reactions between porphyrin donor and **calixarene-bound** quinone acceptor.

Binding of BQ by the calixarene host *via* H-bonding interaction in apolar solvents like CH₂Cl₂ and *via* encapsulation (mediated by π - π interaction) in water rich media (H₂O/THF) has been established earlier.^{24,26} It is reasonable to expect the same interactions to be prevalent in our **P-Calix** compounds in the presence of added BQ. As far as thermodynamics of the PET reaction between the singlet porphyrin and BQ is concerned, free energy change for this reaction (ΔG_{PET}) can be calculated based on the E_{0-0} and redox potential **data**, equn.6. 1.

$$\Delta G_{PET} = E_{1/2}(ox) - E_{1/2} (red) - E_{0-0} \quad (6. 1)$$

where $E_{1/2}(ox)$ and $E_{1/2} (red)$ are the first oxidation potential of the porphyrin and the reduction potential of BQ, respectively. These calculations have been carried out using the data on each new **P-Calix** conjugate investigated in this study and reveal that the PET reactions between the porphyrin singlet and BQ are exoergic by 0.56 ± 0.02 and 0.85 ± 0.01 eV for the free-base and zinc(II) **P-Calix** derivatives, respectively (see: Table 6. 3). In what follows now, details of **supramolecular** PET reactions occurring between the porphyrin and quinone moieties, as revealed by the steady state and time-resolved fluorescence studies in CH₂Cl₂ and H₂O/THF (9:1, v/v) environments, are described.

In the steady state experiments, fluorescence due to **H₂TTP** and **[(TTP)Zn]** ($\lambda_{\text{exc}} = 530 \text{ nm}$) were found to be quenched upon successive addition of BQ in both **CH₂Cl₂** and **H₂O/THF** (9:1, v/v) media. The quenching data was analyzed using **Stern-Volmer** equation, equn.6. 2.⁵⁶

$$I_0/I = 1 + K_{\text{SV}}[\text{BQ}] \quad (6.2)$$

where I_0 and I represent emission intensities of the porphyrin in the absence and the presence of BQ respectively, and K_{SV} is the **Stern-Volmer** quenching constant. K_{SV} is equal to product of the bimolecular quenching constant, k_q , and the excited state lifetime, τ , of the donor porphyrin in the absence of any added quencher. The lifetimes of **H₂TTP** and **[(TTP)Zn^{II}]** in **CH₂Cl₂** and **H₂O/THF** (9:1, v/v) are obtained by the time-resolved single photon counting technique (see: Table 6. 4). The calculated k_q values for the bimolecular reactions involving **H₂TTP** and **[(TTP)Zn^{II}]**, determined from slopes of the corresponding **Stern-Volmer** plots, range between $4.01 - 8.25 \times 10^9 \text{ M}^{-1}\text{s}^{-1}$ ($\pm 10\%$) and are close to those expected for diffusion controlled process.

In the case of isomeric **P-Calix** conjugates, **Stern-Volmer** plots for the quenching by BQ are found to show upward curvature in each case, irrespective of the presence/absence of the zinc(II) ion in the porphyrin crevice or the solvent system employed for the experiments. A representative example is provided in **Fig.6. 5** (inset) which clearly illustrates an upward curvature for

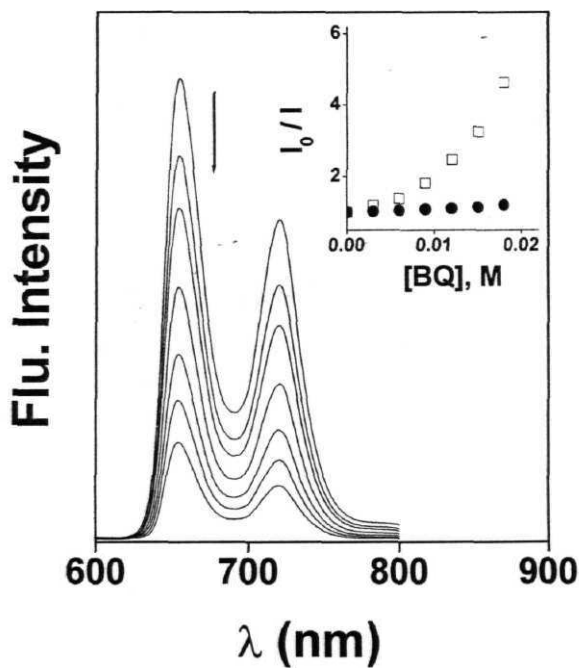
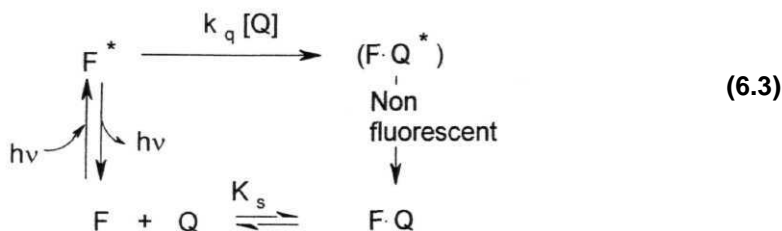


Fig. 6. 5 Fluorescence spectra ($\lambda_{\text{exc}} = 530$ nm) of **[H₂(p-calix)TriTP]** in the absence (top curve) and presence of increasing concentrations of BQ (subsequent curves) in H₂O/THF (9 : 1, v/v). Inset shows Stern-Volmer plots for the quenching of **[H₂(p-calix)TriTP]** (\square) and **[H₂TTP]**(\bullet) by BQ.

the **[H₂(p-calix)TriTP] - BQ** titration in the H₂O/THF (9 : 1, v/v) medium. Such an upward curvature is suggestive of the fact that fluorescence quenching process involves both static and dynamic processes.⁵⁶ Thus, the singlet porphyrin in these isomeric **P-Calix** conjugates is quenched, in part, by 'intra-complex' electron transfer involving the complexed quinone, as shown in eqn.6. 3.



Time-resolved fluorescence studies provide further support for the above scheme. First, control systems **H₂TTP** and **[(TTP)Zn^{II}]** were examined in dry CH₂Cl₂, and THF/H₂O by exciting the sample at 575 nm and monitoring the decay at 650 nm. In the absence of added BQ, singlet state decays of these species were found to be monoexponential. When BQ was added to the above solutions (0 - 6 x 10⁻² M), the fluorescence decay profile remained monoexponential. However, it showed a decreased dynamic lifetime as would be expected for a concentration dependant bimolecular quenching process. The

k_q values estimated by the Stern-Volmer treatment ($2.11 - 5.67 \times 10^9 \text{ M}^{-1} \text{ s}^{-1}$) are close to those obtained by the steady state method (*vide supra*)

When the experiments were carried out with the isomeric **P-Calix** systems in the absence of BQ under identical conditions to those employed for the control systems in CH_2Cl_2 , fluorescence decay of each system was found to follow a first order kinetics with lifetimes (TO) ranging between 7.45 - 7.68 ns and 1.55 - 1.58 ns for the free-base and zinc(II) analogues, respectively (Table 6.4). The corresponding values in $\text{THF}/\text{H}_2\text{O}$ are 6.76 - 6.82 ns and 1.45 - 1.48 ns, respectively. These τ_0 values are close to those of the corresponding unlinked compounds, **H₂TTP** and **[(TTP)Zn^{II}]** (see: Table 6.4). Addition of BQ to each **P-Calix** conjugate dissolved in either CH_2Cl_2 or $\text{THF}/\text{H}_2\text{O}$, however, resulted in a decay profile which could be best analyzed in terms of two components, a long lived component with a concentration dependence (τ_1) and a short lived component with a constant lifetime (τ_2). This fact is illustrated in Fig. 6.6 for **[Zn(o-calix)TriTP]**. The decay profiles were analyzed using eqn. 6.4.

$$I(t) = A_1 \exp(-t/\tau_1) + A_2 \exp(-t/\tau_2) \quad (6.4)$$

Table 6. 4 Data obtained from time-resolved fluorescence studies with P-Calix conjugates.^a

Compound	Life time			k_{PET} (s ⁻¹)	K (M ⁻¹)
	τ_0 (ns)	(ns)	(ns)		
H₂TTP-CH₂Cl₂	8. 12	1. 15			-
[(TTP)Zn^{II}]-CH₂Cl₂	1. 61	0. 71	-		-
[H₂(p-calix)TriTP]-CH₂Cl₂	7. 68	1. 03	0.92	0. 96	15.0
[H₂(m-calix)TriTP]-CH₂Cl₂	7. 52	0. 93	0.87	1. 02	13.8
[H₂(o-calix)TriTP]-CH₂Cl₂	7.45	1. 10	0.75	1.19	16.2
[Zn(p-calix)TriTP]-CH₂Cl₂	1. 58	0. 74	0.61	1. 01	13.2
[Zn(m-calix)TriTP]-CH₂Cl₂	1. 56	0. 78	0.57	1. 11	13.4
[Zn(o-calix)TriTP]-CH₂Cl₂	1. 55	0. 68	0.43	1. 68	15.2
H₂TTP- H₂O/THF	6. 93	1 18	-	-	-
[(TTP)Zn^{II}]- H₂O/ THF	1 49	0 89	-	-	-
[H₂(p-calix)TriTP]- H₂O/THF	6 82	1 12	0.58	1. 57	15.7
[H₂(m-calix)TriTP]- H₂O/THF	6.75	1 23	0.51	1. 81	14.9
[H₂(o-calix)TriTP]- H₂O/THF	6 76	1 08	0.45	2. 04	15.0
[Zn(p-calix)TriTP]- H₂O/THF	1 48	0 84	0.27	2. 95	12.3
[Zn(m-calix)TriTP]- H₂O/THF	1 47	0 88	0.23	3 52	16. 1
[Zn(o-calix)TriTP]- H₂O/THF	1 45	0 79	0. 19	4 52	17. 1

a) Error limits: T and k_{PET} , $\pm 10\%$; K, $\pm 5\%$

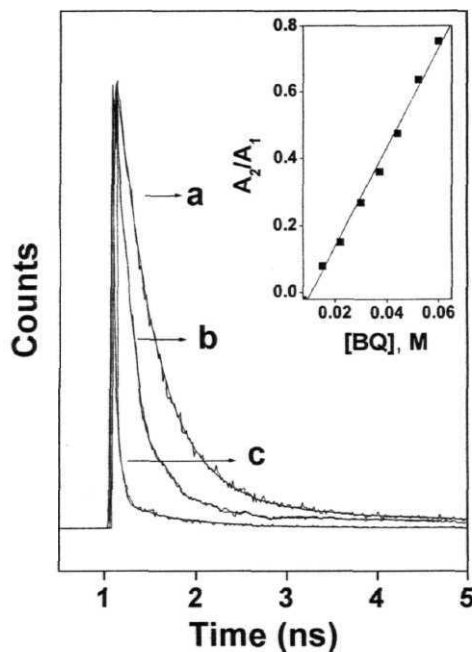


Fig. 6. 6 Time-resolved emission decays ($\lambda_{exc} \approx 575$ nm, $\lambda_{em} = 650$ nm) of [Zn(o-calix)TriTP] at (a) 0, (b) 3×10^{-2} and (c) 6×10^{-2} M of BQ in CH_2Cl_2 . While trace a follows a monoexponential decay, traces b and c could be best fit to a biexponential decay function. Inset shows a plot of ratio of the fractional amplitudes A_2/A_1 vs. $[BQ]$ in CH_2Cl_2 , as derived from the time-resolved emission titration of [Zn(o-calix)TriTP] with BQ.

where A's refer to the fractional amplitudes. The lifetimes of both the long and short lived components obtained at the end of the titration are summarized in Table 6. 4.

It is seen that fractional amplitude of the short lived component (A_2) increases from 0 to 47% as the BQ concentration is increased from 0 to 6×10^{-2} M, (see: Fig. 6. 6 inset). In spite of this increase in the fractional amplitude, life time (τ_2) of this short lived component remained essentially unchanged. However, it could be eliminated by adding methanol (~ 5%) to the original CH_2Cl_2 solution. Under these conditions, fluorescence decay profiles of the isomeric supramolecular complexes in CH_2Cl_2 could be analyzed in terms of single exponentials even in the presence of BQ. In contrast to this, addition of 5% methanol to THF/H₂O solutions containing a given **P-Calix** conjugate and BQ did not affect the decay profile; the profile remained essentially biexponential.

As far as the longer lived component (τ_1) is concerned, not only its life time but also the fractional amplitude was observed to decrease as the concentration of BQ is increased in both CH_2Cl_2 and THF/H₂O. The decrease is in the range of 7. 68 ns to 1. 10 ns and 1. 58 ns to 0. 68 ns respectively, for the isomeric free-base and zinc(II) conjugates in CH_2Cl_2 . In the case of THF/H₂O, the decrease is from 6. 82 to 1. 08 ns and from 1. 48 ns to 0. 79 ns, respectively. The above decrease in the lifetime is similar to that seen during

the titrations that involve the corresponding control systems, viz. **H₂TTP/[(TTP)Zn^{II}]** vs. **BQ**.

The above results can be interpreted by invoking two different quenching pathways operating in the **P-Calix** conjugates in the presence of BQ: (i) The first mechanism involves an unidirectional electron transfer from the singlet porphyrin to **calixarene-bound** BQ within the supramolecular ensemble (short lived component), as illustrated in Fig. 6. 7. Note in this figure that PET is from the porphyrin singlet to BQ that is encapsulated within the calixarene in THF/H₂O medium and it is from the porphyrin singlet to BQ that is H-bonded to the hydroxyl groups of the calixarene in CH₂Cl₂. (ii) The second quenching mechanism involves deactivation of the **uncomplexed P-calix** *via* intermolecular PET that is limited by diffusion (long lived component).

In as much as the above interpretation is correct, the rate constant for the ‘intra-complex’ electron transfer (**k_{PET}**) and the binding constant for the interaction of BQ with the calixarene (**K**)³⁸ can be derived using equns. 6. 5 and 6. 6, respectively.

$$k_{PET} = 1/\tau_2 - 1/\tau_0 \quad (6. 5)$$

$$K = A_2/A_1 [\text{BQ}] \quad (6. 6)$$

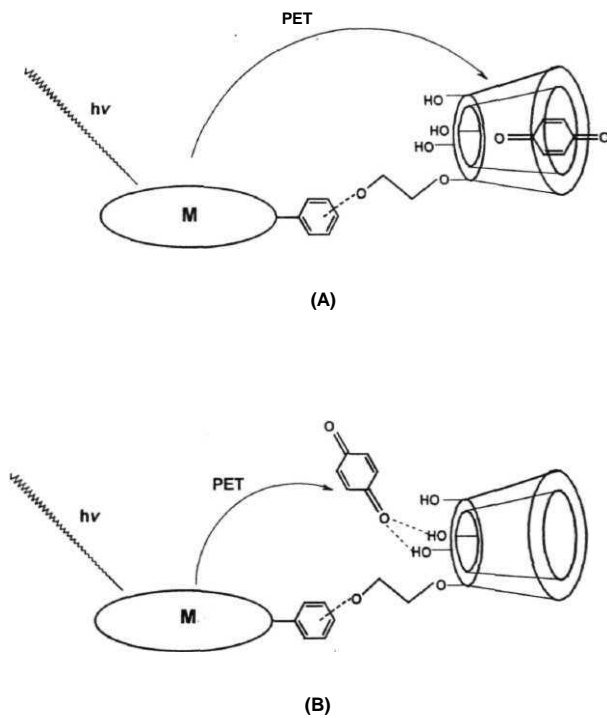


Fig. 6. 7 'Intra-complex' PET for the **P-Calix** conjugates in (A) polar and (B) apolar media.

Table 6. 4 summarizes the k_{PET} and K values for all the free-base and **zinc(II)** derivatives of the isomeric conjugates in CH_2Cl_2 and $\text{THF}/\text{H}_2\text{O}$. Inspection of the data given in Table 6. 4 reveals the following:

- (i) The electron transfer process is invariably faster in the zinc(II) isomers compared to the corresponding free-base systems irrespective of the nature of the isomer (i.e. o-, m- or p-) and also the solvent medium. This observation can be interpreted in terms of the higher exoergicity for the PET reactions in the case of zinc(II) isomers compared to the free-base systems (see: Table 6. 3)
- (ii) PET rate for a given isomeric **P-Calix** conjugate is invariably faster in $\text{THF}/\text{H}_2\text{O}$ than it is in CH_2Cl_2 . This observation is consistent with the higher dielectric constant of $\text{THF}/\text{H}_2\text{O}$ (78. 45)⁵⁷ - a medium in which the electron transfer is expected to be more facile than it is in the solvents having low dielectric constant such as CH_2Cl_2 (0. 89).^{58,59}
- (iii) In general, k_{PET} values follow the order o- > m- > p-, irrespective of the presence/absence of the zinc(II) ion in the porphyrin crevice and the solvent medium employed for the study. Although not quite dramatic, the consistency observed in the variation of the k_{PET} with respect to site of attachment of the calixarene to the porphyrin suggests that the supramolecular PET in these **P-Calix** conjugates is dependent on the distance and orientation between the donor and

acceptor species as is the case with comparable covalently linked porphyrin-quinone systems.⁶¹⁻⁶³ Structure minimization studies reveal that the center-to-center distance (r) between the porphyrin and the calixarene subunits in these conjugates vary as (± 0.3 Å): 8.17 Å (o-) < 10.40 Å (m-) < 12.02 Å (p-). A plot of $\ln(k_{\text{PET}})$ vs. r , illustrated in Fig. 6.8, for the zinc(II)porphyrin isomeric series is consistent with the exponential dependence of the PET rate with the D-A distance.⁶⁴

- (iv) Finally, K values for the binding of BQ with the calixarene, calculated using the fractional amplitude data, are found to be low ($15 \pm 2 \text{ M}^{-1}$) compared to those for the previously investigated **P-calix - BQ** conjugates ($20 - 70 \text{ M}^{-1}$),^{25, 26} but are nearly identical to one another amongst these isomeric complexes in both the investigated solvent media. Moreover, these values are insensitive to the presence/absence of the zinc(II) ion in the porphyrin; nor do they differ with respect to site of attachment of the calixarene to the porphyrin. Thus, the **coordinative/ π - π** interaction between the calixarene and porphyrin subunits in the ground states of o- linked **P-Calix** conjugates, as evidenced by the UV-visible and ^1H NMR results discussed above, does not seem to play a significant role in the singlet state dynamics of these isomers.

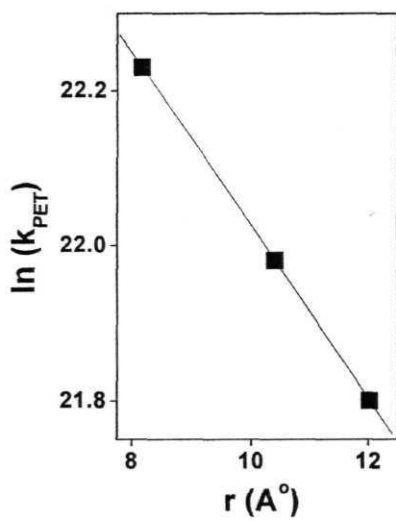


Fig. 6. 8 Plot of $\ln(k_{\text{PET}})$ vs. $r (\text{\AA})$ for $[\text{Zn}(\text{o,m,p-calix})\text{TriTP}]$.

6. 4 Summary

In summary, the present investigation demonstrates the formation of D-A complexes *via* supramolecular contact between the host **P-Calix** conjugate and the guest quinone. The supramolecular contact involves H-bonding in the apolar medium and *n-n* interaction induced by encapsulation of BQ inside the calixarene cavity in the aqueous medium. Steady state and time-resolved fluorescence studies reveal that both dynamic and static quenching mechanisms are involved in the quenching of singlet porphyrin by BQ. The static quenching mechanism has been attributed to an ‘**intra-complex**’ electron transfer occurring between the singlet porphyrin and the ‘**complexed**’ BQ. The efficiency of this ‘intra-complex’ electron transfer is found to be higher in the presence of zinc(II) ion in the porphyrin crevice, more polar solvent medium and shorter distance between the donor and acceptor subunits.

6. 5 References

1. Gutsche, C. D. In *Calixarenes, Monographs in Supramolecular Chemistry, Vol. 1*; Stoddart, J. F., Eds.; The Royal Society of Chemistry: London; 1989.
2. *Calixarenes: A Versatile Class of Macrocyclic Compounds, Topics in Inclusion Science 3*; Vicens, J., Bohmer, V., Eds.; **Kluwer**: Dordrecht, 1991.

3. *Calixarenes in Action*; Mandolini, L., Ungaro, R., Eds.; Imperial College Press: London, 2000.
4. Chou, J. -H.; Kosal, M. E.; Nalwa, H. S.; Rakow, N. A.; Suslick, K. S. In *The Porphyrin Handbook*; Kadish, K.M.; Guillard, R.; Smith, K. M. Eds.; Academic Press: New York; 2000; Vol. 6, pp. 43-131 (and references cited therein).
5. Gust, D.; Moore, T. A. In *The Porphyrin Handbook*; Kadish, K. M., Guillard, R.; Smith, K. M. Eds.; Academic Press: New York, 2000; **Vol. 8**, Chapter 57.
6. Wasielewski, M. R. *Chem. Rev.* **1992**, *92*, 435.
7. Connolly, J. S.; Bolton, J. R. In *Photoinduced Electron Transfer, Part D*; Fox, M.A., Chanon, M., Eds.; Elsevier: Amsterdam, 1988.
8. *Photodynamic Therapy: Basic Principles and Clinical Applications*; Henderson, B. W., Dougherty, T. J., Eds.; Marcel Dekker: New York; 1992.
9. Asfari, Z.; Vicens, J.; Weiss, J. *Tetrahedron Lett.* **1993**, *34*, 627.
10. Rudkevich, D. M.; Verboom, W.; Reinhoudt, D. N. *Tetrahedron Lett.* 1994, *55*, 3171.
11. Nagasaki, T.; Fujishima, H.; Takeuchi, M.; Shinkai, S. *J. Chem. Soc. Perkin Trans. 1* **1995**, **1883**.
12. Nagasaki, T.; Fujishima, H.; Shinkai, S. *Chem. Lett.* **1994**, *35*, 989.
13. Kobayashi, N.; Mizuno, K.; Osa, T. *Inorg. Chim. Acta* **1994**, *224*, 1

14. Rudkevich, D. M.; Shivanyuk, A. N.; Brzozka, Z.; Verboom, W.; Reinhoudt, D. N. *Angew. Chem. Int. Ed. Engl.* **1995**, *34*, 2124.
15. Rudkevich, D. M.; Verboom, W.; Reinhoudt, D. N. *J. Org. Chem.* **1995**, *60*, 6585
16. Khoury, R. G.; Jaquinod, L.; Aoyagi, K.; Olmstead, M. M.; Fisher, A. J.; Smith, K. M. *Angew. Chem. Int. Ed. Engl.* 1997, *36*, 2497.
17. Fiammengo, R.; Timmerman, P.; Jong, F.D.; Reinhoudt, D.N. *Chem. Commun.* **2000**, 2313.
18. Arimura, T.; Ide, S.; Suga, Y.; Nishioka, T.; Murata, S.; Tachita, M.; Nagumura, T.; Inoue, H. *J. Am. Chem. Soc.* **2001**, *123*, 10744.
19. Di Costanzo, L.; Geremia, S.; Randaccio, L.; Purrello, R.; Lauceri, R.; Sciotto, D.; Gulino, F. G. *Angew. Chem. Int. Ed.* **2001**, *40*, 4245.
20. Iwamoto, H.; Yukimasa, Y.; Fukazawa, Y. *Tetrahedron Lett.* **2002**, *43*, 8191.
21. Dudic, M.; Lhotak, P.; Stibor, I.; Dvorakova, H.; Lang, K. *Tetrahedron* **2002**, *58*, 5482.
22. Jokic, D.; Asfari, Z.; Weiss, J. *Org. left.* 2002, *4*, 2129.
23. Lauceri, R.; Raudino, A.; Monsu Scolaro, L.; Micali, N.; Purrello, R. *J. Am. Chem. Soc.* **2002**, *124*, 14536.
24. Milbradt, R.; Weiss, J. *Tetrahedron Lett.* **1995**, *35*, 1936.
25. Arimura, T.; Brown, C. T.; Spring, S. L.; Sessler, J. L. *Chem. Commun.* **1996**, 2293.

26. Arimura, T.; Ide, S.; Sugihara, H.; Murata, S.; Sessler, J. L. *New J. Chem.* **1999**, 23, 977.
27. Alder, A. D.; Longo, F. R.; Finarelli, J. D.; Goldmacher, J.; Assour, J.; Korsakoff, L. *J. Org. Chem.* **1967**, 32, 476.
28. Fuhrhop, J. -H; Smith, K. M. In *Porphyrins and Metalloporphyrins*; Smith, K. M., Ed.; Elsevier : Amsterdam, 1975: p. 769.
29. Gutsche, C. D.; Dhawan, B.; Muthukrishnan. R. *J. Am. Chem. Soc.* **1981**, 103, 3782.
30. Moghadam, G. E.; Ding, L.; Tadj, F.; Meunier, B. *Tetrahedron* **1989**, 45, 2641.
31. Li, Z. T.; Ji, G. Z.; Zhao, C. X.; Yuan, S. D.; Ding, H.; Huang, C; Diu, A. L.; Wei. M. *J. Org. Chem.* **1999**, 64, 3572.
32. Gust D.; Moore, T. A.; Moore, A. L. *Acc. Chem. Res.* **1993**, 26, 198.
33. Kurreck, H.; Huber, M. *Angew. Chem., Int. Ed. Engl.* **1995**, 34, 849
34. Ward, M. D. *Chem. Soc. Rev.* **1997**, 26, 365.
35. Gust, D. *Nature (London)* **1997**, 386, 21.
36. Harriman, A.; Magda, D. J.; Sessler, J. L. *Chem. Commun.* **1991**, 345.
37. Harriman, A.; Magda, D. J.; Sessler, J. L. *J. Phys. Chem.* **1991**, 95, 1530.
38. Sessler, J. L.; Wang, B.; Harriman, A. *J. Am. Chem. Soc.* **1993**, 115, 10418.
39. D'Souza, F. *J. Am. Chem. Soc.* **1996**, 118, 923.

40. D'Souza, F.; Deviprasad, G. R.; Hsieh, Y. Y. *Chem. Commun.* **1991**, 533.
41. D'Souza, F.; Deviprasad, G. R.; *J. Org. Chem.* **2001**, 66, 4601.
42. Hayashi, T.; Ogoshi, H. *Chem. Soc. Rev.* **1997**, 26, 355.
43. Piotrowiak, P. *Chem. Soc. Rev.* **1999**, 28, 143.
44. Turro, C.; Chang, C. K.; Leroi, G. E.; Cukier, R. I.; Nocera, D. G. *J. Am. Chem. Soc.* **1992**, 114, 4013.
45. Hunter, C. A.; Hyde, R. K. *Angew. Chem., Int. Ed. Engl.* **1996**, 35, 1936.
46. Mizutani, T.; Kurahashi, T.; Murakami, T.; Matsumi, N.; Ogoshi, H. *J. Am. Chem. Soc.* **1997**, 119, 8991.
47. Lang, K.; Karl, V.; Kapusta, P.; Kubat, P.; Vasek, P. *Tetrahedron Lett.* **2002**, 43, 4919.
48. Myles, A. J.; Branda, N. J. *J. Am. Chem. Soc.* **2001**, 123, 177.
49. Aoyama, Y.; Asakawa, M.; Matsui, Y.; Ogoshi, H. *J. Am. Chem. Soc.* **1991**, 113, 6233.
50. Hunter, C. A.; Sander, J. K. M. *J. Am. Chem. Soc.* **1990**, 112, 5525.
51. Abraham, R. J.; Bedford, G. R.; McNeillie, D.; Wright, B. *Org. Magn. Reson.* 1980, 74, 418.
52. Nicholson, R. S.; Shain, I. *Anal. Chem.* **1964**, 36, 706.

53. Ho, T-F.; **McIntosh**, A. R.; Bolton, J. R. *Nature (London)* **1980**, 286, 254.
54. Harriman, A.; Porter, G.; Searle, N. J. *Chem. Soc. Faraday Trans. 2* 1979, 75, 1515.
55. Ganesh, K. N.; Sanders, J. K. M. *Chem. Commun.* **1980**, 1129.
56. Lakowicz, J. R. *Principles of Fluorescence Spectroscopy* (2nd ed.); **Kluwer/Plenum**: New York, 1983.
57. Hasted, J. B. *Dielectric properties in Water. A Comprehensive Treatise, Vol. II*, Plenum Press : New York; 1973; Chapter 7, pp. 405–458.
58. Murov, S. L. *Handbook of Photochemistry*, Marcel Dekker Inc.: New York, 1973.
59. Suppan, P. *Chimica* **1988**, 42, 320.
60. Sessler, J. L.; Johnson, M. R.; Lin, T. R.; Creager, S. E. *J. Am. Chem. Soc.* **1988**, 110, 3659.
61. **Sakata**, Y.; Tsue, H.; O'Neil, M. P.; Wiederrecht, G. P.; Wasielewski, M. R. *J. Am. Chem. Soc.* **1994**, 116, 6904.
62. Wasielewski, M. R.; Johnson, D. G.; Niemczyk, M. P.; **Gaines**, G. L.; O'Neil, M. P.; Svec, W. A. *J. Am. Chem. Soc.* **1990**, 112, 6842.
63. Hayashi, T.; Takimura, T.; **Hitomi**, Y.; **Ohara**, T.; Ogoshi, H. *Chem. Commun.* **1995**, 575.
64. Marcus, R. A. *J. Chem. Phys.* **1956**, 24, 966.

CHAPTER 7

Conclusions

The common genesis of the various topics discussed in this thesis is the knowledge that "photochemically active porphyrin-based arrays and D-A systems are of immense utility in a range of modern research areas". Literature on the recently reported photochemically active **porphyrin** arrays and D-A systems, as relevant to the present thesis, has been reviewed in Chapter 1. Results obtained during the present investigation that deal with the design, synthesis, characterization and photochemical properties of new porphyrin arrays and D-A systems derived from 'axial' or 'peripheral' site substitution of free-base, metallo- and metalloid porphyrins are reported in Chapters 3, 4, 5 and 6.

7.1 'Axial-bonding' type porphyrin arrays

The majority of hitherto reported porphyrin arrays have been obtained *via* cumbersome and often, low-yielding organic synthesis protocols involving manipulation at either the **β -pyrrole** or the **meso-phenyl position/s** of the monomers. On the other hand, relatively few studies have been carried out on the so-called 'axial-bonding' type systems. In addition, less attention seems to have been paid towards the construction of functionally active, hybrid (unsymmetrical) systems.

During the course of the present set of investigations, it was noticed that **bis-axially** ligated, six co-ordinate metalloid porphyrins have been conveniently employed for the synthesis of 'vertically linked' porphyrin trimers and D-A systems.¹ⁿ³ Further realization that it should be possible to synthesize more elaborate hybrid-type arrays by utilizing the reactivities at both the peripheral and axial sites of a metalloid porphyrin species guided the construction of new a nonameric array **(H₂)₆Sn₃**. Details of design, synthesis, spectroscopy, electrochemistry and singlet state activity of this 'axial-bonding' type hybrid porphyrin array are discussed in Chapter 3 of this **thesis**. In doing so, the characteristic features of **(H₂)₆Sn₃** have been compared with those of its structural predecessors, viz. **(H₂)₄Sn₂** and **(H₂)₂Sn**.

Each synthetic step involved during the construction of **(H₂)₆Sn₃** is straightforward and provides good yields of the desired products in pure form. It should, however, be noted that synthesis of an 'all free-base' homologue is clearly outside the scope of this approach. The ground state spectroscopic and redox data of **(H₂)₆Sn₃**, as probed by the UV-visible, ¹H NMR and differential pulse voltammetric techniques, collectively indicate that there exists minimum interaction between **π-planes** of the constituent monomeric porphyrins in this 'axial-bonding' type array. Thus, an architecture involving a symmetric but, a non-parallel disposition of the two axial porphyrins with respect to plane of the central porphyrin is appropriate for this nonamer. Analysis of the emission and excitation spectral data suggested that an electronic energy transfer (EET) from

the central tin(IV) porphyrin to the axial free-base as well as the photoinduced electron transfer (PET) from axial free-base (ground state) to the singlet state of the central porphyrin occur in this nonamer. It is interesting that the EET reactions of $(\text{H}_2)_6\text{Sn}_3$ and $(\text{H}_2)_4\text{Sn}_2$ are more efficient than the corresponding reaction reported for $(\text{H}_2)_2\text{Sn}$.^{1,3} The reason/s for the efficient EET observed for the higher homologues compared to the trimer in this class of 'axial-bonding' type hybrid arrays is still unclear. However, it should be noted that the number of acceptors (i. e. free-base porphyrins) in the neighborhood of a given donor (i. e. tin(IV) porphyrin) increases as one moves from the lower homologue to the higher D-A ensembles in this series.

The 'axial-bonding' strategy for building porphyrin arrays has been extended to the next Chapter. Here, a bimetallic trimer $(\text{Ru})_2\text{Sn}$ has been self-assembled utilizing the hard and soft acid-base (HSAB) principle. The HSAB principle has been employed earlier for the construction of multimetallic porphyrin arrays but, the process of generating the monomeric species, in itself, involved cumbersome organic reaction sequences and required the availability of complex 'tailor made' porphyrin monomers.⁴ The results discussed in Chapter 4 clearly demonstrate that $(\text{Ru})_2\text{Sn}$ can be conveniently self-assembled by using complementary binding properties of the readily available ruthenium(II)- and tin(IV) porphyrins with a ditopic ligand (pyridine-4-carboxylic acid). In accordance with general principles of the self-assembly process, it was possible to achieve the synthesis of $(\text{Ru})_2\text{Sn}$ in near quantitative yields by both 'step-

wise' and 'one-pot' methods. An interesting aspect noticed during this study is that **[(DTPP)Ru^{II}(CO)(Py)]** - the ruthenium(II) precursor used for the construction of this array - exists, in the solid state, as a 'benzoic acid' type dimer. It is reasonable to expect the same dimeric nature to be retained in apolar CH₂Cl₂ medium for this compound. The construction of **(Ru)₂Sn** achieved in CH₂Cl₂ solutions can thus be conceived to proceed with the breaking of these weak H-bonds prior to the competing strong 'Sn - O' interaction.

As is the case with the 'axial-bonding' type nonameric array **(H₂)₆Sn₃** described in the previous Chapter, the spectroscopic and redox data of the trimer **(Ru)₂Sn** are also found to be a superposition of those of its constituent monomeric partners. The quenching of fluorescence due to the tin(IV) porphyrin part of the trimer has been rationalized in terms of a PET from the axial ruthenium(II) porphyrin to the excited state of basal tin(IV) porphyrin.

7. 2 Non-covalently bound D-A conjugates

Two types of non-covalently bound D-A **conjugates** have been reported in this thesis: (i) a porphyrin-calix[4]diquinone conjugate (Chapter 5) and (ii) a series of **isomeric**, free-base and zinc(II) derivatives of **P-Calix** conjugates (Chapter 6). While the construction of porphyrin-calix[4]diquinone conjugate relies on the 'axial-bonding' theme employed in Chapters 3 and 4, the **P-Calix** conjugates, in each of which a calix[4]arene subunit is connected at the peripheral position of the porphyrin, are obtained by employing the long-

established 'all organic' approach. An additional difference between these two types of D-A conjugates is that while the acceptor (i.e. the diquinone) is an integral part of the assembly in the porphyrin-calix[4]diquinone system, the **P-Calix** conjugates, can, at best, be termed as the 'pre D-A systems'. This is because generation of a truly, **non-covalently** bound D-A system is accomplished here only upon addition of BQ to solutions containing **P-Calix** conjugates and the subsequent **H-bonding/encapsulation** of BQ with the calix[4]arene part of these systems. In any case, the photophysical results obtained in both these D-A systems were found to be interesting and could be explained in terms of the well-known $^1(\text{porphyrin}) \rightarrow \text{quinone}$ PET process in each case.

The porphyrin-calix[4]diquinone system described in Chapter 5 has been assembled *via* axial coordination of $[(\text{TTP})\text{Zn}^{\text{II}}]$ with calix[4]diquinone bearing a pendant pyridine as the coordinating ligand. The new pyridine ligand cyclo-25, 27-diethoxy 26,28-calix[4]diquinone 3,5- pyridine dicarboxylate (**CalixQ-py**) has been synthesized in three steps in moderate yield. UV-visible, ^1H NMR and electrochemical titration studies revealed the formation of a stable complex between $[(\text{TTP})\text{Zn}^{\text{II}}]$ and **Calix-py** / **CalixQ-py**. In the steady state and time-resolved fluorescence studies, it was observed that fluorescence intensity and lifetime of $[(\text{TTP})\text{Zn}^{\text{II}}]$ are both drastically decreased upon successive addition of **CalixQ-py**, but not **Calix-py**. The quenching of $[(\text{TTP})\text{Zn}^{\text{II}}]$ fluorescence in

the presence of **CalixQ-py** has been attributed to a PET from the singlet $[(\text{TTP})\text{Zn}^{\text{II}}]$ to the axially ligated calix[4]diquinone.

It should be noted here that the porphyrin-calix[4]diquinone assembly is really a D-A1-A2 (i.e. **porphyrin-quinone₁-quinone₂**) system and hence, there exists a possibility of a sequential electron transfer in this triad (i. e. $\text{D-A1-A2} \rightarrow \text{D}^+-\text{A1-A2} \rightarrow \text{D}^+-\text{A1}^--\text{A2} \rightarrow \text{D}^+-\text{A1-A2}^-$). However, the steady state fluorescence method employed here is inadequate to monitor this electron transfer chain. Another interesting result to be noticed here is the observation that $K([(TTP)Zn^{\text{II}}]^+) / K([(TTP)Zn^{\text{II}}])$ is ≈ 250 , as revealed by the electrochemical data. This suggests that the reduced calix[4]diquinone does not dissociate itself from the PET product, namely, $[(TTP)Zn^{\text{II}}]^+ - \text{CalixQ-py}^-$; instead, it is expected to be more strongly bound at the zinc(II) center in this state. At a first glance, this analysis seems quite encouraging but then, note that stability of the $[(TTP)Zn^{\text{II}}]^+ - \text{CalixQ-py}^-$ state has the potential in it to enhance the possibility of the so-called reverse electron transfer (charge recombination). It is thus instructive to construct a D-A system in which the **porphyrin⁻ - Quencher⁺** state can be photogenerated. As **porphyrin⁻** is expected to binds the extraneous ligands less strongly than the neutral **porphyrin** itself, charge separation rather than the charge recombination is expected to be facilitated in such a system leading to enhanced yield of the redox product.

The series of isomeric free-base and zinc(II) derivatives of **P-Calix** conjugates reported in Chapter 6 have been characterized by mass (MALDI-

TOF), UV-visible, ^1H NMR and fluorescence spectroscopic methods. During these spectral characterizations, it was observed that, except for the o-isomers of the free-base- and zinc(II)porphyrin-calixarene conjugates (i. e. $[\text{H}_2(\text{o-calix})\text{TriTP}]$ and $[\text{Zn}(\text{o-calix})\text{TriTP}]$), the data of all the **P-Calix** systems investigated in this study are within the same range as those of their individual, unlinked components. The red shifts in the UV-visible spectral bands and upfield shifts in the ^1H NMR resonances due to the appended calixarene subunits observed for these o-isomers have been interpreted in terms of either *n-n* ($[\text{H}_2(\text{o-calix})\text{TriTP}]$) or intramolecular coordination between zinc(II) center of the porphyrin and one of the three hydroxyl groups of the calix[4]arene moiety ($[\text{Zn}(\text{o-calix})\text{TriTP}]$). All of the isomeric P-Calix conjugates can bind BQ *via* hydrogen bonding in apolar (CH_2Cl_2) and through π - π interaction in polar ($\text{H}_2\text{O}/\text{THF}$, 9 : 1 v/v) media. The results of steady state and time-resolved fluorescence studies reveal that static as well as dynamic quenching processes are involved in the quenching of fluorescence due to these conjugates by BQ in both polar and apolar media. The quenching mechanism is attributed to an 'intra-complex' PET from the singlet porphyrin to the supramolecularly bound quinone in each case. The rate of this PET is found to follow the order: 'o- > m- > p-' in these **P-Calix** conjugates, as is the case with the analogous, covalently linked porphyrin-quinone systems.⁵ Thus, the coordinative/ π - π interaction between the calixarene and porphyrin subunits in the ground states of o-linked **P-Calix**

conjugates does not seem to play a significant role in the singlet state dynamics of these isomers.

7.3 Future scope

The present study has been helpful, to some extent, not only in formulating strategies towards the design of new types of porphyrin arrays and D-A systems but also in probing certain intricacies involved in the PET reactions in these compounds. Notwithstanding this fact, an in-depth analysis of the results described in various chapters of this thesis suggests that a lot more remains to be done to generate more sophisticated D-A compounds/arrays and to arrive at a better understanding of the EET and PET mechanisms. For example, more elaborate photophysical experiments involving the time-resolved absorption and fluorescence techniques can be carried out to learn more about the mechanistic details of the PET and EET reactions occurring in these D-A systems. Axial-bonding type, D-A systems based on metalloid porphyrins bearing rigid spacers can be built and the intricacies involved in the PET and EET reactions occurring in them can be compared with those of systems described in Chapters 3 and 4. The experience gained in this study while working on various arrays and D-A systems can be advantageously used for the construction of dendrimeric D-A ensembles. Axial bonding type D-A systems having solubility in aqueous environments can also be prepared.

The results described in Chapters 5 and 6 provide some useful insights into the design aspects of more appealing D-A systems such as, for example, porphyrin - triazacalix[4]diquinone or porphyrin - calix[4]triquinone diads. The triaza calix[4]diquinone class of receptors have the ability to bind both anions and transition metal ions. Thus porphyrin - triazacalix[4]diquinone type systems can act as sensors for both anions and transition metal ions (amphiphilic sensor). D-A1-A2-A3 type porphyrin - calix[4]triquinone systems (Fig. 7. 1), being able to bind and sense alkali metal ions in their calix[4]triquinone subunits, are expected form ideal candidates for studying multi-step PET reactions.

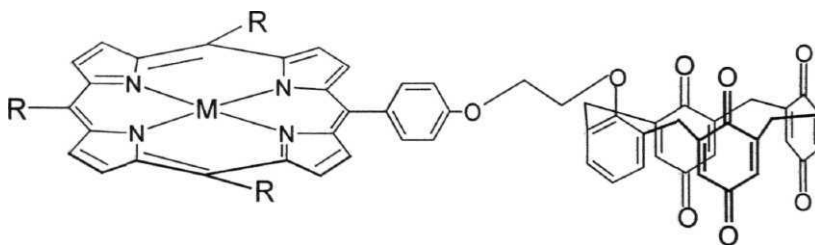


Fig. 7. 1

7. 4 References

1. Rao, T. A.; Maiya, B. G. *Chem. Commun.* **1995**, 939.

2. Rao, T. A.; Maiya, B. G. *Inorg. Chem.* **1996**, *35*, 4829.
3. Giribabu, L.; Rao, T. A.; Maiya, B. G. *Inorg. Chem.* **1999**, *38*, 4971.
4. Kim, H. J.; Bampos, N.; Sanders, J. K. M. *J. Am. Chem. Soc.* **1999**, *121*, 8120.
5. Wasielewski, M. R. *Chem. Rev.* **1992**, *92*, 435.

APPENDIX I

X-ray Crystallographic Data of [(DTPP)Ru^{II}(CO)(Py)]

Table 1 Atomic coordinates ($\times 10^4$) and equivalent isotropic displacement parameters ($\text{\AA}^2 \times 10^3$) for [(DTPP)Ru^{II}(CO)(Py)]. U(eq) is defined as one third of the trace of the orthogonalized Uij tensor.

atom	x	y	z	U(eq)
Ru(1)	5372(1)	2125(1)	7619(1)	25(1)
O (1)	9033(3)	1031(2)	5174(1)	51(1)
O (2)	9500(3)	-313(2)	5643(1)	48(1)
O(3)	3559(3)	2851(3)	8494(1)	59(1)
N(1)	5770(3)	3282(2)	7454(1)	28(1)
N(2)	4334(3)	2613(2)	7067(1)	28(1)
N(3)	5061(3)	936(2)	7748(1)	27(1)
N(4)	6485(2)	1610(2)	8137(1)	26(1)
C(1)	5309(3)	4028(3)	7122(2)	29(1)
C(5)	3091(3)	2742(3)	6536(2)	34(1)
C(10)	5098(4)	-500(3)	8040(2)	37(1)
C(15)	7692(3)	1488(3)	8689(2)	33(1)
C(20)	5739(4)	4715(3)	7157(2)	37(1)
C(25)	2659(4)	6266(3)	6193(2)	46(1)
C(30)	1012(11)	6886(8)	6861(3)	76(1)
C(40)	2146(3)	782(3)	7236(2)	36(1)
C(50)	6001(3)	1032(3)	9167(2)	35(1)
C(60)	9629(5)	2838(5)	8208(3)	80(2)
C(70)	6398(5)	4516(5)	9811(3)	83(2)
C(75)	6630(3)	1578(2)	6944(1)	27(1)
C(80)	7957(3)	334(3)	6529(2)	34(1)
C(100)	3320(20)	3237(15)	1842(7)	88(2)
C(105)	3572(19)	1174(13)	3587(10)	88(2)
C(200)	3100(40)	3770(20)	1587(10)	88(2)
C(205)	3180(30)	1400(20)	3703(11)	88(2)
C(300)	3670(30)	8030(18)	6827(9)	88(2)
C(305)	3870(20)	5030(16)	8538(13)	88(2)
C(400)	3470(30)	8258(15)	6980(10)	88(2)
C(405)	3520(30)	4976(15)	8502(13)	88(2)

Table 2 Anisotropic displacement parameters ($\text{\AA}^2 \times 10^3$) for **[(DTPP)Ru^{II}(CO)(Py)]**. The anisotropic displacement factor exponent takes the form: $-2\pi^2 [h^2 a^{*2} U_{11} + \dots + 2hk a^* b^* U_{12}]$

Atom	U ₁₁	U ₂₂	U ₃₃	U ₂₃	U ₁₃	U ₁₂
Ru(1)	25(1)	24(1)	23(1)	-3(1)	0(1)	8(1)
O(1)	53(2)	51(2)	30(2)	-9(1)	11(1)	-4(2)
O(2)	44(2)	45(2)	38(2)	-10(1)	5(1)	3(2)
O(3)	43(2)	79(3)	39(2)	-17(2)	10(2)	-4(2)
N(1)	27(2)	27(2)	28(2)	-4(1)	0(1)	-9(1)
N(2)	27(2)	27(2)	27(2)	-5(1)	0(1)	-7(1)
N(3)	26(2)	27(2)	28(2)	-3(1)	-1(1)	-10(1)
N(4)	26(2)	27(2)	25(2)	-3(1)	-2(1)	-8(1)
C(1)	31(2)	26(2)	28(2)	-4(2)	1(2)	-8(2)
C(5)	32(2)	38(2)	33(2)	-3(2)	-6(2)	-11(2)
C(10)	43(2)	28(2)	40(2)	1(2)	-8(2)	-14(2)
C(15)	31(2)	36(2)	33(2)	-4(2)	-8(2)	-11(2)
C(20)	42(2)	28(2)	40(2)	-2(2)	-6(2)	-11(2)
C(25)	50(3)	34(2)	45(3)	4(2)	-10(2)	-7(2)
C(30)	67(3)	45(3)	42(3)	8(2)	3(2)	-25(3)
C(35)	29(2)	34(2)	38(2)	-6(2)	-5(2)	-12(2)
C(40)	31(2)	36(2)	41(2)	-6(2)	-5(2)	-12(2)
C(50)	33(2)	34(2)	35(2)	-4(2)	0(2)	-10(2)
O(60)	63(4)	72(4)	72(4)	-15(3)	4(3)	14(3)
C(70)	59(4)	120(6)	75(4)	-58(4)	3(3)	-20(4)
C(75)	37(3)	54(3)	66(3)	-19(3)	5(2)	-21(2)
C(80)	34(2)	27(2)	35(2)	-6(2)	0(2)	-5(2)
C(100)	52(2)	82(2)	48(2)	-20(2)	1(2)	-20(2)
C(105)	65(2)	48(2)	45(2)	-3(2)	6(2)	-12(2)
C(200)	39(2)	29(2)	55(2)	-6(2)	8(2)	-2(2)
C(205)	49(2)	18(2)	58(2)	-5(2)	7(2)	-6(2)
C(300)	58(4)	28(2)	28(2)	-7(2)	8(2)	-9(2)
C(305)	68(4)	19(2)	38(2)	-8(2)	7(2)	-6(2)
C(400)	54(2)	29(2)	28(2)	-6(2)	4(2)	-5(2)
C(405)	53(2)	28(2)	38(2)	-3(2)	2(2)	-2(2)

Table 3 Bond length and Bond angles for $[(DTTP)Ru^II(CO)(Py)]$.

Bond Length (Å)		Bond angle (deg)	
Ru(1)-C(83)	1.839(4)	C(83)-Ru(1)-N(2)	90.84(15)
Ru(1)-N(2)	2.053(3)	C(83)-Ru(1)-N(3)	91.40(16)
Ru(1)-N(3)	2.057(3)	N(2)-Ru(1)-N(3)	90.63(13)
Ru(1)-N(4)	2.059(3)	C(83)-Ru(1)-N(4)	92.47(15)
Ru(1)-N(1)	2.063(3)	N(2)-Ru(1)-N(4)	176.69(12)
Ru(1)-N(5)	2.200(3)	N(3)-Ru(1)-N(4)	89.41(13)
O(1)-C(82)	1.274(5)	C(83)-Ru(1)-N(1)	92.26(16)
O(1)-H(100)	0.8400	N(2)-Ru(1)-N(1)	89.66(13)
O(2)-C(82)	1.245(5)	N(3)-Ru(1)-N(1)	176.32(12)
O(3)-C(83)	1.137(5)	N(4)-Ru(1)-N(1)	90.09(13)
N(1)-C(1)	1.367(5)	C(83)-Ru(1)-N(5)	176.79(15)
N(1)-C(1)	1377(5)	N(2)-Ru(1)-N(5)	86.33(12)
N(2)-C(3)	1.372(5)	N(3)-Ru(1)-N(5)	87.11(12)
N(2)-C(6)	1.378(5)	N(4)-Ru(1)-N(5)	90.36(12)
N(3)-C(11)	1.377(5)	N(1)-Ru(1)-N(5)	89.25(12)
N(3)-C(8)	1.379(5)	C(82)-O(1)-H(100)	109.5(12)
N(4)-C(13)	1.373(5)	C(18)-N(1)-C(1)	107.0(3)
N(4)-C(16)	1.380(5)	C(18)-N(1)-Ru(1)	126.1(3)
C(1)-C(2)	1.406(6)	C(1)-N(1)-Ru(1)	126.5(3)
C(10)-C(11)	1.442(6)	C(3)-N(2)-C(6)	107.3(3)
C(25)-C(26)	1.384(6)	C(3)-N(2)-Ru(1)	126.9(3)
C(30)-H(30C)	0.9800	C(6)-N(2)-Ru(1)	125.8(3)
C(50)-C(51)	1.390(6)	C(11)-N(3)-C(8)	107.3(3)
C(100)-C(101)	1.469(10)	C(11)-N(3)-Ru(1)	126.9(3)
C(105)-H(10N)	0.9800	C(8)-N(3)-Ru(1)	125.8(3)
C(200)-H(20B)	0.9800	C(13)-N(4)-C(16)	107.2(3)
C(300)-H(30H)	0.9800	C(13)-N(4)-Ru(1)	126.7(3)
C(350)-H(40A)	0.9800	C(16)-N(4)-Ru(1)	125.9(3)
C(400)-H(40M)	0.9800	N(1)-C(1)-C(2)	125.5(4)
C(405)-H(40C)	0.9800	N(1)-C(1)-C(20)	109.0(4)

APPENDIX II

List of publications

1. A new family of donor-acceptor systems comprising of tin(IV)porphyrin and anthracene subunits: Synthesis, spectroscopy and energy transfer studies, A. Ashok **Kumar**, L. Giribabu, Bhaskar G. Maiya, **Proc. Ind. Acad. Sci. (Chem. Sci.)**, 2002, **114**, 565-578
2. Orientation dependence of energy transfer in an anthracene-porphyrin donor-acceptor system, L. Giribabu, **A. Ashok Kumar**, V. Neeraja and Bhaskar G. Maiya, **Angew. Chemie (Int. Ed.)**, 2001, **40**, 3621-3624
3. New Molecular Arrays Based on Tin(IV) Porphyrin Scaffold, **A. Ashok Kumar**, L. Giribabu, D. R. Reddy and Bhaskar G. Maiya, **Inorg. Chem.** 2001, **40**, 6757 - 6766.
4. A supramolecular array assembled via the complementary binding properties of ruthenium(II) and tin(rV) porphyrins, Bhaskar G. Maiya, N. Bampos, **A. Ashok Kumar**, N. Feeder and **J.K. M. Sanders**, **New J. Chem.** 2001, 797-800.

5. **Cobalt(III)**, nickel(II) and ruthenium(II) complexes of 1, 10-phenanthroline family of ligands: DNA binding and photocleavage studies, S. Arounagiri, D. Eswaramoorthy **A. Ashok Kumar**, A. Dattagupta and Bhaskar G. Maiya, **Proc. Ind. Acad. Sci (Chem. Sci.)**, 2000, 112, 1-17.
6. A new 'axial-bonding' type donor-acceptor system assembled *via* coordination of zinc(II) porphyrin with pyridine-linked calix[4]diquinone, **A. Ashok Kumar** and Bhaskar G. Maiya. (Manuscript under preparation)
7. 'Intra-complex' electron transfer in a series of quinone-bound porphyrin-calix[4]arene conjugates, **A. Ashok Kumar** and Bhaskar G. Maiya. (Manuscript under preparation)